ABSTRACT

Title of Dissertation: Existence and Stability of Vortex Solutions of Certain Nonlinear Schrödinger Equations

Richard Kollár, Doctor of Philosophy, 2004

Dissertation directed by: Professor Robert L. Pego
Department of Mathematics

The nonlinear Schrödinger equation models a wide variety of different physical phenomena ranging from nonlinear optics, water waves, magnetization of ferromagnets to Bose-Einstein condensates (BEC). The structure of the equation supports existence of topologically non-trivial solutions – vortices. Surprisingly, we demonstrate that the Landau-Lifshitz magnetization equation which is formally also a nonlinear Schrödinger equation does not admit such solutions unless they are stationary. On the other hand, the contrary is true for the Gross-Pitaevskii equation which describes the mean-field approximation of BEC. We investigate stability of vortex solutions by means of a very reliable, sensitive and robust technique – the Evans function. This method, although limited to two dimensions, allows us to study rotating axisymmetric BEC for large particle numbers which can be unattainable by other means. We found a singly-quantized vortex linearly stable. The linear stability of multi-quantized vortices depends on the diluteness of a condensate, with alternating intervals of stability and instability.

Existence and Stability of Vortex Solutions of Certain Nonlinear Schrödinger Equations

by

Richard Kollár

Dissertation submitted to the Faculty of the Graduate School of the
University of Maryland, College Park in partial fulfillment
of the requirements for the degree of
Doctor of Philosophy
2004

Advisory Committee:

Professor Robert L. Pego, Chairman/Advisor
Professor C. David Levermore
Professor Jian-Guo Liu
Professor Ricardo H. Nochetto
Professor Steven L. Rolston

DEDICATION

To all whom it may concern

ACKNOWLEDGEMENTS

I would like to thank all the people who intelectually and emotionally supported me through my graduate studies, my family, my friends both in Slovakia and in the U.S.A., both in mathematics and in the outside world. Particularly, I am extremely grateful for all the help I received from my advisor Robert Pego and from Jian-Guo Liu; besides helping me with my thesis they both opened my eyes wide and showed me that math is interesting. I would also like to thank Daniel Ševčovič for fruitful discussions and advices; the whole Math department at the University of Maryland, College Park, for a nice supportive environment for work; Institute of Applied Mathematics, Comenius University, Bratislava, for hospitality during my stay; UMD Graduate School for a generous financial support through the Dissertation Fellowship; all members of my dissertation and oral exam committee for their dedication and my soon-to-be-wife Katka for patience. I would also like to acknowledge the financial support of the National Science Foundation under grants nos. DMS 00-72609, DMS 03-05985.

TABLE OF CONTENTS

LIST OF FIGURES

Chapter 1

Introduction

One of the central problems in the field of nonlinear partial differential equations and nonlinear waves particularly is *the behavior of coherent structures supported by an underlying system*. There exist a large variety of such structures: solitary waves, phase-interfaces and various types of singularities. Investigations in fluid flows, superconductors, reaction-diffusion processes or material coarsening are just a few examples of the practical significance of research in the field. Although these patterns have often only a local character, they are frequently the dominant features of evolution of a system. Because in some cases these objects persist without any change for a long time, while in other cases they can evolve and interact with similar objects or with a physical boundary it is not possible to describe their nature in general.

The focus of this thesis is primarily on the problem of stability and instability of vortices in Bose-Einstein condensates modeled by the Gross-Pitaevskii equation

$$i\hbar\psi_t = \left(-\frac{\hbar^2}{2M}\triangle + V(x) + i\hbar\Omega\partial_\theta + g|\psi|^2\right)\psi\,,$$

an equation with the structure of a nonlinear Schrödinger equation. Non-existence of vortex and vortex-like solutions to another nonlinear Schrödinger equa-

tion, the Landau-Lifshitz magnetization equation

$$m_t = m \times \triangle m - \lambda m \times m \times \triangle m,$$

which written in the stereographic projection has the form

$$iw_t = -\triangle w - 2\,\frac{\nabla w \cdot \nabla w}{1+|w|^2}\bar{w}\,,$$

is also proved.

In the case of the Gross-Pitaevskii equation which models in the Hartree-Fock approximation Bose-Einstein condensates confined in rotating harmonic traps, we study stability of localized (encapsulated) vortex solutions of the reduced two-dimensional problem. First, we numerically obtain accurate vortex solutions by tracing the bifurcation branch out of a trivial solution and then we improve its precision by the multiple shooting method. Then we rigorously derive the proper linearization of the Gross-Pitaevskii equation about these solutions. The linearization procedure is analogous to one used in [1]. This justifies the Bogoliubov equations well-known in the physics literature obtained by the linearization of the associated Hamiltonian in the field operator formalism. The "classical" treatment of linearization can be also found in [2] and [3] but without any reasoning behind the choice of the form of the small perturbation used. The derivation here shows how the necessary coupling naturally appears starting from an arbitrary perturbation.

Next, we prove that if the relative trap rotational frequency Ω is smaller than 1, the essential spectrum of the linearized operator is empty. This proof is to our knowledge not known in the literature. Since we show that the eigenvalues (the discrete spectrum) of the linearized problem suffer only a shift by a purely imaginary number depending on rotation, stability of this part of the spectrum

is unaffected by rotation of the trap. This reduces the number of free parameters in the problem to a single one, denoted by p, nonlinearly depending upon the number of the particles in the condensate N,

$$N = \int_{\mathbb{R}^2} |\psi|^2 dx^2 \,.$$

The linearized equations are then decomposed into an infinite system of coupled pairs for the Fourier modes. We prove that the unstable eigenvalues may exist only for finitely many of them with a bound dependent only on the vortex charge (the proof is not new and its sketch can be found in [4]). Moreover, all the possible unstable eigenvalues are located in a vertical strip symmetric with respect to the imaginary axis. Also the number of possible unstable eigenvalues is bounded by the number of negative eigenvalues of the corresponding self-adjoint Hamiltonian. We also prove the precise asymptotic behavior of the solutions to the linearized equations.

To determine the location of both stable and unstable eigenvalues we use the Evans function technique. This robust method allows us to study the problem for a wide range of the parameter p corresponding to the size of the condensate ranging from an effectively linear regime far up to the fully nonlinear Thomas-Fermi regime corresponding to a large number of particles N in a dilute state.

We find singly-quantized ($m = 1$) vortices linearly stable in agreement with both experimental and theoretical results in literature. On the other hand, multi-quantized vortices ($m = 2$) are found to be linearly stable and unstable as reported by [5] using a less reliable method. For a fixed inter-particle interaction strength the stability or instability depends on the size of the condensate, with intervals of stability and instability alternating with increasing number of particles starting with unstable phase for a very small number of particles. The

intervals of stability or instability show a repeating pattern eventually continuing to any number of particles, although the proportion of length of intervals of instability seems to grow. Experimental creation of a multi-quantized vortex may therefore require some other means of stabilization than just a harmonic trap. Nevertheless, we emphasize the instability we observe is weak, with the real part of the unstable eigenvalues small and only slowly increasing with the growing parameter p.

The presence of the instability is checked by direct numerical simulations using the Strang time-splitting scheme designed in [6]. A rough approximation of the eigenvectors for the detected eigenvalues is calculated by a simple Galerkin approximation.

For the Landau-Lifshitz magnetization equation we prove that all the non-stationary solutions with a vortex-like structure have their modulus oscillating and approaching π as $|x| \to \infty$ in such a way that their energy is infinite. On the other hand, the stationary vortex solutions, the Belavin-Polyakov instantons, have finite energy. We emphasize that this statement is true also for the dissipation-less model $\lambda = 0$ and for any frequency $\omega \neq 0$. This suggests a strong energetic instability of any non-stationary vortex structures for $\omega \neq 0$.

1.1 Thesis outline

This section gives an overview on how the material is organized in the chapters and appendices of this thesis.

The two sections of Chapter 2 serve as an introduction and an historical survey into the concept of vortex solutions to nonlinear Schrödinger equations. Some results on existence and stability for certain nonlinear Schrödinger equations (ex-

cluding the Gross-Pitaevskii and the Landau-Lifshitz equation) are also briefly discussed.

The whole of Chapter 3 contains analysis and results on stability of vortex solutions in Bose-Einstein condensates. First, the motivation and a summary of known results are presented. A mathematical justification of the numerical approach used to generate vortex solutions follows. The next step is a rigorous derivation of linearized equations (which turn out to be equivalent to the Bogoliubov equations well-known in the physics literature) and an introduction to the Evans function method used to determine stability or instability of vortex solutions. Finally, a description of the numerical procedure and its results are discussed. Note that although the results of analysis required by this approach are also mentioned, details of the necessary proofs and long calculations are omitted and included only in the appendices. (The material in Chapter 3 is a joint work with Dr. Robert L. Pego.)

On the other hand, Chapter 4 is self-contained and is devoted to the Landau-Lifshitz magnetization equation. After an outline of a derivation from the general torque equation and from a free energy functional, the Landau-Lifshitz equation is transformed into spherical coordinates. Then results and their connection to the general vortex concept mentioned in Chapter 2 are described. The remaining sections contain full mathematical proofs of non-existence of non-stationary pure vortex solutions and of an infinite-energy property of all the vortex-like solutions in this model. The main techniques used in these arguments come from the theory of ordinary differential equations, namely the Pohozaev identity and oscillation theory. (The material in Chapter 4 was recently submitted by the author for publication [7].)

Chapter 5 discusses some of the important issues arising in this work and also lists possibilities for further investigations.

All of the appendices are related to the Gross-Pitaevskii equation treated in Chapter 3. Appendix A contains details of justification of use of the Crandall-Rabinowitz theorem in Chapter 3. The theorem describing spatial properties of a radial vortex profile is in Appendix B. The proof that the essential spectrum of the linearized Gross-Pitaevskii equation is empty can be found in Appendix C.

Appendix D contains two proofs for bounds on unstable eigenvalues which were for the sake of clarity of presentation omitted in Chapter 3. Asymptotic analysis of solutions to the Gross-Pitaevskii equation and to its linearization is located in Appendix E.

Appendix F serves as a source for all the formulas necessary for the proper rescaling of systems of ordinary differential equations in the numerical implementation of the Evans function evaluation. Finally, Appendix G describes the numerical procedure (a Galerkin method) for solving the linearized Gross-Pitaevskii equation assuming the approximate eigenvalue is known.

Chapter 2

Vortex solutions to nonlinear Schrödinger equations

There is a good reason for the fact that nonlinear Schrödinger equations (NLS) are ubiquitous both in physics and mathematics. They model a wide variety of different physical phenomena including water waves, nonlinear optics, optical fibers or Bose-Einstein condensates. From the mathematical point of view they play an important role as the lowest order perturbation approximation for weakly nonlinear dispersive wave systems.

The nonlinear Schrödinger equations [8] that are considered here have the general form

$$i\psi_t = -\triangle\psi + f(x, \psi, \nabla\psi)\,, \tag{2.1}$$

where $\psi : \mathbb{R}^D \to \mathbb{C}$ (here $D = 2$ or $D = 3$). The nonlinearity f is assumed to preserve the structure of NLS, namely the rotational invariance

$$f(x, e^{i\alpha}\psi, \nabla e^{i\alpha}\Psi) = e^{i\alpha} f(x, \psi, \nabla\psi)$$

and the invariance with respect to complex conjugacy

$$f(x, \overline{\psi}, \nabla\overline{\psi}) = \overline{f(x, \psi, \nabla\psi)}\,.$$

The simplest nonlinearities with these properties are the *cubic nonlinear Schrödinger equation*

$$i\psi_t = -\triangle\psi + |\psi|^2\psi \tag{2.2}$$

and the *cubic-quintic nonlinear Schrödinger equation*

$$i\psi_t = -\triangle\psi - (|\psi|^2 - |\psi|^4)\psi\,. \tag{2.3}$$

These equations model laser beams in defocusing and self-focusing-defocusing media in nonlinear optics, respectively, and they also serve as simple models for more complicated gauge theories of mathematical physics. The cubic-quintic NLS can be also obtained by a truncation of the Taylor series for a so-called saturable media nonlinearity of the form $f(\psi) = \frac{|\psi|^2\psi}{1+|\psi|^2}$. The focus of this thesis is on the different nonlinear Schrödinger equations — the Gross-Pitaevskii equation (GP) and the Landau-Lifshitz equation (LL), which are discussed in details in Chapters 3 and 4.

The structure of the nonlinear Schrödinger equation supports existence of solitary wave solutions. Aside from the traditional solitary wave solutions (solitons) one may also expect existence of solutions with a singular phase – *vortex solutions* with localized topological defects [9]. At a center of a vortex, the associated wave function has a nontrivial winding number. Although vortices are only local structures they dominate the geometry and topology of the flow. Their name is derived from a well-known analogy to fluid vortices [10]. Contrary to the fluid dynamics or superconductors setting, the experimental realization of such solutions in the context of NLS was demonstrated only quite recently (for Bose-Einstein condensates). The significance of vortices is underlined by the fact that they appear to be a key to understanding the underlying physics, particularly in the Ginzburg-Landau theory of superconductivity and in superfluidity.

The vortex phenomena in NLS and related equations is known in physics at least from the early 20th century. One of the first accounts related to the subject in the mathematics literature is due to P.L. Lions [11] who studied stationary solutions to a nonlinear wave equation

$$u_{tt} = \triangle u + f(u) \tag{2.4}$$

in two-dimensions of the form

$$u(r, \theta) = e^{im\theta} w(r)\,,$$

where (r, θ) are the polar coordinates in $\mathbb{R}^2$. The partial differential equation (2.4) then reduces to an ordinary differential equation

$$w'' + \frac{1}{r} w' - \frac{m^2}{r^2} w + f(w) = 0 \tag{2.5}$$

for an unknown real function $w(r)$. Such a solution has a topological singularity at the origin – the winding number of the field $u(x)$ around the origin equals m.

The systematic study of such solutions in the frame of NLS (and a corresponding nonlinear heat equation (NLH)) began in 1990 with the work of J.C. Neu [12]. He studied stationary solutions to NLS (and NLH) of the form

$$i\psi_t = -\triangle\psi - (1 - |\psi|^2)\psi$$

in two dimensions. He observed that except for the trivial uniform states $\psi = e^{i\theta_0}$ there are also solutions given by

$$\psi(x) = U(r) e^{i(n\theta + \theta_0)}\,.$$

The modulus $U(r)$ then satisfies the ordinary differential equation

$$U'' + \frac{1}{r} U' - \frac{n^2}{r^2} U + (1 - U^2)U = 0\,, \tag{2.6}$$

which is well-posed with the boundary conditions

$$U(0) = 0 \qquad \text{and} \qquad U(\infty) = 1\,. \tag{2.7}$$

He formally obtained a description of the asymptotic behavior of the solution $U(r)$ as $r \to 0$ and $r \to \infty$:

$$\begin{aligned} U(r) &\sim a r^{|n|} + O(r^{|n|+2}) \qquad \text{as } r \to 0, \\ &\sim 1 - \tfrac{n^2}{2r^2} + O\left(\tfrac{1}{r^4}\right) \qquad \text{as } r \to \infty. \end{aligned}$$

Although it was not particularly stated, the form of NLS equation considered implicitly implies that $\Psi(x)$ generates a stationary state solution to (2.2) of the form

$$\psi(x,t) = e^{i\omega t} e^{in\theta} U(r)\,, \tag{2.8}$$

for $\omega = -1$.

Any solution of the form (2.8) to NLS for an arbitrary ω gives rise to a traveling wave solution to the same equation by means of the *Galilean boost transformation*. Setting $u_n(x) = e^{in\theta}U(r)$ the traveling wave solution is given by

$$\psi(x,t) = \exp\left((i/2)(x\cdot v) - (i/4)|v|^2 t + it\omega + i\theta_0\right) u_n(x - vt - x_0)\,, \tag{2.9}$$

where $v \in \mathbb{R}^2$ is an arbitrary velocity.

2.1 Overview of existence and stability results

The significance of the problem spurred a broad and extensive investigations in the field of nonlinear Schrödinger equations. Here, only the mathematical results closely related to existence and stability of vortex solutions (or solutions with a similar structure) will be mentioned.

The first paper on vortices for NLS [12] focused on *stability* and interaction of vortex solutions. In the case of the nonlinear heat equation he gave a numerical evidence that solutions with topological degrees $n = 1$ and $n = -1$ are topologically stable and solutions with $|n| > 1$ tend to dissolve into vortices of a smaller degree. On the other hand, the dynamics of NLS due to the non-dissipative character of the equation remains an open problem.

In the broader context of *defects* the vortex solutions for both the Gross-Pitaevskii equation and the dissipative form of Landau-Lifshitz equation were studied by Pismen and Rubinstein [9]. Their analysis reveals that vortex solutions are only a special case of the more general defects. This connects the focus problems of this thesis with problems of interface dynamics in reaction-diffusion and Klein-Gordon equations.

A variational setting for a vortex in the scalar field was introduced by Weinstein [13]. The problem to overcome in the variational approach is that the energy of a vortex is infinite. Weinstein also precisely formulates questions regarding linear and nonlinear stability of a single vortex.

Existence of pure and encapsulated (exponentially localized) vortex solutions for various nonlinearities was proved by Iaia and Warchall [14, 15]. This particularly covers the cubic and cubic-quintic NLS. The argument is based on various ordinary differential equations techniques; many of them are similar to those used here in Chapter 4.

Linear stability of singly-quantized vortex solutions for cubic NLS was proved by Weinstein and Xin [16] using a simple argument based on a lemma of Pego and Weinstein [17].

The cubic-quintic problem was studied by Pego and Warchall [1] and Towers *et al.* [18]. Vortices of all degrees $|m| \geq 1$ (numerical evidence is given for $|m| = 1, \ldots, 5$) are found to be stable for a certain frequencies in the interval (ω_{cr}, ω_*) that shrinks with growing m, and unstable for frequencies outside of this interval. The upper bound ω_* is the same for all m's and is determined solely by the nonlinearity. The authors also pointed out that stability of $m = 0$ spinless ground states can be analyzed by the convenient criterion introduced by Grillakis, Shatah and Strauss [19].

Among other related results, stability and existence of so-called stationary bubble solutions was studied by A. De Bouard [20]. Bubble solutions have a boundary condition $\psi(x) \to 1$ as $|x| \to \infty$ and contrary to vortices, these solutions are real in the whole domain. De Bouard proved a sufficient condition for existence of stationary bubbles for a wide class of nonlinearities.

Chapter 3

Linear stability of vortices in Bose-Einstein condenstates

Since the experimental creation of Bose-Einstein Condensates (BEC) in alkali vapors in 1995 independently by groups of Cornell, Wieman and Ketterle [21, 22], BEC are one of the most active areas of modern condensed-matter physics, as it is demonstrated in numerous experimental and numerical results. BEC is in many ways an ideal system for scientific and technological exploration, since on the one hand they are rather well-characterized by theoretical models (mean-field theory), and on the other hand they are susceptible to optical and magnetic manipulation by a variety of sensitive techniques. A general overview of the subject can be found in Pethick [23] and Dafovo *et al.* [2].

In recent years, in numerous experiments at temperatures smaller than the critical condensation temperature, condensates confined in magnetic or optical traps and consisting of a large number of atoms in the same quantum state were created with almost 100% of the atoms in the condensed state. Such a high purity allows them to be described in the Hartree-Fock approximation by a single macroscopic wave function. This model leads to a nonlinear Schrödinger equation (NLS) with a non-local nonlinearity. A traditional simplification, replacing the non-local interaction potential with a localized short-range interaction propor-

tional to the delta function, leads to the Gross-Pitaevskii equation

$$i\hbar\psi_t = \left(-\frac{\hbar^2}{2M}\triangle + V(x) + i\hbar\Omega\partial_\theta + g|\psi|^2\right)\psi\,,$$

which is a nonlinear Schrödinger equation with a cubic (focusing or defocusing depending on whether the interaction is repulsive or attractive, respectively) nonlinearity and with a spatially dependent trap potential.

Mathematical results in this field are rare due to the strong nonlinearity and complexity of the system. The major development is the derivation of the Gross-Pitaevskii equation under various limits directly from many-body Schrödinger equations, and thus the justification of the model, which was proved in a series of papers of Lieb *et al.* [24, 25, 26]. On the other hand, the sketch of the proof of well-posedness of the Gross-Pitaevskii equation can be found in Jackson and Weinstein [27]. From the point of view of nonlinear waves, the interesting phenomena is that the structure of the Gross-Pitaevskii equation, similarly to some other nonlinear Schrödinger equations, supports existence of various types of solitary solutions, and particularly of vortex solutions. In the recent years, their presence and stability is extensively studied by both experimental and analytical means.

In the beginning of the experimental explorations of BEC, the goal was to create and detect vortices in the condensate. Nowadays, after large arrays of singly-quantized vortices have been created, one of the goals is to create a (stable) multi-quantized vortex, which can be possibly used to store a quantum information in the future. Results on stability of these vortices are very pertinent to experimentalists and in many cases they served as a guide for design of experiments. In general, two different concepts of stability are considered in literature, the energetic and linear stability. A solution is energetically stable if it mini-

mizes an associated energy functional within a class of functions satisfying some constraint. Unfortunately, most work on energetic stability is based only on a heuristic argument. Instead of minimizing the functional within a general class of functions, many other restrictions are imposed. The simplest approach where the minimization only goes through single vortex solutions with different charges reveals that a high enough trap rotation frequency can eventually stabilize a vortex of any degree [28]. On the other hand, the energy of a single multi-quantized vortex of charge m is larger that the energy of m singly-quantized vortices and thus multi-quantum vortices are believed to be unstable. The total energy in this case also depends on the relative location of vortices as they tend to form regular hexagonal arrays in harmonic traps.

A mathematical framework for a rigorous variational approach was discussed by Aftalion and Du [29]. Their method for effectively 2D condensates uses the method parallel to the Ginzburg-Landau theory of superconductors. In [30] the authors claim that a sufficiently fast rotation in combination with a strong pinning potential is capable to make even multi-quantum vortices energetically stable. Another heuristic energy argument suggests that for a trap rotation frequencies Ω bigger or equal to a critical angular velocity Ω_c (for which the centrifugal force balances the trapping potential) the condensate becomes unstable and spins out of a trap.

More rigorous analysis was conducted by Seiringer [31] where he studies when a vortex solution can be a global energy minimizer. He proves that for any $0 < \Omega < \Omega_c$ there exists N_Ω (independent of an interaction potential) such that all vortices with charge $m > N_\Omega$ are energetically unstable, i.e. they are not global minimizers (ground states) of the energy functional. Moreover, he proves that

all multi-quantized vortices, $m \geq 2$, become energetically unstable for a value of the chemical potential of the condensate large enough. Finally, he proves that symmetry breaking of the axi-symmetrical vortex solution is inevitable for any m, even for a singly-quantized vortex for a large enough interaction strength, since no ground state is an eigenfunction of the angular momentum. The symmetry breaking of the ground state is also demonstrated by a geometric analysis in [27] in the case of a double-well trapping potential.

Energetic stability should describe approximately the behavior after dissipation is introduced into the system. Such a concept may sometimes not be the most relevant because of the superfluid nature of BEC; instead one should rather study non-linear stability. On the other hand, ground states of the energy functional are nonlinearly orbitally Lyapunov stable, i.e. if the initial data are "close" to the ground state solution then the perturbed solution remains close to the ground state solution (in the same sense) for all times (see [27] and references therein).

On the other hand, nonlinear stability does not imply energetic stability. Therefore no conclusions on nonlinear instability can be inferred directly from considerations of the energy functional. Linear stability which properly describes the system behavior for a very short time can detect possible nonlinear instabilities by presence of eigenvalues in the right half-plane.

The linear stability of singly- and multi-quantized vortices was studied numerically by Pu *et al.* [5]. Similarly as in this thesis they describe the eigenvalues of the linearized Gross-Pitaevskii equation. They observe that the singly-quantized vortex is linearly stable, while the stability of $m = 2$ and $m = 3$ vortex depends on a parameter characterizing diluteness of the condensate. They also propose

a quantum-mechanical mechanism of transition to instability. Nevertheless, the numerical method used (finite elements) is completely different and a priori less reliable than the approach used here.

In [4] Garcia-Ripoll and Perez-Garcia use the same setting to study linear stability of a singly-quantized vortex but they restrict their search for instability only to the so-called *anomalous modes*. As pointed later in [32], these modes are not intrinsically unstable in that sense that some dissipation mechanism must be introduced into the system for them to become relevant. The numerical technique used in [4] relies on the Galerkin type approximation and Newton iteration. The finite temperature model generalization is further studied in [33].

Among the other related results, the instability of a vortex solution under a change of a shape of a trap for a weakly interacting condensate was studied in [34]. Deconinck and Kutz [35] numerically observed that the Gross-Pitaevskii equation (with a periodic trap potential) with a localized inter-particle interaction potential is not asymptotically equivalent to the same equation with a non-local interaction potential, i.e. stability of solutions is not preserved in the limit as non-local potential approaches the local one. Stability of various other solitary solutions (dark, bright, dark-in-bright, soliton vortices, etc.) other than vortices is discussed in [36, 37, 38].

In this work a robust numerical algorithm for finding a stationary-state vortex profile and its stability is designed and implemented. It makes use of the Evans function method originally proposed in [39] and further developed in [17]. This method proved to be a proper tool for detecting eigenvalues even in cases where other available methods failed and provides a justification of the finite element [5], Galerkin approximation [4], or finite difference approaches used before.

Particularly, the method here closely follows the approach of [1] for cubic–quintic nonlinear Schrödinger equation. Due to the robustness and high reliability of the method, this allows to describe in detail stability/instability parameter regimes far into the important Thomas-Fermi regime, corresponding to large numbers of particles and very dilute gas.

The Gross-Pitaevskii equations are rigorously "classically" linearized. The linearization procedure demonstrates why the perturbation must have the particular structure widely used in the literature (see [3], where a field-operator linearization is derived as well). The essential spectrum of the linearized operator is empty, which reduces the problem of linear stability to discrete spectrum. The linearized equation breaks into an infinite system of coupled pairs of equations for Fourier modes. Fortunately, only finitely many of them are relevant for possible instability. Moreover, the precise asymptotic description of the eigenfunctions is proved, which is necessary for construction of the Evans function used to detect presence and location of eigenvalues.

The numerical results presented here are consistent with all the previous results on energetic and linear stability; this is particularly true for [5]. The simply-quantized ($m = 1$) vortex is found linearly stable for any particle number and any trap rotation frequency. Stability of a multi-quantized $m = 2$ vortex depends on the interaction strength g and the particle number N. There is numerical evidence that the regions of stability and instability alternate with the growing parameter Ng. The presence of unstable eigenvalues for certain parameters is also justified by a direct evolution calculation based on the Strang splitting scheme recently proposed in [6].

3.1 The Gross-Pitaevskii equation

The behavior of low-temperature Bose-Einstein condensates (BEC) trapped in the harmonic potential $V(x)$ rotating with the angular velocity Ω about the z-axis is well described by the time-dependent Gross-Pitaevskii equation. The wave function $\psi(x,t)$ satisfies (in three dimensions)

$$i\hbar\psi_t = \left(-\frac{\hbar^2}{2M}\triangle + V(x) + i\hbar\Omega\partial_\theta + g|\psi|^2\right)\psi \tag{3.1}$$

with

$$\begin{aligned} V(x) &= V_{3D}(x) = \frac{1}{2}M\left(\omega_x^2x^2 + \omega_y^2y^2 + \omega_z^2z^2\right), \\ g &= g_{3D} = \frac{4\pi\hbar^2a}{M}, \end{aligned}$$

where g is the interaction strength, M is the atomic mass of atoms in the condensate, a is the s-wave scattering length [26] and θ is an azimuthal angle in cylindrical coordinates. The term $\Omega\partial_\theta$ corresponds to the angular momentum $\mathbf{\Omega}\cdot(\mathbf{r}\times\nabla)$ of the condensate caused by a rotating frame of coordinates. The total number of particles in the condensate N is given by the integral

$$\int_{\mathbb{R}^3}|\psi|^2dx^3 = N, \tag{3.2}$$

and is conserved during the evolution of the system. For disc-shaped (pancake) traps ($\omega_z^2 >> \omega_x^2$, $\omega_z^2 >> \omega_y^2$) it was recently justified [6] that the system is well approximated by a planar two-dimensional reduced model. The equation (3.1) formally does not change, one only needs to set

$$\begin{aligned} V(x) &= V_{2D}(x) = \frac{1}{2}M\omega_{tr}^2\left(x^2 + \lambda_{tr}^2y^2\right), \\ g &= g_{2D} = g_{3D}\cdot\left(\frac{M\omega_z}{2\pi\hbar}\right)^{1/2}, \end{aligned}$$

where $\omega_x = \omega_{tr}$ and $\omega_y = \omega_{tr}\lambda_{tr}$. For purpose of numerical investigations in this work the same values of parameters were used as in [5]: a condensate consisting of atoms of ^{23}Na is considered with $a = 2.75$ nm, $\omega_z = 2\pi \times 200$ Hz, $\omega_{tr} = 2\pi \times 10$ Hz ($\omega_z >> \omega_{tr}$), $M = 10^{-26}$ kg and the Planck constant $\hbar = 6.6261 \times 10^{-34} Js$. A similar set of parameters used in the experiment (as cited in [30, 40]) with a ^{87}Rb condensate is: $M = 3.81 \times 10^{-26}$ kg, $a = 5.77\,\text{nm}$, $\omega = \omega_z = \omega_{tr} = 2\pi \times 200\,\text{Hz}$. In these experiments the number of particles was approximately $N = 2 \times 10^5$, horizontal and vertical condensate sizes were $R = 20$ μm, $L = 10$ μm and the temperature $T_c = 1$ μK. Both ^{23}Na and ^{87}Rb represent alkali gases with a repulsive interaction potential. As an example of an attractive interaction ^{7}Li with $a = -1.45$ nm can serve. Note that the parameter a can be tuned via Feshbach resonance [41].

There appear to be two important scalings of time, length and magnitude of the wave function. First, setting

$$t = (1/\omega_{tr})\, t'\,, \qquad x = \sqrt{\hbar/M\omega_{tr}}\, x'\,, \quad \psi = \sqrt{NM\omega_{tr}/\hbar}\,\psi'$$

(i.e. time is measured relatively to the frequency of rotation of the trap and distance is measured relatively to the size of the trap) leads to (dropping the primes)

$$i\psi_t = -\frac{1}{2}\triangle\psi + \frac{1}{2}(x^2 + \lambda_{tr}^2 y^2)\psi + i\Omega_{rel}\psi_\theta + U|\psi|^2\psi \tag{3.3}$$

with

$$\int_{\mathbb{R}^2} |\psi|^2 dx^2 = 1\,, \tag{3.4}$$

where $\Omega_{rel} = \Omega/\omega_{tr}$ and $U = gNM/\hbar^2$. In this scaling the energy functional is given by

$$E(\psi) = \int_{\mathbb{R}^2} \frac{1}{2}|\nabla\psi|^2 - i\Omega\overline{\psi}\partial_\theta\psi + \left(\frac{1}{2}(x^2 + \lambda_{tr}^2 y^2) + U|\psi|^2\right)|\psi|^2 dx^2\,. \tag{3.5}$$

This scaling is very suitable and was widely used for investigations of energetic stability since a ground state of (3.3)–(3.4) can be obtained by solving the minimization problem for the energy functional (3.5) with respect to a fixed constrain (3.4).

On the other hand, setting

$$t = (1/\omega_{tr})\, t' \,, \qquad x = \sqrt{\hbar/M\omega_{tr}}\, x' \,, \quad \psi = \sqrt{\hbar\omega_{tr}/|g|}\, \psi'$$

yields (dropping the primes)

$$i\psi_t = -\frac{1}{2}\triangle\psi + \frac{1}{2}(x^2 + \lambda_{tr}^2 y^2)\psi + i\Omega_{rel}\psi_\theta + \frac{g}{|g|}|\psi|^2\psi \tag{3.6}$$

with

$$\int_{\mathbb{R}^2} |\psi|^2 dx^2 = K \,, \tag{3.7}$$

where $\Omega_{rel} = \Omega/\omega_{tr}$ and $K = |g|NM/\hbar^2 \geq 0$. Note that the scaling of time and space is the same as in the first scaling. The energy functional (3.5) is the same as in the first scaling with U replaced by $g/|g|$.

In this work the following assumptions will be made. Only two-dimensional radial wave functions of the form $\psi = \psi(r, \theta)$ will be considered. The relative trap frequency Ω_{rel} will be for simplicity denoted by Ω. One usually studies the case $0 < \Omega_{rel} < 1$ since the physical intuition suggests that $\Omega_{rel} \geq 1$ destabilizes the condensate. For such frequencies the centrifugal force dominates the trapping potential and all the particles eventually spiral out of the trap. Nevertheless, such a restriction is not in agreement with current experiments [42] and does not influence eigenvalues (discrete spectrum) of the linearized problem as it will be proved later. Nevertheless, the assumption $\Omega_{rel} < 1$ will be needed to properly define the linearized operator and to determine its essential spectrum. This issue will be further discussed in the summary. On the other hand, the method

used here only deals with a case of a disc trap, $\lambda_{tr} = 1$. However, it can be conjectured that the qualitative behavior (stability/instability) should be to some extent preserved also for elongated traps. Moreover, the model includes both attractive and repulsive interaction inter-particle potential (sign of the nonlinear term) but for simplicity only the case of repulsive potential will be considered here (questions concerning stability in transition between repulsive and attractive potential via Feshbach resonance will be a subject of future investigations; some results can be found in [5]).

Under these assumptions (3.6) has the form

$$\begin{aligned} i\psi_t(t,r,\theta) &= -\frac{1}{2}\triangle\psi(t,r,\theta) + \frac{1}{2}r^2\psi(t,r,\theta) + i\Omega\psi_\theta(t,r,\theta) \\ &\quad +|\psi(t,r,\theta)|^2\psi(t,r,\theta) \end{aligned} \tag{3.8}$$

with

$$\int_0^\infty \int_0^{2\pi} |\psi(r,\theta)|^2 r d\theta dr = K \tag{3.9}$$

and the energy functional (3.5) for a stationary solution ψ (minimizer of energy) satisfies

$$E(\psi) = \mu K - \frac{1}{2}\int_{\mathbb{R}^2} |\psi|^4 dx^2 \,.$$

Note that the Thomas-Fermi regime [10, 26] $Na/d_0 >> 1$ (here d_0 is the mean oscillator length, $d_0 = \sqrt{\hbar/M\omega_0}$ and ω_0 is the mean trap frequency $\omega_0^3 = \omega_x\omega_y\omega_z$), corresponds to $K \to \infty$ since $K = 2|a|N\sqrt{2\pi M\omega_z/\hbar}$, i.e.

$$K = \frac{N|a|}{d_0} 2\sqrt{2\pi}\left(\frac{\omega_{tr}}{\omega_z}\right)^{1/3} . \tag{3.10}$$

This is the limit under which Lieb and Seiringer [26] justified the Gross-Pitaevskii energy functional to be a good approximation for the N-body quantum system.

Note, that the only two free parameters which stay in (3.8)–(3.9) are K, the L^2-norm of the wave function ψ, and Ω, the relative angular velocity of the trap.

Also note, that the Galilean boost (2.9) does not produce solutions to the Gross-Pitaevskii equation since the equation is not translationally invariant. Instead, there is a different boost introduced in [43]. For any solution $\psi(x)$, to (3.8) this transformation gives rise to a family of solutions to the same equation. For simplicity, only a non-rotating case is presented here, the generalization to rotating traps can be found in [43]. The transformation has the form

$$\Psi_R(x,t) = \Psi(x - R(t), t)e^{i\theta(x,t)}\,, \tag{3.11}$$

where $R(t)$ solves the harmonic oscillator equation

$$R_{tt}(t) = -R(t) \qquad \text{and} \qquad \theta(x,t) = x \cdot R_t + f(t)\,,$$

where $f(t) = \int_0^t (R_t \cdot R_t - R \cdot R)\, dt$.

3.2 Vortex solutions

The Gross-Pitaevskii equation has the structure of the nonlinear Schrödinger equation and therefore one may expect the presence of vortex solutions of the general form

$$\psi(r,\theta,t) = e^{i(-\mu t + m\theta)}w(r)\,, \tag{3.12}$$

where m is a vortex degree (or charge) and μ is a non-dimensional parameter corresponding to frequency or chemical potential ($\mu > 0$). In BEC it is plausible to search for localized vortices with

$$w(0) = 0 \qquad \text{and} \qquad w(\infty) = 0 \tag{3.13}$$

due to the influence of the trapping potential. The radial profile function $w(r)$ then satisfies

$$w_{rr} + \frac{1}{r}w_r - \frac{m^2}{r^2}w + 2(m\Omega + \mu)w - r^2 w - 2|w|^2 w = 0\,. \tag{3.14}$$

Since the dependence of a solution on parameters Ω and μ is solely through the profile parameter $p = m\Omega+\mu$, it is possible to restrict the search to stationary traps:

$$w_{rr} + \frac{1}{r}w_r - \frac{m^2}{r^2}w + 2pw - r^2w - 2|w|^2w = 0\,. \tag{3.15}$$

Since the equation (3.8) is written in the rotating frame of coordinates, any fixed parameter p represents a fixed parameter μ relative to a fixed observer (lab frame). Therefore the profile shape can be considered independent of the trap rotation frequency Ω. On the other hand, the stability of solutions for a fixed parameter p may, in general, depend on Ω.

The asymptotic behavior of a vortex profile can be determined directly from (3.15). It is not difficult to see that as $r \to 0^+$ the equation has the same character as the linear Schrödinger equation and

$$w(r) \sim r^m \quad \text{for } m \geq 1.$$

As $r \to \infty$, the nonlinear term for an exponentially localized solution becomes negligible and the linear Schrödinger equation with a potential is a good approximation:

$$w_{rr} + \frac{1}{r}w_r - \frac{m^2}{r^2}w + 2pw - r^2w = 0\,. \tag{3.16}$$

The proof of a statement that the positive solution $w(r)$ to (3.15) approaching 0 as $r \to \infty$ satisfies $w(t) = O(r^p e^{-r^2/2})$ is given in Appendix E. Other properties of a vortex profile satisfying (3.13), (3.15) are summarized and proved in Appendix B.

The goal of this chapter is to study linear stability of solutions to (3.15). Naturally, it is crucial to obtain very precise numerical solutions of (3.15) first.

The approach used here is based on path-following of a bifurcating branch out of the trivial solution $w = 0$ and is similar to the one used in [3]. It requires

some information about the localized solutions to (3.16). This equation has two independent general solutions — products of a polynomial, a decaying Gaussian and a confluent hypergeometric function. The exact solutions are

$$\begin{aligned} w_{(1)}(r) &= r^m e^{-r^2/2} M\left(\frac{m}{2}+\frac{1-p}{2}, m+1, r^2\right), \\ w_{(2)}(r) &= r^m e^{-r^2/2} U\left(\frac{m}{2}+\frac{1-p}{2}, m+1, r^2\right). \end{aligned}$$

The confluent hypergeometric functions $M(a,b,x)$ and $U(a,b,x)$ are, in general, independent solutions to $xf''+(b-x)f'-af=0$ [44]. Their asymptotics as $r\to\infty$ yields

$$w_{(1)}(r)\sim r^p e^{r^2/2}, \qquad w_{(2)}(r)\sim r^p e^{-r^2/2},$$

and the Wronskian of $w_{(1)}(r)$ and $w_{(2)}(r)$ is given by

$$W(w_{(1)},w_{(2)}) = -\frac{\Gamma(m+1)}{\Gamma(\frac{m}{2}+\frac{1-p}{2})r^2}. \tag{3.17}$$

The only possibility for $w_{(1)}(r)$ (and similarly for $w_{(2)}(r)$) to satisfy the boundary conditions at both ends is when the Wronskian (3.17) vanishes. This happens if $|\Gamma(m/2+(1-p)/2)|=\infty$, so $m/2+(1-p)/2=-n$, n a nonnegative integer. Therefore a non-trivial solution $w_n(r)$ to (3.16) approaching zero as $r\to 0^+$ and as $r\to\infty$ exists for $p=p_n$, where

$$p_n = m+1+2n. \tag{3.18}$$

In that case both solutions $w_{(1)}(r)$ and $w_{(2)}(r)$ reduce to the single solution $w_n(r) = r^m e^{-r^2/2} L_n^{(m)}(r^2)$, where $L_n^{(m)}(r)$ is the generalized Laguerre polynomial with n the number of zeros of $L_n^{(m)}(r)$ for $r>0$. The non-negative solution (the ground state of the associated energy functional) corresponds to $n=0$, $p_0=m+1$ and $w=w_0$.

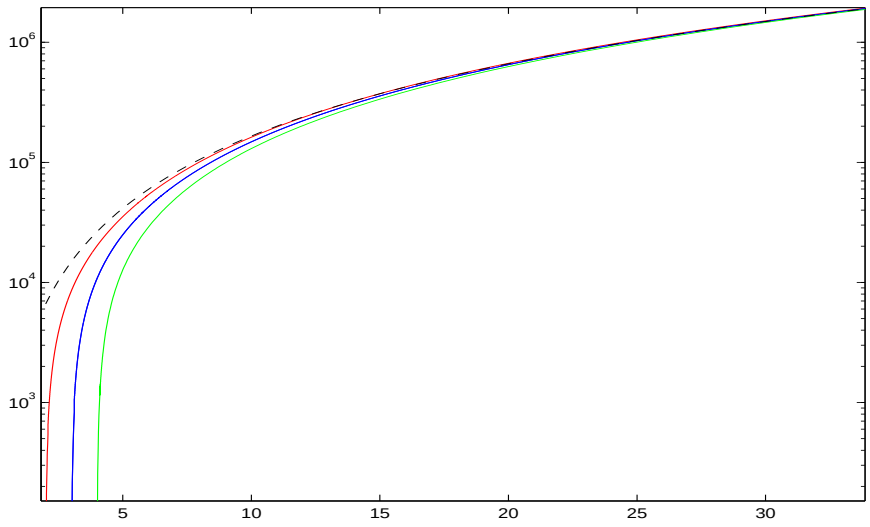

(a)

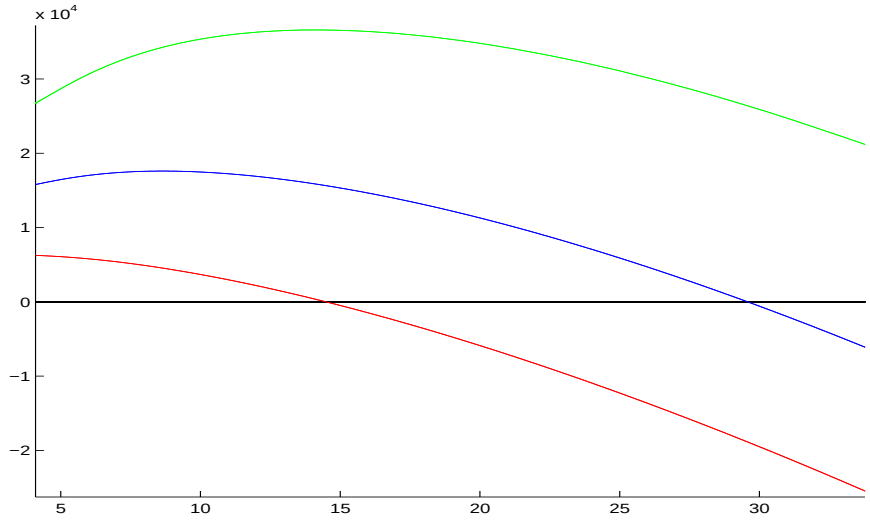

(b)

Figure 3.1: (a) ($\log N$ vs. p) plot of branches of vortex solutions for $m = 1, 2, 3$ (from left to right) emerging at $p_0 = m+1$ for ^{23}Na data. Dashed curve represents the number of particles for $w_{tf}(r) = \sqrt{p_0 - r^2/2}$ in the Thomas-Fermi regime. (b) The difference between the number of particles of vortex solutions for $m = 1, 2, 3$ and number of particles of w_{tf}. The number of particles increases with m.

The numerical algorithm designed to find solutions to (3.15) is based on the following observation. It is reasonable to expect that introduction of the nonlinear term leads to the existence of a solution branch $(p(s), w_p(s))$ bifurcating from the trivial solution $w = 0$ for $p = p_0$. To justify such a behavior one can use the Crandall-Rabinowitz theorem [45] (details can be found in Appendix A).

Theorem 3.2.1. *The solutions* (w_p, p), $p = m\Omega + \mu$, *to (3.15) near* $(0, p_0)$, $p_0 = m + 1$, *form a curve*

$$(p(s), w(s)) = (\tau(s), sw_0 + sz(s)),$$

where $s \to (\tau(s), z(s)) \in \mathbb{R} \times span\{w_0\}^{\perp}$ *is a continuously differentiable near* $s = 0$, $\tau(0) = \tau'(0) = 0$, $z(0) = 0$ *and*

$$\begin{aligned} w(s) \in X &= \{w : w \in L^2(\mathbb{R}, \mathbb{R}; r), e^{im\theta} w(r) \in \mathcal{H}\}, \\ \mathcal{H} &= \{u : u \in H^2(\mathbb{R}^2, \mathbb{R}^2), (x^2 + y^2)u \in L^2(\mathbb{R}^2, \mathbb{R}^2)\}. \end{aligned}$$

Hence it is possible to numerically trace the solution curve (p, w_p) from the branching point $(p_0, 0)$, see Fig. 3.1 (a). The behavior of norms relatively to the norm of the pure Thomas-Fermi regime is illustrated on Fig. 3.1 (b). The first point on the approximate solution curve is set to be $(p_0, \varepsilon w_0)$ which is by the Crandall-Rabinowitz theorem an $O(\varepsilon^2)$ approximation of the exact solution. Then an implementation of a predictor-corrector algorithm [46] is used to get solutions for large values of the parameter p. Since a further stability study will require evaluations of the profile values at any given point within the computational domain, the precision of calculations is improved by optimizing the already calculated profile for any given p by a multiple shooting procedure [47] with a very

small tolerance. This allows to achieve high precision in evaluations of $w(r)$ by simple integration from a nearby mesh point. Note, that the calculation is almost independent of the size of the parameter p since the size of the computational domain, and so the number of necessary nodes, grows very slowly. Therefore it is possible to reach large values of p. Also note, that with the growing parameter p, L^2-norm (3.10) of profiles grows (Fig. 3.1) and hence states far in the physically interesting Thomas-Fermi regime ($Na/d >> 1$) for a wide range of p's are obtained for a small computational cost. On the other hand, for a computation for a single value of p this method has a significant overhead. A similar method was also used in [3].

3.3 Linear stability

The goal of this section is to obtain a proper mathematical formulation of the linearization of (3.15) around solutions constructed in the previous section – localized vortex profiles. The derived equations have the same form as the Bogoliubov equations [23, 3] commonly used in physics literature. Note that the analogy between the derivation here and the usual derivation of the Bogoliubov equations is by no means straightforward (this issue will be addressed in more details later in the section).

A small general perturbation of the vortex solution $\psi(t, r, \theta) = e^{i(-\mu t + m\theta)} w(r)$, where $w(r) = w_p(r)$ for a fixed parameter p, has the form

$$u(t, r, \theta) = e^{-i\mu t} \left(e^{im\theta} w(r) + \varepsilon v(t, r, \theta) \right) .$$

Neglecting the higher order nonlinear terms in (3.8) yields

$$iv_t = -\frac{1}{2} \triangle v + i\Omega \partial_\theta v - \mu v + \frac{1}{2} r^2 v + 2|w|^2 v + |w|^2 e^{2im\theta} \overline{v} \, . \tag{3.19}$$

The complex character of the equation (3.19) significantly complicates the analysis. Therefore, decompose the complex wave function v as

$$\Phi = \begin{pmatrix} \Phi_1 \\ \Phi_2 \end{pmatrix} = \begin{pmatrix} \text{Re } v \\ \text{Im } v \end{pmatrix} .$$

The equation (3.19) is then equivalent to the real system

$$\partial_t \Phi = A\Phi = J\left[\frac{1}{2}\triangle - J\Omega\partial_\theta - \left(\frac{1}{2}r^2 - \mu + 2|w|^2\right) - |w|^2 e^{2m\theta J} R\right]\Phi\,, \qquad (3.20)$$

where

$$J = \begin{pmatrix} 0 & -1 \\ 1 & 0 \end{pmatrix} \qquad \text{and} \qquad R = \begin{pmatrix} 1 & 0 \\ 0 & -1 \end{pmatrix} .$$

To determine the linear stability of the vortex solution ϕ one needs to study the spectrum of the operator A as an unbounded operator $D(A) \to L^2(\mathbb{R}^2, \mathbb{R}^2)$.

The precise definition of the operator A is somewhat involved and requires the concept of a quadratic form [49]. Denote (for now only formally)

$$L_c = -\frac{1}{2}\triangle + \frac{1}{2}r^2 I + J\Omega\partial_\theta\,, \qquad L_w = 2|w|^2 I + |w|^2 e^{2m\theta J} R - \mu\,,$$

where I is the 2×2 identity matrix. Then

$$A = -J(L_c + L_w)\,.$$

Then define a quadratic map

$$q_{Lc} : D(q) = \left(H^1(\mathbb{R}^2, \mathbb{R}^2) \cap L^2(\mathbb{R}^2, \mathbb{R}^2; r^2 dr)\right) \to \mathbb{C}$$

by

$$q_{Lc}(\Psi, \Psi) = \int_0^{2\pi}\int_0^{\infty}\left[\frac{1}{2}|\nabla\Psi|^2 + \frac{r^2}{2}|\Psi|^2 + J\Omega(r \times \nabla\Psi)\cdot\Psi\right] r dr d\theta\,.$$

Here $L^2(\mathbb{R}^2, \mathbb{R}^2; f(r)dr)$ represents the space of functions $\Psi : \mathbb{R}^2 \to \mathbb{R}^2$ with the bounded norm

$$||\Psi||^2_{L^2(\mathbb{R}^2,\mathbb{R}^2;f(r)dr)} = \int_0^{2\pi} \int_0^{\infty} |\Psi|^2(r) f(r) r dr d\theta \,.$$

Then for $0 \leq \Omega < 1$ the quadratic form q_{Lc} is semibounded (details can be found in Appendix C):

$$q_{Lc}(\Psi, \Psi) \geq 0 \,.$$

Note that the space $D(q) = H^1(\mathbb{R}^2, \mathbb{R}^2) \cap L^2(\mathbb{R}^2, \mathbb{R}^2; r^2 dr)$ is dense in $L^2(\mathbb{R}^2, \mathbb{R}^2)$ since the Schwartz space is a subset of $D(q)$ and is dense in $L^2(\mathbb{R}^2, \mathbb{R}^2)$. The quadratic form q_{Lc} is closed if it has a closed graph, i.e. if $D(q)$ is complete under the graph norm $||\Psi||_{+1} = \sqrt{q_{Lc}(\Psi, \Psi) + ||\Psi||^2_{L^2}}$. This is true since both H^1 and $L^2(r^2 dr)$ can be obtained from L^2 by completing the space C_0^∞ functions under the H^1 and $L^2(r^2 dr)$ norms respectively. Also it is necessary to observe that for $0 \leq \Omega < 1$:

$$C\left(||\Psi||^2_{H^1} + ||\Psi||^2_{L^2(r^2dr)}\right) \geq q_{Lc}(\Psi, \Psi) + ||\Psi||^2_{L^2} \geq c\left(||\Psi||^2_{H^1} + ||\Psi||^2_{L^2(r^2dr)}\right)$$

for some $C > c > 0$ (the lower bound follows from the semiboudedness, the proof of the upper bound is analogous). Then Theorem VIII.15, pp. 278 of [49] claims that q_{Lc} is the quadratic form of a unique self-adjoint operator L_c. The domain of the operator L_c denoted by $D(L_c)$ is dense in L^2, also clearly $H^2(\mathbb{R}^2, \mathbb{R}^2) \cap L^2(\mathbb{R}^2, \mathbb{R}^2; r^2 dr) \subset D(L_c)$ and

$$L_c \Psi = \left(-\frac{1}{2}\triangle + \frac{1}{2} r^2 I + J\Omega\partial_\theta\right)\Psi \,,$$

for $\Psi \in D(L_c)$ in the sense of distributions.

It is easy to see that the operator $L_w : L^2(\mathbb{R}^2, \mathbb{R}^2) \to L^2(\mathbb{R}^2, \mathbb{R}^2)$ can be defined as

$$L_w \Psi = 2|w|^2 \Psi + |w|^2 e^{2m\theta J} R\Psi - \mu\Psi \,,$$

and is bounded. Therefore the operator $A = -J(L_c + L_w)$ with the domain $D(A) = D(L_c)$ is densely defined in $L^2(\mathbb{R}^2, \mathbb{R}^2)$.

The essential spectrum of the operator A is empty, as stated in the next theorem.

Theorem 3.3.1. *For any m, μ and for $0 \leq \Omega < 1$ the essential spectrum of the operator A is empty, $\sigma_{ess}(A) = \emptyset$, i.e. spectrum of A consists of its eigenvalues.*

The proof of the Theorem 3.3.1 is in Appendix C. Unfortunately, it is not clear whether the essential spectrum is empty also for $\Omega \geq 1$.

If λ is an eigenvalue of the operator A, it satisfies

$$A\Phi = \lambda\Phi \tag{3.21}$$

which can be rewritten as

$$\left[\lambda J + \frac{1}{2}\triangle - J\Omega\partial_\theta - \left(\frac{1}{2}r^2 - \mu - 2|w|^2\right)\right]\Phi + |w|^2 e^{2m\theta J} R\Phi = 0\,. \tag{3.22}$$

Similarly as in [1] it is useful to represent (3.22) in the basis of the eigenvectors of the matrix J:

$$\Phi = \Phi_+ \begin{pmatrix} 1/2 \\ -i/2 \end{pmatrix} + \Phi_- \begin{pmatrix} 1/2 \\ i/2 \end{pmatrix}\,.$$

Since $D(A) \subset L^2(\mathbb{R}^2, \mathbb{R}^2)$, then $\Phi_\pm \in L^2(\mathbb{R}^2, \mathbb{C})$. Consequently, (3.22) has the form

$$\left(i\lambda + \frac{1}{2}\triangle - i\Omega\partial_\theta - \frac{1}{2}r^2 + \mu - 2|w|^2\right)\Phi_+ - |w|^2 e^{2im\theta}\Phi_- = 0\,, \tag{3.23}$$

$$\left(-i\lambda + \frac{1}{2}\triangle + i\Omega\partial_\theta - \frac{1}{2}r^2 + \mu - 2|w|^2\right)\Phi_- - |w|^2 e^{-2im\theta}\Phi_+ = 0\,. \tag{3.24}$$

One can deduce by a simple bootstrap argument that $\Phi_\pm \in H^m_{loc}$ for each $m > 0$, so $\Phi_\pm \in C^\infty(\mathbb{R}^2, \mathbb{C}) \cap L^2(\mathbb{R}^2, \mathbb{C}) = C^\infty(\mathbb{R}^2, \mathbb{R}^2) \cap L^2(\mathbb{R}^2, \mathbb{R}^2)$.

The system (3.23)–(3.24) has the same form as the *Bogoliubov linearized system* [23]. Although the Bogoliubov equations are a widely accepted model in the physics literature, a connection between the "classical" linearization treatment used here and the process of "linearization" used in the derivation of the Bogoliubov system is unclear.

The usual procedure starts with a Hamiltonian formulation using the formalism of the second quantization, namely the so-called *field operator*. The first approximation used in this process is considering ladder operators of the associated operator algebra as N-dependent constant multipliers. In this formalism the field operator is approximated by a "large" ground-state part and a "small" reminder representing excited states. Such a decomposition is then inserted into the Hamiltonian. The second approximation comes when in the expansion of the Hamiltonian (in the small correction remainder) only terms up to quadratic order are retained. A diagonalization procedure transforms the system into a form equivalent with the linearization obtained here.

It is important to emphasize that the derivation in the physical literature is on a formal level and its justification is unclear. Nevertheless, the result obtained this way is in a perfect agreement with the rigorous approach here. It would be particularly interesting to understand what assumptions in the mathematical derivation correspond to the ladder-operator approximation. Although this "classical" approach is not new, it gives the reasoning behind the particular choice of the perturbation used in [2] and [3].

To find the eigenvalues of (3.22), further decompose $\Phi_\pm(r,\theta)$ at each fixed r into Fourier modes (with shifted indices for a notational ease)

$$\Phi_\pm(r,\theta) = \sum_{j=-\infty}^{\infty} e^{i(j\pm m)\theta} y_\pm^{(j\pm m)}(r)\,. \tag{3.25}$$

After the introduction of the Fourier modes the equation (3.22) transforms to an infinite-dimensional system of linear equations.

The system decouples to coupled pairs for unknown nodes $y_+ = y_+^{(j+m)}, y_- = y_-^{(j-m)}$ (note that $p = m\Omega + \mu$):

$$\left[i\lambda + \frac{1}{2}\triangle_r - \frac{(j+m)^2}{2r^2} - \frac{1}{2}r^2 + (p + j\Omega) - 2|w|^2\right] y_+ = |w|^2 y_- \quad (3.26)$$

$$\left[-i\lambda + \frac{1}{2}\triangle_r - \frac{(j-m)^2}{2r^2} - \frac{1}{2}r^2 + (p - j\Omega) - 2|w|^2\right] y_- = |w|^2 y_+ \quad (3.27)$$

with appropriate boundary conditions

$$\lim_{r\to 0^+} y_\pm(r) \quad \text{exists} \qquad \text{and} \qquad \lim_{r\to\infty} y_\pm(r) = 0\,. \quad (3.28)$$

By the symbol $\triangle_r$ we denote the radial Laplace operator $\triangle_r = \frac{\partial^2}{\partial r^2} + \frac{1}{r}\frac{\partial}{\partial r}$.

Finally, the eigenproblem (3.21) is decomposed into countable many problems

$$L_j y - j\Omega R y = i\lambda R y\,, \qquad y = (y_+, y_-)^T\,, \quad (3.29)$$

where

$$L_j = \begin{pmatrix} L_j^+ - p & 0 \\ 0 & L_j^- - p \end{pmatrix} + |w|^2 \begin{pmatrix} 2 & 1 \\ 1 & 2 \end{pmatrix}\,,$$

and

$$L_j^+ = -\frac{1}{2}\triangle_r + \frac{(j+m)^2}{2r^2} + \frac{1}{2}r^2\,,$$
$$L_j^- = -\frac{1}{2}\triangle_r + \frac{(j-m)^2}{2r^2} + \frac{1}{2}r^2\,.$$

Similarly as before the bootstrap argument gives $y \in C^\infty \cap L^2(\mathbb{R}^+, \mathbb{C}^2; rdr)$. The associated inner product is given by

$$\langle y, z\rangle = \int_0^\infty \left(y_+(r)\overline{z_+(r)} + y_-(r)\overline{z_-(r)}\right) rdr\,.$$

The next theorem summarizes the results of this section.

Theorem 3.3.2. *A complex number λ is an eigenvalue of A if and only if for some integer j the system of equations (3.29) have a nontrivial solution satisfying (3.28). An eigenfunction associated with an eigenvalue λ has the form*

$$v_{\lambda,j,m}(x,t) = Ce^{\lambda t}e^{i(j+m)\theta}y_+^{(j+m)}(r) + \overline{Ce^{\lambda t}e^{i(j-m)\theta}y_-^{(j-m)}(r)}\,.$$

The "only if" part of the statement of the theorem was already proved in this section. The reverse implication can be proved analogously as the parallel theorem in [1].

3.3.1 Reduction to non-rotating traps

The structure of the system of equations (3.29) allows to determine the location of eigenvalues for rotating traps ($\Omega \neq 0$) directly from the eigenvalues for stationary traps ($\Omega = 0$).

Lemma 3.3.3. *There is an one-to-one correspondence between the eigenvalues λ_Ω of the operator A corresponding to the mode j and trap frequency Ω and the eigenvalues of A corresponding to the mode j and zero frequency which is given by*

$$\lambda_\Omega = \lambda_0 + j\Omega i\,.$$

The claim immediately follows from (3.29) since if

$$i\lambda_0 = i\lambda_\Omega + j\Omega \tag{3.30}$$

then λ_0 is an eigenvalue of the reduced problem

$$L_j y = i\lambda_0 R y\,, \tag{3.31}$$

which is independent of Ω. The relation (3.30) reveals that $\lambda_\Omega = \lambda_0 + ij\Omega$, i.e. λ_Ω and λ_0 have the same real part. Therefore any linear instability of the vortex solution in a rotating trap caused by the existence of an eigenvalue with a nontrivial real part must be present also in a stationary trap.

3.3.2 Bounds for eigenvalues

At a first glance it may seem impossible to solve infinitely many systems of the form (3.29). Fortunately, it is not necessary, as stated in the next proposition (the proof is included in Appendix D and is the same as in [4]).

Proposition 3.3.4. *The unstable eigenvalues of the problem (3.21) must be solutions of (3.28)–(3.29) for j satisfying*

$$|j| \leq 2m\,. \tag{3.32}$$

One can also prove the following estimate (the proof is also included in Appendix D).

Proposition 3.3.5. *The real part of every eigenvalue of the the operator A (3.21) is bounded with*

$$|\Re\lambda| < 3 \max_{r>0} |w(r)|^2 < \infty\,. \tag{3.33}$$

Both propositions restrict the search for unstable eigenvalues to a finite number of equations and to a vertical strip. Unfortunately, it is not clear how to obtain any bound for the imaginary part of the possible unstable eigenvalues. Since one can expect infinitely many stable eigenvalues in both directions on the

imaginary axis it is hopeless to prove that the imaginary part of an eigenvalue is bounded.

Nevertheless, the possible number of unstable eigenvalues is limited. To explain in detail a way to obtain an upper bound for the number of unstable eigenvalues, set $\hat{J} = -iR$. The equation (3.31) reduces to

$$\hat{J}L_j y = \lambda_0 y\,, \tag{3.34}$$

where $\hat{J}$ is skew-symmetric ($\hat{J}^2 = -I$) and L_j is self-adjoint. The number of unstable eigenvalues in the right-half plane ($\Re\lambda > 0$) is then limited by the number of the negative eigenvalues of the self-adjoint operator L_j [17, 50]. This explains the observation of Pu *et al.* [5] that the instability for $m \geq 2$ appears when L_j is an indefinite operator. On the other hand, the indefiniteness of L_j does not guarantee the instability of $\hat{J}L_j$; the connection between the spectra of L_j and $\hat{J}L_j$ is more involved.

Moreover, there is also a way how to justify that there are no other unstable eigenvalues and how to reduce the computational cost significantly. The key is to take into account also the Krein signature of the eigenvalues [50].

For simplicity assume that all the eigenvalues of $\hat{J}L_j$ are simple. The total number of the negative eigenvalues (counting multiplicities) of L_j is equal to the number of negative directions in the indefinite metric space with the indefinite metric given by the Krein signature $\langle L_j\Psi, \Psi\rangle$ and the non-negative inner product given by $\langle |L_j|\Psi, \Psi\rangle$. A simple observation reveals, that the unstable eigenvalues of $\hat{J}L_j$ have zero Krein signature, and so each pair of eigenvalues symmetric with respect to the imaginary axis represents one negative direction in the indefinite space. But there are also possible stable eigenvalues on the imaginary axis with the negative Krein signature.

Therefore, a possible numerical justification that there are no other unstable eigenvalues could be the following. First, determine the number n_{total} of negative eigenvalues of L_j. If the number is zero, there are no unstable eigenvalues of $\hat{J}L_j$. If $n_{total} > 0$, the number gives the total number n_u of pairs of unstable eigenvalues of $\hat{J}L_j$ plus the number n_s of stable eigenvalues with the negative Krein signature. If the present method (the Evans function technique) detects the presence of the same number of pairs of eigenvalues off the imaginary axis $n_u = n_{total}$, there are no other unstable eigenvalues. If $n_u < n_{total}$, perform a calculation of the Krein signature for eigenvalues on the imaginary axis. If $n_u + n_s = n_{total}$ there are no other unstable eigenvalues, otherwise, increase the area of search and repeat the whole process.

Since the numerical results suggest patterns in the behavior of the eigenvalues, this would also allow to reduce the computations even more. If n_{total} is known, one only needs to find stable eigenvalues of $\hat{J}L_j$ on imaginary axis within a reasonable interval and their Krein signatures. Only if their total number differs from n_{total}, i.e. $n_s < n_{total}$, a search off the imaginary axis is necessary. As pointed by Sandstede *et al.* [50], a deeper breakthrough would be if one could detect the Krein signature directly from the Evans function. These issues are subject to further investigations by the author.

3.3.3 Special eigenvalues

The symmetries of the Gross-Pitaevskii equation and its linearization and boosts of the solutions imply the presence of a special set of eigenvalues.

For any m

$$j = 0 \quad \text{and} \quad \lambda = 0$$

is a constant double eigenvalue for all $p \geq p_0$. Its multiplicity comes from the symmetry of the Gross-Pitaevskii equation under a phase change (this generates an eigenvector) and under a change of standing-wave frequency (this generates a generalized eigenvector). A detailed discussion on these two symmetries and its implications on spectra is given in [1], Appendix B.

Due to the presence of potential the other usual invariants of the nonlinear Schrödinger equation – spatial translations, do not apply. Also, the Galilean boost (2.9) does not work. Instead, the García-Ripoll–Pérez-García–Vekslerchik (GGV) boost [43] introduced in (3.11) applies.

As discussed in [1], any one parameter family u_τ of solutions to (3.8) give rise to a solution to the corresponding equation linearized about u_0. This fact follows from the simple differentiation of (3.8) for u_τ with respect to τ. The solution is then given by

$$\tilde{u} := \partial_\tau u_\tau|_{\tau=0} \,.$$

In the case of GGV boost, setting $R(t) = \tau(\cos t, \sin t)^T$ ($R(t)$ can chosen any linear combination of $\cos t$ and $\sin t$, it only must satisfy $R_{tt} = -R$) provides $\theta(r, \theta, t) = \tau r \cos(\theta - t)$. Then u_τ is in polar coordinates given by

$$u_\tau = \psi\left(r(\cos(\theta) - \tau\cos(t), \sin(\theta) - \tau\sin(t))^T\right) \exp(i\tau r\cos(\theta - t)) \,.$$

where ψ is given by (3.12) and $w(r)$ satisfies (3.15). Hence

$$\tilde{u} = \begin{pmatrix} \cos t \\ \sin t \end{pmatrix} \cdot \nabla\psi(r, \theta, t) + ir\cos(\theta - t)\psi(r, \theta, t) \,,$$

which can be also written as

$$\tilde{u} = e^{-i\mu t} e^{im\theta} \left[w'(r)\cos(\theta - t) + i\frac{mw}{r}\sin(t - \theta) + irw\cos(t - \theta) \right] .$$

The vector $\tilde{\Psi} = (\Re\tilde{u}, \Im\tilde{u})^T$ then satisfies the linearized equations (3.20) and has the form

$$\begin{aligned} e^{\mu t}\tilde{\Psi} &= \begin{pmatrix}\cos m\theta \\ \sin m\theta\end{pmatrix}\begin{pmatrix}\cos\theta \\ \sin\theta\end{pmatrix}\cdot\begin{pmatrix}\cos t \\ \sin t\end{pmatrix}w'(r) \\ &+\begin{pmatrix}-\sin m\theta \\ \cos m\theta\end{pmatrix}\left[-\begin{pmatrix}\cos\theta \\ \sin\theta\end{pmatrix}\cdot\begin{pmatrix}-\sin t \\ \cos t\end{pmatrix}\frac{mw(r)}{r} + \begin{pmatrix}\cos\theta \\ \sin\theta\end{pmatrix}\cdot\begin{pmatrix}\cos t \\ \sin t\end{pmatrix}rw(r)\right]. \end{aligned}$$

In the decoupling to Fourier modes this solution yields a solution to the system (3.26)–(3.27) for $j = 1$, $\lambda = i$ and

$$y_+ = \frac{1}{2}\left[w'(r) - \frac{mw(r)}{r} + rw(r)\right], \quad y_- = \frac{1}{2}\left[w'(r) + \frac{mw(r)}{r} - rw(r)\right].$$

The similar solution can be also obtained for $\lambda = -i$. Therefore the GGV boost implies the existence of the eigenvalues (for any m)

$$j = 1 \quad \text{and} \quad \lambda = \pm i\,.$$

Note, that the numerical results discussed further in this chapter indicate that for

$$j = 0 \quad \text{and} \quad \lambda = \pm 2i$$

is also a pair of constant eigenvalues. We conjecture that this pair of eigenvalues corresponds to some other boost of the Gross-Pitaevskii equation.

3.4 The Evans function

While the finite element and the Galerkin approximation methods provide a fast and simple way to find eigenvalues of the problem (3.29), the Evans function technique method has proved to be the most reliable and robust in certain cases. This approach will be implemented here. It is parallel to [1], where the reader can find many details of the procedure.

The main idea of this approach is to identify eigenvalues of the operator L_j as zeros of an analytic function $E_j(\lambda)$. First, write the system (3.31) as a 4×4 system of first order ordinary differential equations:

$$y' = B(r, j, \lambda)y \tag{3.35}$$

where

$$B = B_\infty + B_w\,, \quad y = \left(y_+^{(j+m)}(r), \partial_r y_-^{(j+m)}(r), y_+^{(j-m)}(r), \partial_r y_-^{(j-m)}(r)\right)^T \tag{3.36}$$

and

$$B_\infty = \begin{pmatrix} 0 & 1 & 0 & 0 \\ k^+ & -1/r & 0 & 0 \\ 0 & 0 & 0 & 1 \\ 0 & 0 & k^- & -1/r \end{pmatrix}\,, \qquad B_w = |w|^2 \begin{pmatrix} 0 & 0 & 0 & 0 \\ 4 & 0 & 2 & 0 \\ 0 & 0 & 0 & 0 \\ 2 & 0 & 4 & 0 \end{pmatrix}\,.$$

The coefficients k^+ and k^- are given by

$$\begin{aligned} k^+(r,\lambda) &= \frac{(j+m)^2}{r^2} + r^2 - 2p - 2i\lambda\,, \\ k^-(r,\lambda) &= \frac{(j-m)^2}{r^2} + r^2 - 2p + 2i\lambda\,. \end{aligned}$$

The asymptotic behavior of solutions to (3.35) is described in the next theorem.

Theorem 3.4.1. *For fixed parameters $\lambda \in \mathbb{C}$ and $m > 0$, p real, j integer, there exist solutions $y_i^{(0)}(r)$ and $y_i^{(\infty)}(r)$, $i = 1, 2, 3, 4$, to the system (3.35) with the following asymptotic behavior,*

$$\begin{aligned} y_i^{(0)}(r) &\sim y_{0i}(r) \qquad\qquad as \quad r \to 0^+\,, \\ y_i^{(\infty)}(r) &\sim y_{\infty i}(r) \qquad\qquad as \quad r \to \infty\,. \end{aligned}$$

Here y_{0i} and $y_{\infty i}$, $i = 1, 2, 3, 4$, are independent solutions of the asymptotic systems

$$y_0 = B_0(r, j, \lambda)y_0\,, \qquad y_\infty = B_\infty(r, j, \lambda)y_\infty\,,$$

where

$$B_0 = \begin{pmatrix} 0 & 1 & 0 & 0 \\ l^+ & -\frac{1}{r} & 0 & 0 \\ 0 & 0 & 0 & 1 \\ 0 & 0 & l^- & -\frac{1}{r} \end{pmatrix}$$

and

$$l^+(r) = \frac{(j+m)^2}{r^2}\,, \qquad l^-(r) = \frac{(j-m)^2}{r^2}\,.$$

The asymptotic behavior of these solutions as $r \to +\infty$ *is given by*

$$\begin{aligned} y_{\infty 1} &\sim e^{r^2/2} r^{\alpha_+} \left(1/r, 1, 0, 0\right)^T\,, & y_{\infty 2} &\sim e^{r^2/2} r^{\alpha_-} \left(0, 0, 1/r, 1\right)^T\,, \\ y_{\infty 3} &\sim e^{-r^2/2} r^{-\alpha_+} \left(1/r, -1, 0, 0\right)^T\,, & y_{\infty 4} &\sim e^{-r^2/2} r^{-\alpha_-} \left(0, 0, 1/r, -1\right)^T\,, \end{aligned}$$

where $\alpha_+ = p + i\lambda$, $\alpha_- = p - i\lambda$, *and as* $r \to 0^+$ *by*

$$\begin{aligned} y_{01} &\sim r^{|j+m|} \left(1, |j+m|/r, 0, 0\right)^T\,, & y_{02} &\sim r^{|j-m|} \left(0, 0, 1, |j-m|/r\right)^T\,, \\ y_{03} &\sim r^{-|j+m|} \left(1, -|j+m|/r, 0, 0\right)^T\,, & y_{04} &\sim r^{-|j-m|} \left(0, 0, 1, -|j-m|/r\right)^T\,. \end{aligned}$$

The proof of the theorem is included in Appendix E.

The asymptotic analysis reveals that (3.35) has two exponentially growing solutions asymptotically equivalent to $y_1^{(0)}(r)$ and $y_2^{(0)}(r)$ for $r << 1$ and two exponentially decreasing solutions asymptotically equivalent to $y_3^{(\infty)}(r)$ and $y_4^{(\infty)}(r)$ for $r >> 1$. Note that these solutions are not in any way unique. From now on the notation $y_1^{(0)}$, $y_2^{(0)}$, $y_3^{(\infty)}$ and $y_4^{(\infty)}$ will always refer to solutions with the given asymptotics. The two-dimensional growing and decaying subspaces nontrivially intersect only if λ is an eigenvalue. Their intersection can be detected by vanishing of the Wronskian $W(r,\lambda) = \det(y_1^{(0)}, y_2^{(0)}, y_3^{(\infty)}, y_4^{(\infty)})$. Although the determinant seems to be a proper quantity at a first glance, it has many disadvantages. First, it can be a priori dependent on r. This problem can be resolved

by setting

$$E_j(\lambda) = -r^2 \det(y_1^{(0)}(r), y_2^{(0)}(r), y_3^{(\infty)}(r), y_4^{(\infty)}(r)) \,. \tag{3.37}$$

This function is by Abel's formula independent of r. (The determinant satisfies a differential equation $W'(r) = \mathrm{Tr}\,(B)\, W(r)$.)

It is evident that $E_j(\lambda) = 0$ is a necessary and sufficient condition for the existence of an eigenvalue. The disadvantage of the direct approach described is that it does not guarantee that $E_j(\lambda)$ is an analytic function. On the other hand, analyticity of the Evans function would enable to study the presence and location of eigenvalues by means of contour integrals via the argument and generalized-argument principle.

An alternative way to construct and evaluate the Evans function is to introduce the adjoint system

$$z' = -zB(r, j, \lambda) \,. \tag{3.38}$$

The fundamental matrices $Y(z)$ (its columns are y_i) and $Z(z)$ (with rows z_i) of systems (3.35) and (3.38) are related by $ZY = I$. Therefore Theorem 3.4.1 (by a simple direct calculation of the inverse matrix) also guarantees existence of four independent solutions of (3.38) as $z_1^{(\infty)}$, $z_2^{(\infty)}$, $z_3^{(\infty)}$ and $z_4^{(\infty)}$ such that the matrices $Z^{(\infty)}$ with columns $z_i^{(\infty)}$ and $Y^{(\infty)}$ with columns $y_i^{(\infty)}$ satisfy $Z^{(\infty)}Y^{(\infty)} = I$. One can also easily deduce the asymptotic behavior of $z_i^{(\infty)}$ as $r \to \infty$. Furthermore, a simple calculation [1] shows that

$$E_j(\lambda) = \det \begin{pmatrix} z_1^{(\infty)} \cdot y_1^{(0)} & z_1^{(\infty)} \cdot y_2^{(0)} \\ z_2^{(\infty)} \cdot y_1^{(0)} & z_2^{(\infty)} \cdot y_2^{(0)} \end{pmatrix} \,. \tag{3.39}$$

Unfortunately, $E_j(\lambda)$ constructed in this way can still depend on a particular choice of solutions $y_i^{(0)}$ and $z_i^{(\infty)}$. The idea how to overcome this difficulty is quite simple [1]. Instead of considering the system (3.35) one can construct a larger

6×6 system for pairs (exterior products) of solutions to (3.35). This exterior system will than have the unique solution of maximum growth and the unique solution of maximal decay $\hat{y}_{12}^{(0)} = y_1^{(0)} \wedge y_2^{(0)}$ and $\hat{y}_{34}^{(\infty)} = y_3^{(\infty)} \wedge y_4^{(\infty)}$. Properties of the adjoint system are similar as for 4×4 systems. Evaluation of the Evans function is then given by the simple formula

$$E_j(\lambda) = \hat{z}_{34}^{(\infty)} \cdot \hat{y}_{12}^{(0)} \,. \tag{3.40}$$

It is important to realize that the Evans function given by (3.40) is analytic in $\mathbb{C}$ and it is solution- and spatially- independent. On the other hand, the values are the same as given by (3.39) and (3.37).

3.4.1 Symmetries of the Evans function

Before a description of the numerical implementation it is useful to list the symmetries of the Evans function constructed. The proof of the Proposition is the same as in [1].

Proposition 3.4.2. *For all integers j and complex numbers $\lambda \in \mathbb{C}$,*

- $\overline{E_j(\lambda)} = E_j(-\lambda)$;
- $E_j(\lambda) = E_{-j}(-\lambda)$.

Particularly, $E_j(\lambda)$ is real for λ purely imaginary and $E_0(\lambda) = E_0(-\lambda) = \overline{E_0(\overline{\lambda})}$.

3.5 Numerical implementation

All the computations in this thesis were performed on a PC with 512 MB memory and 2.2 GHz AMD processor. The codes were implemented in Fortran 77 except

for time-splitting direct evolution simulations and all visualizations which were done in Matlab. Moreover, all computations were performed in real arithmetic.

3.5.1 Evans function evaluation

To attain high precision and stability for all computations, exterior products were used throughout the whole numerical implementation of the evaluation of the Evans function. As one can easily see from the asymptotic description of the solutions, the behavior of the system is significantly different for $r << 1$ and $r >> 1$. Therefore it is necessary to subsequently rescale the solution during the integration process over the interval $[0, \infty)$ (the actual implementation approximate this interval with $[\varepsilon, R]$, where $\varepsilon = 10^{-7}$ and $R = R(p)$, $R(p)$ is set in such a way that the vortex solution is negligible at $R = R(p)$; $R(p)$ is an increasing function, $R(0) = 5$, $R(35) = 25$). The aim is to rescale the system in a such a way that the matrix $B(r, \lambda, j)$ (and so the solution) will be bounded through the whole integration. The details of the rescaling used are included in Appendix F.

The presence of the unstable eigenvalues is detected by a contour integration using the argument principle, similarly as in [1]. The algorithm adaptively calculates the argument of the Evans function $E_j(\lambda)$ for j's restricted by Proposition 3.3.4 along a contour Γ which encloses a bounded region in $\mathbb{R}^2$. The region is pictured on Fig. 3.2. Note that Proposition 3.4.2 allows to confine the integration into the right half plane (the total argument will be then twice as large) and also reduces the set of j's for which the calculation is necessary to non-negative values. Moreover, Proposition 3.3.5 restricts the location of unstable eigenvalues into a vertical strip. Naturally, it is not possible to perform numerical calculations without imposing also some vertical bound for the region enclosed by the

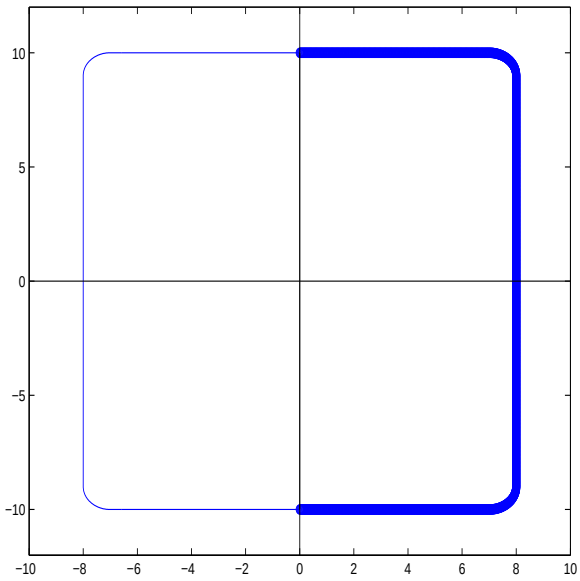

Figure 3.2: Contour used for counting of eigenvalues. Due to the symmetry of the Evans function, the computation was restricted to the thick contour in the right-half plane.

contour. The vertical bound in the implementation is chosen is such a way that the behavior of the stable eigenvalues becomes predictable. Although there is no mathematical justification provided here that the contour encloses all the unstable eigenvalues, the number of possible unstable eigenvalues is limited and can be eventually numerically determined as it was discussed in Subsection 3.3.2.

Stable eigenvalues on the imaginary axis are, thanks to the symmetry of the Evans function, zeros of the real valued function $E(\lambda)$. Hence one can plot that real function and determine the location and multiplicity of its zeros within a finite interval. In the actual implementation this is done automatically — one first interpolates the real function by a cubic spline and then uses the Newton

method for locating zeros. In a small neighborhood of a possible double zero, a very fine mesh was used to resolve any ambiguity.

The total number of unstable eigenvalues of $E_j(\lambda)$ enclosed in the region is then determined by the difference $n_u = n_{s+u} - n_s$ of

$$n_{s+u} = \frac{1}{2\pi i} \oint_\Gamma \frac{E_j'(\lambda)}{E_j(\lambda)} d\lambda = \frac{1}{2\pi i} \oint_\Gamma \arg\left(E_j(\lambda)\right) d\lambda$$

and the number of (stable) eigenvalues n_s on the imaginary axis, including their algebraic multiplicity. If n_u is not equal to zero it must by Proposition 3.4.2 be an even positive integer. The precise location of pairs of unstable eigenvalues can be determined by the generalized argument principle. The quantity

$$s_1 = \sum \lambda_i = \oint_\Gamma \lambda \frac{E_j'(\lambda)}{E_j(\lambda)} d\lambda \tag{3.41}$$

gives the sum of positions of all eigenvalues enclosed by Γ. Since the location of all eigenvalues on imaginary axis (within Γ) was already approximated by zeros of the spline interpolation of $E_j(\lambda)$, the formula (3.41) allows to find a sum of positions of pairs of eigenvalues symmetric with respect to an imaginary axis. Hence, if $n_u = 2$, it completely determines the imaginary part of those unstable eigenvalues. Their respective real parts (with the same absolute value) can be further calculated using the generalized argument principle (the second moment):

$$s_2 = \sum \lambda_i^2 = \oint_\Gamma \lambda^2 \frac{E_j'(\lambda)}{E_j(\lambda)} d\lambda \,.$$

Once again, one subtracts the sum of squares of the approximated purely imaginary eigenvalues from s_2. The calculation of the real part of unstable eigenvalues is then straightforward.

In theory this procedure describes the location of unstable eigenvalues (in the case $n_u = 2$). Unfortunately, the numerical error involved can be significant with

a major contribution coming from a finite difference approximation of $E_j'(\lambda)$. Therefore the obtained values are considered only approximate. The calculated location is further used to construct a smaller contour Γ_s which lies solely in the right-half plane and encloses only a single eigenvalue. The presence of a zero of $E_j(\lambda)$ inside a smaller contour is again calculated by the argument principle. Its location is then determined by (3.41). This process can be repeated a few times until a desired precision is attained. In the implementation the threshold for a precision was set up to be 10^{-3}. If there are more than 2 unstable eigenvalue present ($n_u \geq 4$) inside Γ, it is easier to guess their location first and then continue as in this case $n_u = 2$ than to use higher moments.

Note that this method does not allow to calculate the eigenfunction directly and for that another method must be used. A simple Galerkin method which was implemented is described in Appendix G.

3.5.2 Direct simulations

For direct simulations of the evolution of the Gross-Pitaevskii equation (3.8), either starting with initial data to be exact solutions or its perturbation, a time-splitting scheme [6] was used (see [51] for a different schemes comparison).

The goal is to solve

$$i\varepsilon\frac{\partial\Psi(x,t)}{\partial t} = -\frac{\varepsilon^2}{2}\triangle\Psi(x,t) + V(x)\Psi(x,t) + |\Psi(x,t)|^2\Psi(x,t)\,, \tag{3.42}$$

on $(t,x) \in [0,T]\times\Omega = [0,T]\times[-a,a]^2$ with the initial condition

$$\Psi(x,t)|_{t=0} = \Psi^0(x)\,, \qquad \text{for all } x\in\Omega,$$

and periodic boundary conditions

$$\Psi(x,t)|_{x_i=-a} = \Psi(x,t)|_{x_i=a}, \quad \Psi_{x_i}(x,t)|_{x_i=-a} = \Psi_{x_i}(x,t)|_{x_i=a}\,,$$

for $i = 1, 2$ and $t > 0$. Set $\triangle x = \triangle y = 2a/M > 0$ and $\triangle t > 0$ to be a spatial and a temporal discretization step respectively, $x_j = -a + j\triangle x$, $y_j = -a + j\triangle y$, $t_n = n\triangle t$. Denote by Ψ_{ij}^n the approximation of $\Psi(x_i, y_j, t_n)$.

The time-splitting spectral method uses the fact that the operator on the right-hand side of (3.42) can be written as a sum of two operators, for which it is possible to solve the evolution equation exactly.

First, one can solve (integrate in time) exactly

$$i\varepsilon\Psi_t(x,t) = -\frac{\varepsilon^2}{2}\triangle\Psi(x,t) \tag{3.43}$$

by the Fourier spectral method. Although the second evolution equation is non-linear

$$i\varepsilon\Psi_t(x,t) = V(x)\Psi(x,t) + |\Psi(x,t)|^2\Psi(x,t)\,, \tag{3.44}$$

and it seems impossible to solve it exactly, the contrary is true. The equation (3.44) preserve the norm $|\Psi|$ and therefore it is effectively linear and can be integrated exactly. On an interval $t \in [a, b]$ it becomes

$$i\varepsilon\Psi_t(x,t) = V(x)\Psi(x,t) + |\Psi(x,a)|^2\Psi(x,t)\,. \tag{3.45}$$

These two half-steps will be combined via the standard Strang splitting: when integrating over $[t_n, t_{n+1}]$ first integrate (3.45) over the first half of the interval, then integrate (3.43) over the whole interval and finally integrate (3.45) again over the remaining half of the interval.

Assume that the data at t_n are given by Ψ_{jl}^n, $j, l = 0, \ldots, M-1$. In two-dimensional case, integration steps on $[t_n, t_{n+1}]$ are represented by the following

formulas:

$$\begin{aligned}
\Psi^*_{jl} &= \Psi^n_{jl} \exp\left[-i\left(V(x_j,y_l)+|\Psi^n_{jl}|^2\right)\frac{\triangle t}{2\varepsilon}\right], \qquad j,l=0,1,2,\ldots,M-1,\\
\hat{\Psi}^*_{uv} &= \sum_{j=0}^{M-1}\sum_{l=0}^{M-1}\Psi^*_{jl}\exp\left[-i\left(\omega_u(x_j+a)+\omega_v(y_l+a)\right)\right], \\
&\qquad\qquad u,v=-\frac{M}{2},\ldots,\frac{M}{2}-1,
\end{aligned}$$

and

$$\begin{aligned}
\hat{\Psi}^{**}_{uv} &= \hat{\Psi}^*_{uv}\exp\left[-i\varepsilon\triangle t\left(\frac{\omega_u^2+\omega_v^2}{2}\right)\right], \qquad u,v=-\frac{M}{2},\ldots,\frac{M}{2}-1,\\
\Psi^{**}_{jl} &= \frac{1}{M^2}\sum_{u=-M/2}^{M/2-1}\sum_{v=-M/2}^{M/2-1}\hat{\Psi}^{**}_{uv}\exp\left[i\left(\omega_u(x_j+a)+\omega_v(y_l+a)\right)\right], \\
&\qquad\qquad j,l=0,1,2,\ldots,M-1,\\
\Psi^{n+1}_{jl} &= \Psi^{**}_{jl}\exp\left[-i\left(V(x_j,y_l)+|\Psi^{**}_{jl}|^2\right)\frac{\triangle t}{2\varepsilon}\right], \qquad j,l=0,1,2,\ldots,M-1,
\end{aligned}$$

where $\omega_u = u\pi/a$ is the Fourier frequency. Clearly, the second step represents a two-dimensional discrete Fourier transform and the fourth step its inverse (both steps are implemented using FFT). In the case considered here $\varepsilon = 1$ and $a = 10$.

As reported in [51] and [6], the scheme is infinite order of accuracy in spatial discretization and second order in time, i.e. the error is $O\left((\triangle t)^2,(\triangle x)^p)\right)$ for all $p > 0$. The performance of the scheme is shown on Fig. 3.3, where errors of the numerical solutions $\Psi^{(\triangle t)}_{num}$ initialized as a singly-quantized vortex rotating with a given frequency μ are compared with the analytically predicted solution (exact rotation of the initial data). Here, the norm used is

$$|f|^2_{\triangle x} = (\triangle x)^2\sum_{ij} f^2_{ij}\,. \tag{3.46}$$

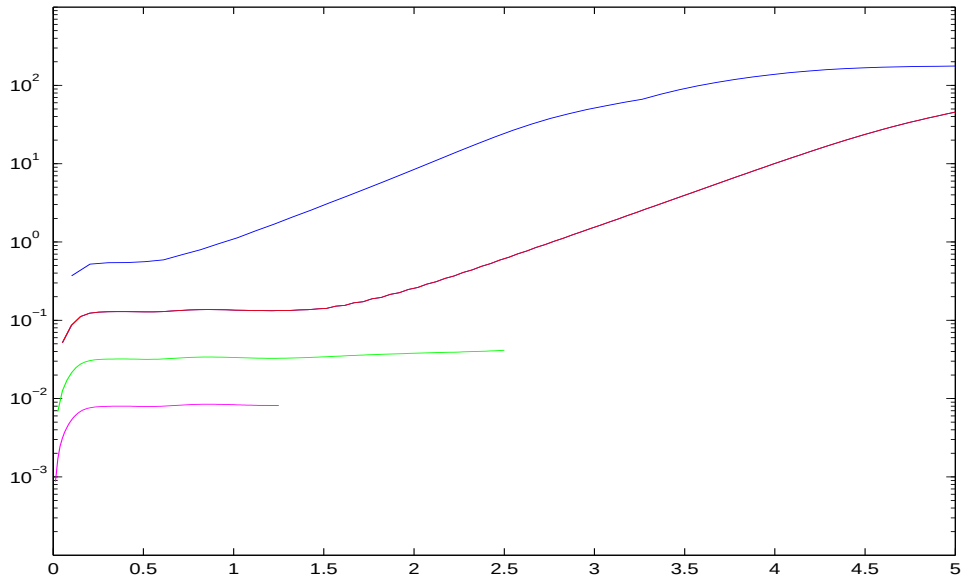

Figure 3.3: The $|\cdot|_{\triangle x}$ norm of the error produced by the time-splitting scheme is plotted vs. time. The four different curves correspond (from above) to $\triangle t = 0.1, 0.05, 0.025\ 0.0125$, $\triangle x = 20/256$.

By subsequently setting the time step to half its value the error decreases approximately by a factor of 4. This test was performed for $\triangle x = 20/256$ and $\triangle t = 0.0125, 0.025, 0.05$ and 0.1.

The Gross-Pitaevskii equation solved here is not periodic, particularly the potential $V(x) = |x|^2/2$ has singularity in its first derivative at the boundary of the proposed periodic box. To avoid this problem, it is helpful to mollify the quadratic potential by replacing it with

$$V(x) = \begin{cases} \frac{1}{2}|x|^2 & \text{for } |x| < a - \delta_V, \\ \frac{1}{2}|x|^2\left[1 - c_V(a - \delta_V - |x|)^2\right] & \text{for } a - \delta_V < |x| < a, \\ \frac{1}{2}a^2(1 - \varepsilon_V) & \text{for } |x| > a, \end{cases}$$

where ε_V is chosen small, $\varepsilon = 0.05$, and

$$\delta_V = \frac{a\varepsilon_V}{1-\varepsilon_V}\,, \qquad c_V = \frac{(1-\varepsilon_V)^2}{a^2\varepsilon_V}$$

are chosen in such a way that $V(x)$ and its derivative are periodic in both x and y direction.

3.6 Numerical results

Numerical results will be discussed separately for singly- and multi-quantized vortices since the stability diagrams (diagrams of stable and unstable eigenvalues) reveal different patterns.

3.6.1 Singly-quantized vortices m = 1

The radial vortex profile obtained by the predictor-corrector algorithm and refined by the multiple shooting method as described in Section 3.2 is drawn on Fig. 3.4. For a better illustration the modulus of the corresponding vortex solution in the right-half plane is visualized on Fig. 3.5.

The singly-quantized vortex, $m = 1$ is found to be linearly stable for all values of the parameter p investigated, $p \in (0, 35)$, corresponding to number of particles $N \in (0, 10^6)$ for ^{23}Na data given in Section 3.1. By Theorem 3.32 the unstable eigenvalue can appear only for $|j| \leq 2$. Location of the stable eigenvalues (p vs. $\mathrm{Im}\,\lambda$) for $j = 0, 1, 2, 3$ is plotted on Fig. 3.6. For the sake of clarity only eigenvalues with $|\Im\lambda| < 5$ are presented here. The bound $|\Im\lambda| < \max(5, p/2)$ was imposed in the numerical implementation.

For a small value of p, close to $p_0 = m + 1$ the eigenvalues are close to the eigenvalues of the reduced uncoupled linear problem neglecting the $|w|^2$ depen-

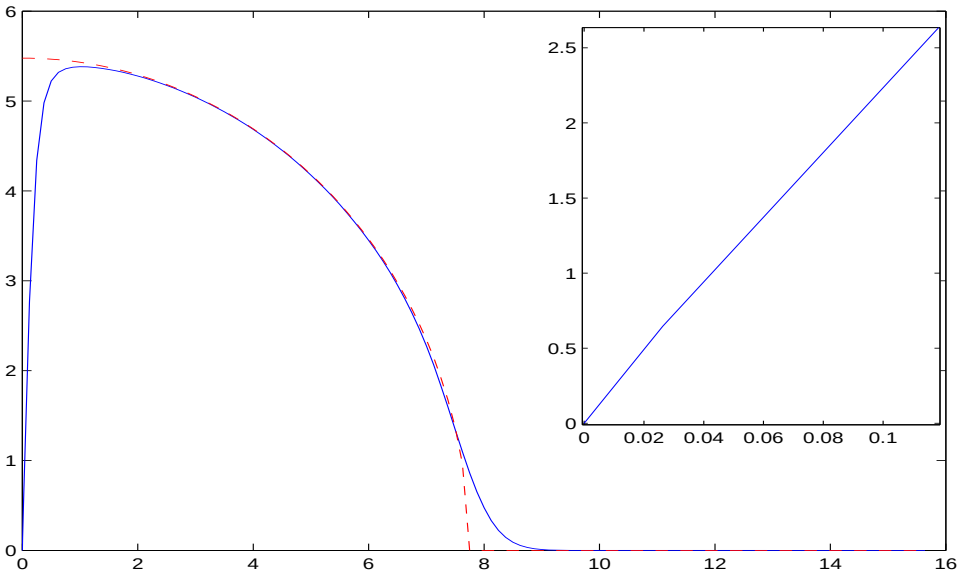

Figure 3.4: The radial vortex profile of a singly-quantized vortex for the dimensionless parameter $p \approx 30$ corresponding to $N \approx 10^6$ particles of ^{23}Na

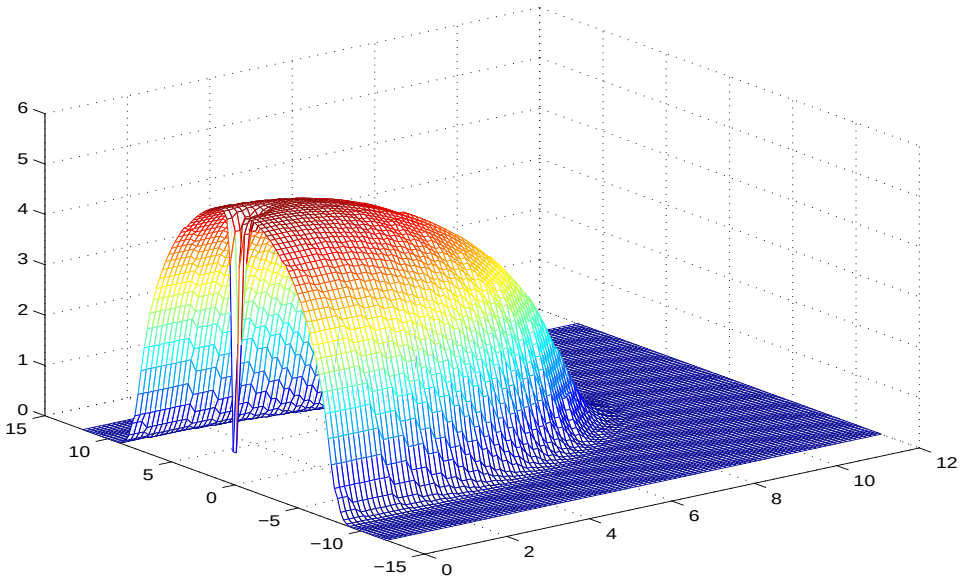

Figure 3.5: The modulus of the singly-quantized vortex solution for the dimensionless parameter $p \approx 30$ corresponding to $N \approx 10^6$ particles of ^{23}Na.

$m = 1$	$j = 1$	$\lambda_0 = -3$	$\lambda(s) = -2.64 - 1.24\, s^{-1.02}$
		$\lambda_0 = -1$	$\lambda(s) = 0.01 - 1.48\, s^{-0.80}$
		$\lambda_0 = 3$	$\lambda(s) = 2.73 - 0.17\, s^{-0.14}$
	$j = 2$	$\lambda_0 = -2$	$\lambda(s) = -1.41 - 1.82\, s^{-1.04}$
		$\lambda_0 = 0$	$\lambda(s) = 1.41 - 1.61\, s^{-1.04}$
		$\lambda_0 = 2$	$\lambda(s) = 3.16 - 2.43\, s^{-1.02}$

Table 3.1: Approximate asymptotic behavior of eigenvalues for $m = 1$.

dence. This is not a surprise since for p close p_0 the modulus of $|w|^2$ is small and the nonlinear problem "decouples" to a pair of linear equations with solutions close to the corresponding eigenfunction for $p = p_0$. As shown before these solutions exist for $p_0 + 2n$, $n \geq 0$.

As p increases certain eigenvalues remain constant: a double eigenvalue $\lambda = 0$ and simple eigenvalues $\lambda = \pm 2i$ for $j = 0$ and simple eigenvalues $\lambda = \pm 1$ for $j = 1$. These eigenvalues originate in the symmetries and boosts of the Gross-Pitaevskii equation and are present for every m (see Subsection 3.3.3).

The remaining non-constant eigenvalues after an initial steep decay or growth approach a regime where they slowly monotonically grow. All eigenvalues (for large p) are clearly separated preventing a collision of two eigenvalues on imaginary axis. It would be plausible to describe the asymptotics of the eigenvalues as $p \to \infty$ when the condensate approaches the Thomas-Fermi regime. We were only able to study the asymptotic behavior of purely imaginary eigenvalues numerically by plotting a loglog plot of the first order differences of $\lambda(s)$. We observed a clear linear trend implying an algebraic decay of an exact power.

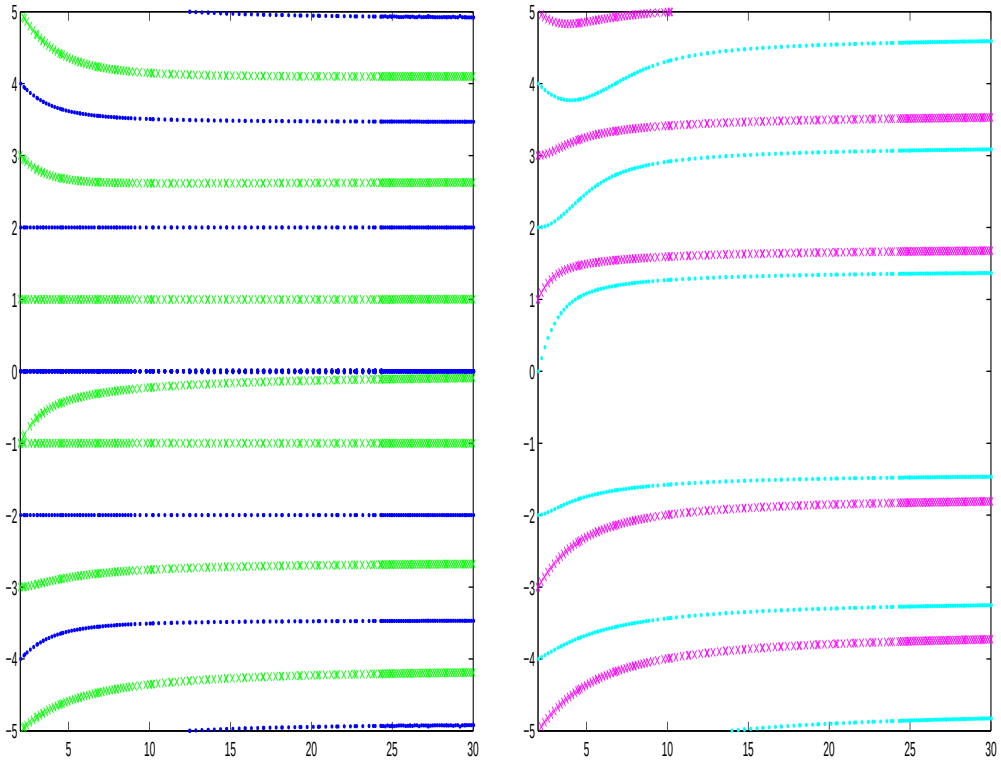

(a) (b)

Figure 3.6: Stable eigenvalues (p vs. $\mathrm{Im}\,\lambda$) of the linearization about a singly-quantized, $m = 1$, vortex solution, $p \in (m+1, 30)$: (a) the eigenvalues corresponding to modes $j = 0$ (marked thin), $j = 1$ (marked thick); (b) the eigenvalues corresponding to $j = 2$ (thin), $j = 3$ (thick).

$m = 2$	$j = 2$	$\lambda_0 = -4$	$\lambda(s) = -1.41 - 2.69\, s^{-0.96}$
		$\lambda_0 = 0$	$\lambda(s) = 1.38 - 7.96\, s^{-1.39}$
		$\lambda_0 = 2$	$\lambda(s) = 3.11 - 27.66\, s^{-1.59}$
	$j = 3$	$\lambda_0 = -3$	$\lambda(s) = -1.74 - 5.14\, s^{-1.06}$
		$\lambda_0 = -1$	$\lambda(s) = 1.73 - 3.97\, s^{-1.02}$
		$\lambda_0 = 1$	$\lambda(s) = 3.61 - 5.30\, s^{-0.97}$

Table 3.2: Approximate behavior of eigenvalues for $m = 2$.

The approximate behavior of eigenvalues with a small imaginary part for $m = 1$, $j = 1, 2$ and $m = 2$, $j = 2, 3$ is presented in Tables 3.1–3.2. As can be seen from the tables — most of the eigenvalues seem to approach a constant limit value L_{λ_0} and their asymptotic behavior as $s >> 1$ is well approximated by

$$\lambda(s) = L_{\lambda_0} - cs^{-1}$$

for a constant c. On the other hand, certain eigenvalues show different rate of growth clearly distinct from $(-s^{-1})$ but we do not have any explanation of this phenomena.

3.6.2 Multi-quantized vortices m $\geq$ 2

The eigenvalue diagrams for multi-quantized vortices, $m = 2$, show higher complexity of the behavior of the eigenvalues than those for $m = 1$. The radial vortex profile for $p \approx 35$ is illustrated on Fig. 3.7 and the modulus of the vortex solution in the right half-plane on Fig. 3.8. For $m = 2$ the vortex solution is within its core well approximated by a paraboloid.

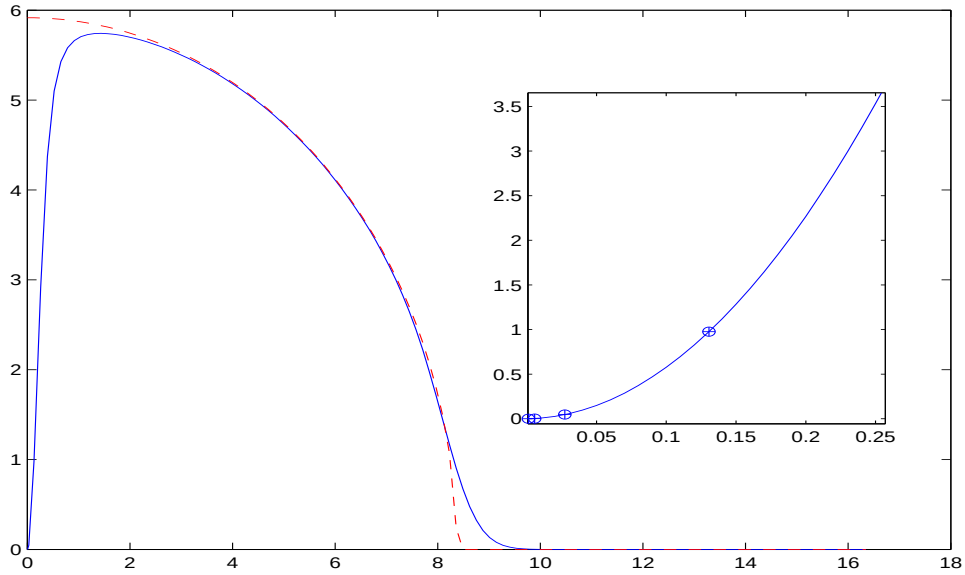

Figure 3.7: The radial vortex profile of a multi-quantized vortex, $m = 2$, for the dimensionless parameter $p \approx 35$ corresponding to $N \approx 10^6$ particles of ^{23}Na.

The modes $j = 0$ and $j = 1$ demonstrate the same features as in the case of the singly-quantized vortex with the same constant eigenvalues: a double eigenvalue $\lambda = 0$ and simple eigenvalues $\lambda = \pm 2i$ for $j = 0$ and simple eigenvalues $\lambda = \pm i$ for $j = 1$ (see Fig. 3.9 (a)).

A different behavior appears for modes $j = 2$ and $j = 3$, as shown on Fig. 3.9 (b) and Fig. 3.11. While for $j = 3$ there are no unstable eigenvalues present and the stable eigenvalues do not collide but rather diverge from each other when they approach each other, the collisions are inevitable for $j = 2$ and cause instability. A collision of two stable purely imaginary eigenvalues produces a pair of unstable eigenvalues symmetric with respect to the imaginary axis. After a further increase of parameter p these two eigenvalues come back to the imaginary axis and split

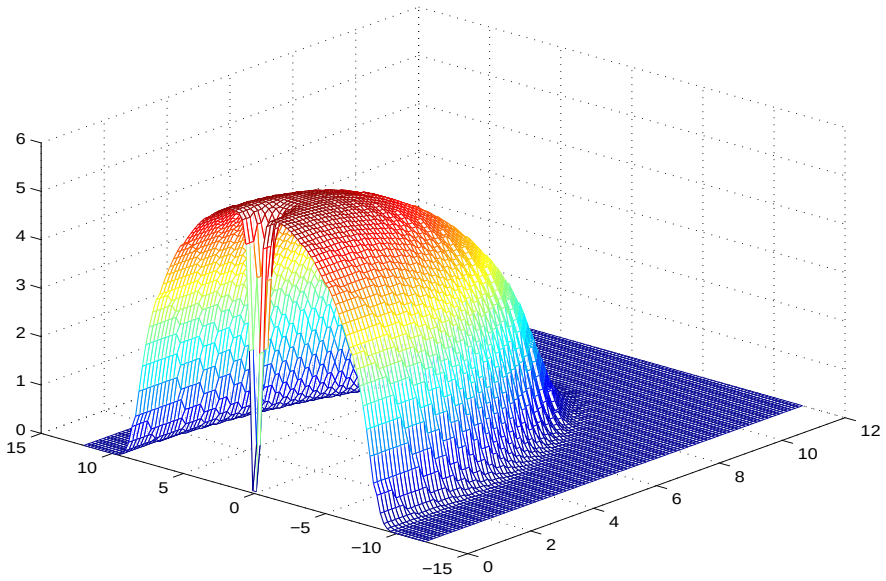

Figure 3.8: The modulus of the multi-quantized vortex solution, $m = 2$, for the dimensionless parameter $p \approx 35$ corresponding to $N \approx 10^6$ particles of ^{23}Na.

back to two stable eigenvalues as illustrated on Fig. 3.10. This "collision – split – collision" process almost periodically repeats for the whole range of p studied.

We conjecture that this behavior is caused by the presence of an eigenvalue with negative Krein signature. The imaginary part of this eigenvalue is decreasing with increasing p and on its way it encounters eigenvalues with the opposite signature. After each collision the eigenvalues split off the imaginary axis and become eigenvalues with zero Krein signature symmetric relative to the imaginary axis. Reversibility of this process suggests that the eigenvalues come back to the imaginary axis and the process repeats itself (for a larger parameter p). This suggest a surprising fact that the transition to instability for large p may happen at a large frequency, i.e. for $\mathrm{Im}\,\lambda$ large, and therefore there is no hope to confine the imaginary parts of unstable eigenvalues to a finite interval independently

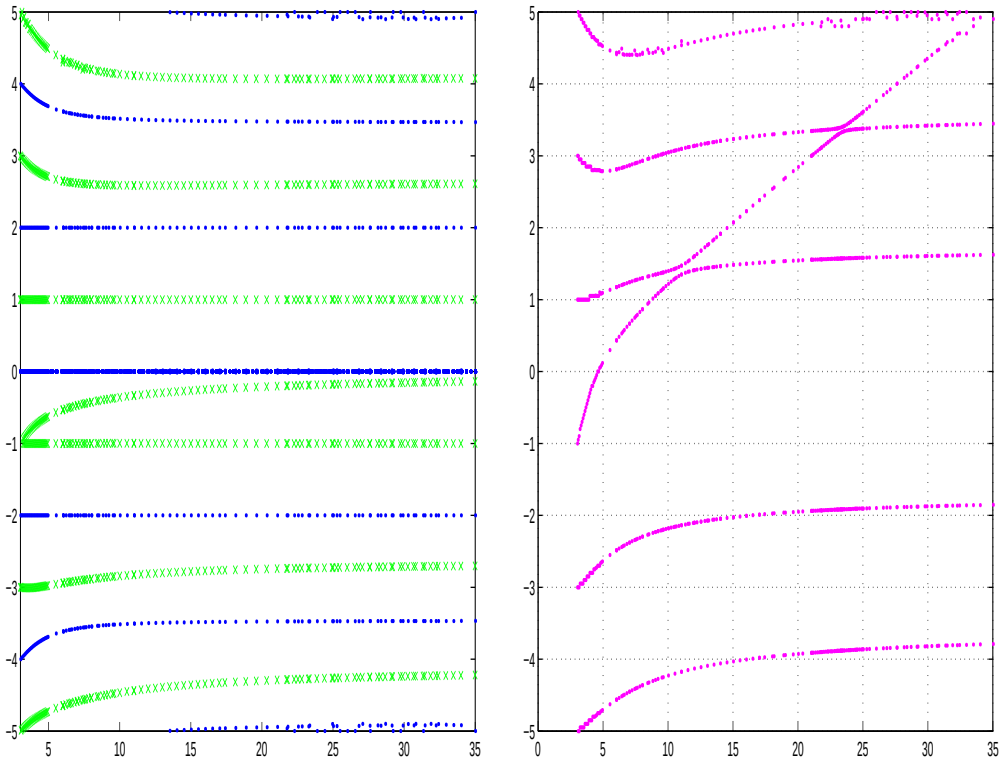

(a) (b)

Figure 3.9: Stable eigenvalues (p vs. $\mathrm{Im}\,\lambda$) of the linearization about a multi-quantized vortex solution, $m = 2$, $p \in (m+1, 35)$: (a) eigenvalues corresponding to modes $j = 0$ (marked thin), $j = 1$ (marked thick); (b) eigenvalues corresponding to $j = 3$.

of p. The behavior of the eigenvalues demonstrates a strong agreement with the earlier work of Pu *et al.* [5] as can be seen also from comparison of Fig. 3.10 and the figure in the paper. This is also in agreement with the results of Seiringer [31] where he proved that for any $m \geq 1$ for large enough p the vortex becomes energetically unstable in that sense that it cannot be a global minimizer of the energy and is subject to symmetry breaking.

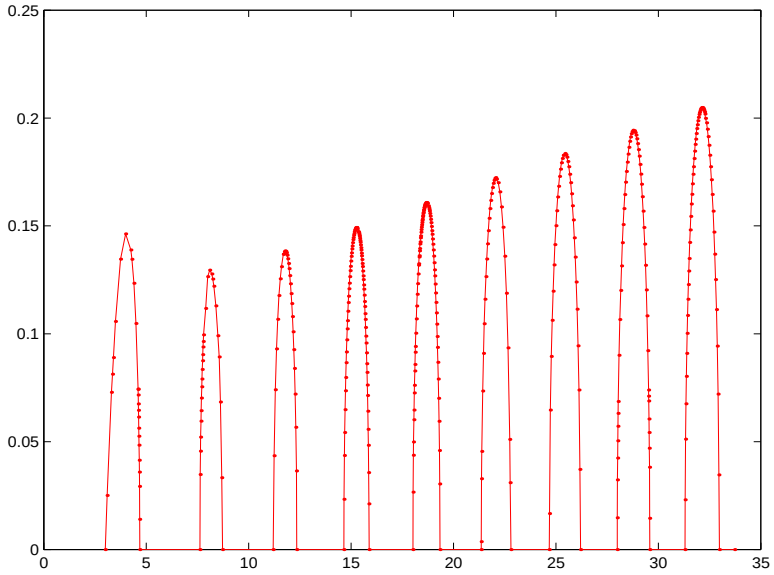

Figure 3.10: Stable and unstable ($\mathrm{Re}\,\lambda$ vs. p) eigenvalues of the linearization about a multi-quantized vortex solution, $m = 2$, $p \in (m+1, 35)$, corresponding to the mode $j = 2$.

In the case $j = 3$ we suspect that the eigenvalues have the same Krein signature and therefore they cannot split off the imaginary axis. Instead, they repel each other when they are too close to each other and do not collide at all.

We also give numerical evidence of the presence of exponential instability. Direct complex-time evolution simulations described in Section 3.5.2 were conducted with with a time step $\triangle t = 0.025$ and spatial discretization $\triangle x = 2a/256$ for $a = 10$ (Fig. 3.12).

First, we consider the exact vortex solution initialized by $\Psi_{p0} = e^{2i\theta}w(r)$. A comparison of the numerically evolving solution $\Psi_p(t)$ and the analytical prediction $e^{-ipt}e^{2i\theta}w(r)$ (but in the case of the singly-quantized vortex) was already performed and is illustrated on Fig. 3.3 with the error measured by the norm $|\cdot|_{\triangle x}$

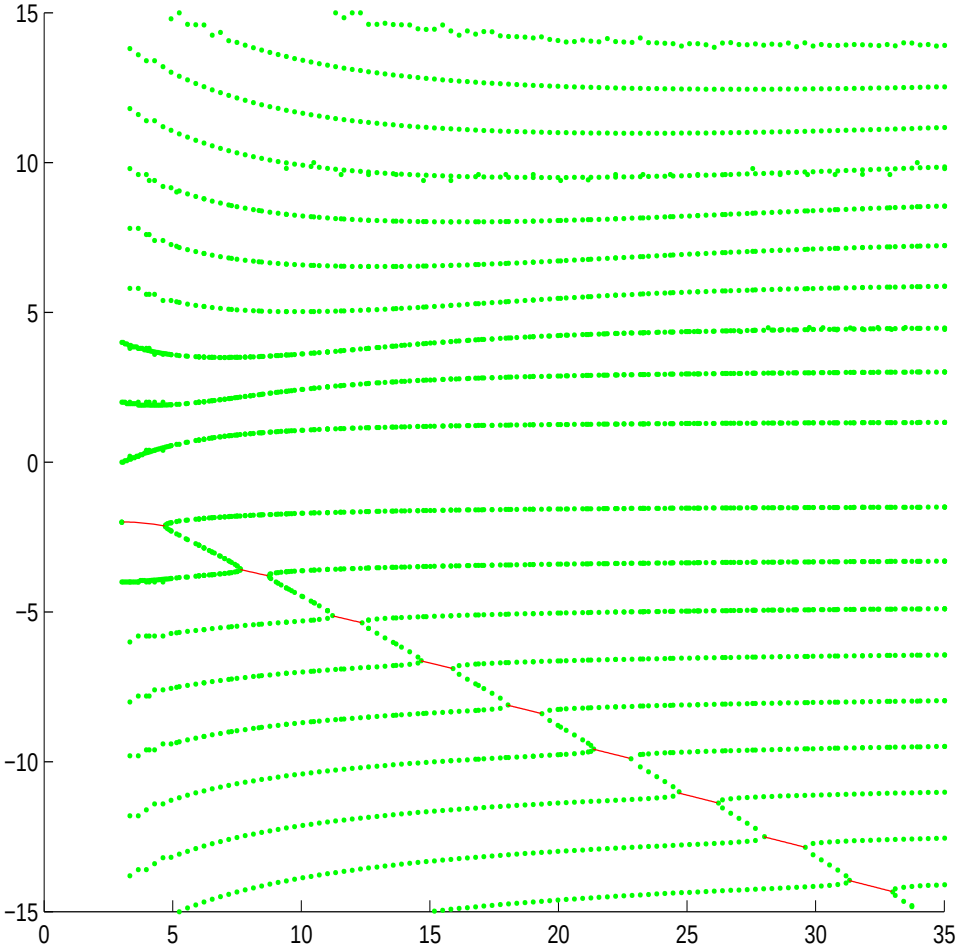

Figure 3.11: Imaginary part of stable and unstable ($\mathrm{Im}\,\lambda$ vs. p) eigenvalues of the linearization about a multi-quantized vortex solution, $m = 2$, $p \in (m+1, 35)$, corresponding to mode $j = 2$. Stable eigenvalues are plotted thick, unstable form thin curves.

introduced in (3.46). Note that the norm $|\Psi_{0p}|^2_{\triangle x} \approx (\triangle x)^2 \cdot 160$ is preserved for the exact equation and varies only slowly in the time-splitting numerical scheme used for direct evolution of the system.

Then, the initial data Ψ_{0p} are perturbed by a random (not necessarily radial modulus) function Ψ_{0rand}, $|\Psi_{0rand}|^2_{\triangle} = (\triangle x)^2$ in the whole domain $[-10, 10] \times$

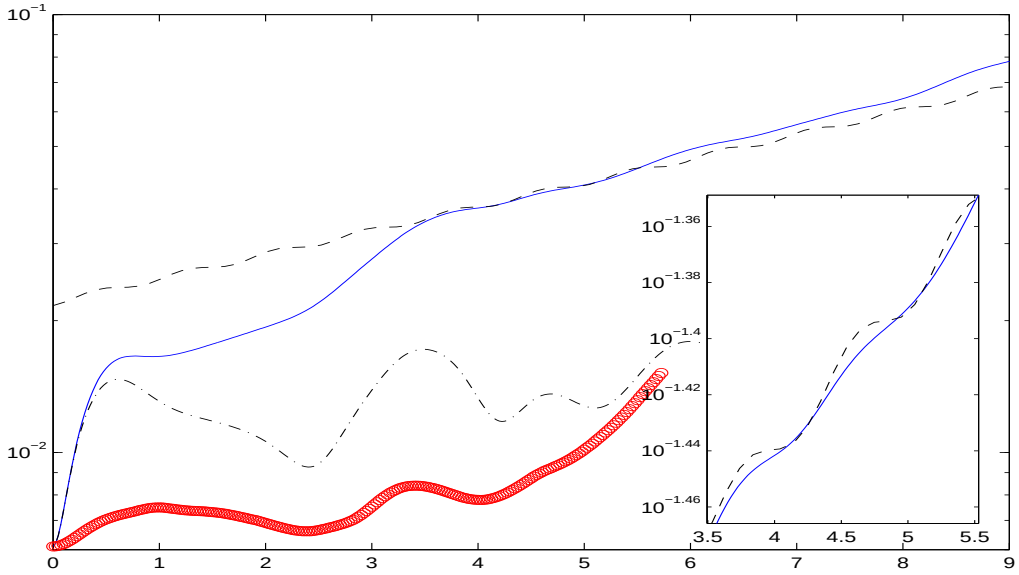

Figure 3.12: A comparison of error growth rates for $m = 2$, $j = 2$, $p \approx 8$. The time evolution of the error functions $E_{rand}(t)$ (the thick solid curve), $E_{inst}(t)$ (the thin solid curve) is plotted vs. time. A comparison with the error function E_{exp} (the dashed curve) is shown and zoomed in the insert. The dash-dotted curve represents an error E_{stab} and corresponds to $p \approx 9$.

$[-10, 10]$. As can be seen from Fig. 3.12, the norm of the difference of the evolving solution

$$E_{rand}(t) = |\Psi_{rand}(t) - \Psi_p(t)|_{\triangle x}$$

does not demonstrate any presence of the localized exponential instability (for $t \leq 5$). But the global character of the initial perturbation (in the whole domain) interacts with the spatial boundary and produces a significant error in a relatively short time $t \approx 5$ and produces a significant error growth at that time.

Also, the exact solution Ψ_{p0} is initially perturbed by data approximating the unstable mode Ψ_{0unst} obtained by the procedure described in Appendix G.

Unfortunately, the Galerkin approximation approach does not produce a pure eigenfunction and the solution is polluted by significant contributions from other eigenstates. The exact eigenfunction has the precise form (by Theorem 3.3.2)

$$\Psi_{0unst}^{exact} = Ce^{\lambda t}e^{i(j+m)\theta}y_+(r) + \overline{Ce^{\lambda t}e^{i(j-m)\theta}y_-(r)}.$$

(Here y_+, y_- are solutions to (3.26)–(3.27) for the unstable eigenvalue λ, $\Re\lambda > 0$.)

Again, the evolution of the error

$$E_{unst}(t) = |\Psi_{unst}(t) - \Psi_p(t)|_{\triangle x}$$

is plotted. Although the behavior of $E_{unst}(t)$ for small t does not correspond to the rate of growth expected for Ψ_{0unst}^{exact} (which may be caused by the presence of the other eigenstates), after a certain time it is well correlated with a multiple of the expected growth $E_{exp} = Ae^{\Re\lambda t}\sqrt{B + C\cos 2t\Im\lambda}$, for some constants A, B and C, where the constants B and C are predicted by the theoretical analysis. Nevertheless, the exponential growth with the predicted growth rate demonstrates the presence of the unstable eigenvalue.

Finally, a comparison was performed with the expected stable solution for $p \approx 9$. The initial perturbations were taken to be a random perturbation and the perturbation by some approximation of the eigenfunction for the stable eigenvalue $\lambda \approx -4$ (see also Fig. 3.12). The random perturbation causes almost the same error as in the previous case and therefore is not plotted. The error $E_{stab}(t)$ produced by a solution given by the initial perturbation by an approximate stable eigenstate demonstrate first the same phenomena as the unstable solution. The difference appears afterwards when the growth rates of the stable and unstable solution clearly separate, with an exponential growth dominating the behavior of the unstable case and oscillatoric behavior in the stable case.

Certainly, we should endeavour to find the precise form of the eigenfunctions since they are relevant not only to the direct simulations but also to numerical calculation of the Krein signature. The proposed methods are finite element method used in [5] or implementation of a multiple shooting method similar to the one already used here for improvement of the exact numerical solutions of the Gross-Pitaevskii equation.

Chapter 4

The Landau-Lifshitz magnetization equation

The material in this Chapter documents that the Landau-Lifshitz equation

$$m_t = m \times \triangle m - \lambda m \times m \times \triangle m, \tag{4.1}$$

($\lambda \in \mathbb{R}$, $m = (m_1, m_2, m_3)$, $m : \mathbb{R}^2 \to \mathbb{S}^2$) does not support existence of any non-stationary vortices or localized vortex-like solutions (e.g. encapsulated vortices) of finite energy. While this is clear if dissipation is present ($\lambda > 0$), surprisingly it remains true in the absence of dissipation (when $\lambda = 0$). Note that although the Landau-Lifshitz equation does not have a priori the structure of the nonlinear Schrödinger equation, written using the stereographic projection, it transforms to such a form [52].

4.1 Derivation of the Landau-Lifshitz equation

The Landau-Lifshitz equation, often called also the magnetization equation, describes the time evolution of the density of the magnetic moment (magnetization) m in a ferromagnetic medium [53]. The magnetic moment is primarily created by electron spins. Its magnitude is approximately constant for temperatures below the Curie point. A detailed discussion of the Landau-Lifshitz equation can be

found in Komineas and Papanicolaou [54], Visintin [55] and Kosevich, Ivanov and Kovalev [56].

The dynamics of the Landau-Lifshitz equation is derived from the general torque equation [57]

$$m_t = \gamma_0 L = \gamma_0 m \times h \,,$$

where L is the magnetic torque, h is the effective intensity of the magnetic field and $\gamma_0 = \frac{ge}{2m_e c}$ is a constant (e is the electron charge, m_e is the unit electron mass, c is the speed of light and g is the gyromagnetic ratio, $g \approx 2$). To preserve the magnitude $|m|$ of the magnetic moment it is traditional to include the Ginzburg-Landau phenomenological dissipative term [54]

$$m_t = \gamma_0 m \times h - \lambda m \times (m \times h) \,, \tag{4.2}$$

where λ is a dissipation constant — typically $\gamma_0 > \lambda$ (often $\gamma_0 >> \lambda$). The equation (4.2) is referred to as the Landau-Lifshitz equation [53] and is formally equivalent to the Gilbert equation:

$$m_t = \gamma(L - \eta m \times m_t) \,.$$

The effective intensity h of the magnetic field is the negative variational derivative of the free energy $E(m)$

$$h = -\frac{\delta E}{\delta m} \,.$$

The free energy $E(m)$ in two-dimensional models consists in general of four different terms [55]:

$$E(m) = \int_\Omega \left(\frac{1}{2} \sum_{i,j=1}^{3} a_{ij} \frac{\partial m}{\partial x_i} \cdot \frac{\partial m}{\partial x_j} + \Phi(m) - H_{app} \cdot m + \frac{1}{8\pi} |H_{dem}(m)|^2 \right) dx \tag{4.3}$$

where the individual contributions in (4.3) represent the exchange, the anisotropy, the applied magnetic field and the demagnetizing field energies. The symmetric

tensor (a_{ij}) is assumed to be positive definite, the function $\Phi : \mathbb{S}^2 \to \mathbb{R}$ depends on the internal structure of the ferromagnet and is assumed to be smooth and convex (as defined on $\mathbb{R}^3$), H_{app} is a prescribed divergence-free applied magnetic field and H_{dem} is the demagnetizing magnetic field given by the magnetostatic equations (a simpler form of the Maxwell equations)

$$\nabla \cdot (H_{dem} + 4\pi m) = 0 \qquad \text{and} \qquad \nabla \times H_{dem} = 0\,.$$

In what follows only the two-dimensional model (i.e. $m : \mathbb{R}^2 \to \mathbb{S}^2$) in the whole plane $\Omega = \mathbb{R}^2$ will be considered. Moreover, assume that the leading term of the free energy — the exchange energy — is uniform and diagonal and dominates all the other sources of the free energy, so

$$E(m) = \int_{\mathbb{R}^2} \frac{1}{2}|\nabla m|^2 dx\,. \tag{4.4}$$

Then (4.2) yields (4.1).

4.1.1 Properties of the Landau-Lifshitz equation

An easy calculation shows that the constraint $|m| = 1$ is preserved in time by (4.1). A numerical scheme for (4.1) was recently proposed by E and Wang [58].

For $\lambda = 0$ the equation (4.1) reduces to

$$m_t = m \times \triangle m \tag{4.5}$$

and describes the Hamiltonian (symplectic) flow of harmonic mappings into $\mathbb{S}^2$. If $\lambda = \infty$ the equation (4.1) reduces to $m_t = \triangle m + |\nabla m|^2 m$ (since $-m\times(m\times\triangle m) = \triangle m + |\nabla m|^2 m$ for $|m| = 1$) and describes heat flow of harmonic maps into $\mathbb{S}^2$.

Another common form of (4.1) is the so-called easy-axis magnetization, for which the one-direction anisotropy energy term dominates the total free energy

(4.3),

$$m_t = m \times \triangle m + \lambda m \times (m_3 \hat{z})\,, \tag{4.6}$$

where $\hat{z}$ is the z-direction unit vector [59].

The effect of individual terms on dynamics of (4.1) can be inferred by the following simplified considerations. First, since $-m \times (m \times h) = h - (m \cdot h)m$ for $|m| = 1$, the second term on the right-hand side of (4.1) act as a projection and forces m to tend to the direction of $h = \triangle m$. It dissipates the energy because

$$\frac{d}{dt}E(m) = -\int m_t \cdot h dx = -\lambda \int |m \times h|^2 dx < 0\,.$$

On the other hand, the term $m \times h$ is not dissipative and is perpendicular to both m and h and forces m to rotate around h. The total effect of terms on the right hand side of (4.1) results in a non-planar spiral revolution of a unit vector m asymptotically tending to $h/|h|$.

4.2 The Landau-Lifshitz equation in spherical coordinates

For further study it is convenient to transform the Landau-Lifshitz equation using spherical coordinates:

$$m_1 = \cos\psi \sin\phi, \qquad m_2 = \sin\psi \sin\phi, \qquad m_3 = \cos\phi\,.$$

The functions ϕ and ψ naturally map the plane $\mathbb{R}^2$ into $[0, \pi)$ and $[0, 2\pi)$ respectively, but they will be allowed to have as their values any real numbers and the value will be always considered modulo the appropriate constant (π and 2π respectively). In this setting (4.1) turns into

$$\phi_t = -F + \lambda G\,, \qquad\qquad \psi_t \sin\phi = G + \lambda F\,, \tag{4.7}$$

where

$$F = \sin\phi\triangle\psi + 2\cos\phi\nabla\phi\cdot\nabla\psi \qquad \text{and} \qquad G = \triangle\phi - \sin\phi\cos\phi(\nabla\psi)^2\,.$$

The goal is to search for standing wave solutions represented in polar coordinates (r,θ) as

$$\phi = \phi(r), \qquad \psi = n\theta + \omega t + \psi_0\,, \tag{4.8}$$

where n is a vortex degree, ω is the angular velocity (frequency) and ψ_0 is the initial phase. Then $F = 0$ and $\phi_t = 0$, so (4.7) becomes

$$\lambda G = 0\,, \qquad \psi_t \sin\phi = G\,.$$

Thus either $G = 0$ and then $\Psi_t \sin\Phi = 0$ or $\lambda = 0$. In the first case any nontrivial solution $\Phi \neq 0$ must have $\omega = 0$ and hence stationary solutions. If $\lambda = 0$ the equation (4.1) reduces to (4.5). Then (4.7) yields

$$\phi_{rr} + \frac{1}{r}\phi_r - \sin\phi\cos\phi\frac{n^2}{r^2} = \omega\sin\phi\,. \tag{4.9}$$

Note the similarity with the structure of the cubic nonlinear Schrödinger equation [15].

To avoid the singularity at $r = 0$ one can exploit with minor modifications the technique of Iaia and Warchal [15]. The proper initial conditions are

$$\lim_{r\to 0^+}\frac{1}{r^n}\phi(r) = d \quad \text{and} \lim_{r\to 0^+}\frac{1}{r^{n-1}}\phi'(r) = nd\,. \tag{4.10}$$

From now on it will be assumed for simplicity that $d > 0$. The form of these conditions implies that to specify a solution one only needs to prescribe one of them. The energy E of a solution of the form (4.8) is given by

$$E = \pi\int_0^\infty \left(\phi_r^2 + \frac{n^2}{r^2}\sin^2\phi\right) r dr\,. \tag{4.11}$$

Similarly, following [15] it is possible to justify the global existence of the solutions and uniqueness for the initial value problem (4.9)–(4.10). If $\Phi(r)$ is approaching a constant value at infinity for $\omega \neq 0$, (4.9) implies $\lim_{r\to\infty} \phi(r) = k\pi$ for an integer k. It will be shown further that k must be 0, 1 or 2. All such solutions have locally finite energy over any finite interval $(0, R)$. Any other initial condition not in agreement with $\phi(0) = 0$ (e.g. $\phi(0) = \frac{\pi}{2}$) clearly leads to a locally infinite energy in some neighborhood of 0.

4.3 The main result

The main result of this Chapter is the following.

Theorem 4.3.1. *For any $\omega \neq 0$, any $\lambda \in \mathbb{R}$ and any $d > 0$ the only solution $\phi(r)$ to (4.9)–(4.10) oscillates infinitely many times about the value π as $r \to \infty$ and has an infinite energy (4.11).*

The statement of Theorem 4.3.1 is particularly interesting if $\lambda = 0$ since in the case of $\lambda \neq 0$ one can use either the above mentioned argument or the Derrick-Pohozaev scaling to rule out any non-stationary solutions. Unfortunately for $\lambda = 0$ the energy associated with (4.1) is invariant in such a scaling and this simple argument cannot be used here. The behavior of a solution is illustrated on Fig. 4.1.

One can use similar arguments to show that the natural energy associated with the Bessel functions,

$$E_B = \int_0^\infty r u_r^2(r) + \frac{1}{r} u^2(r) dr \,,$$

is infinite for every Bessel function, a solution to the Bessel equation

$$r^2 u'' + r u' + (r^2 - n^2) u = 0 \,.$$

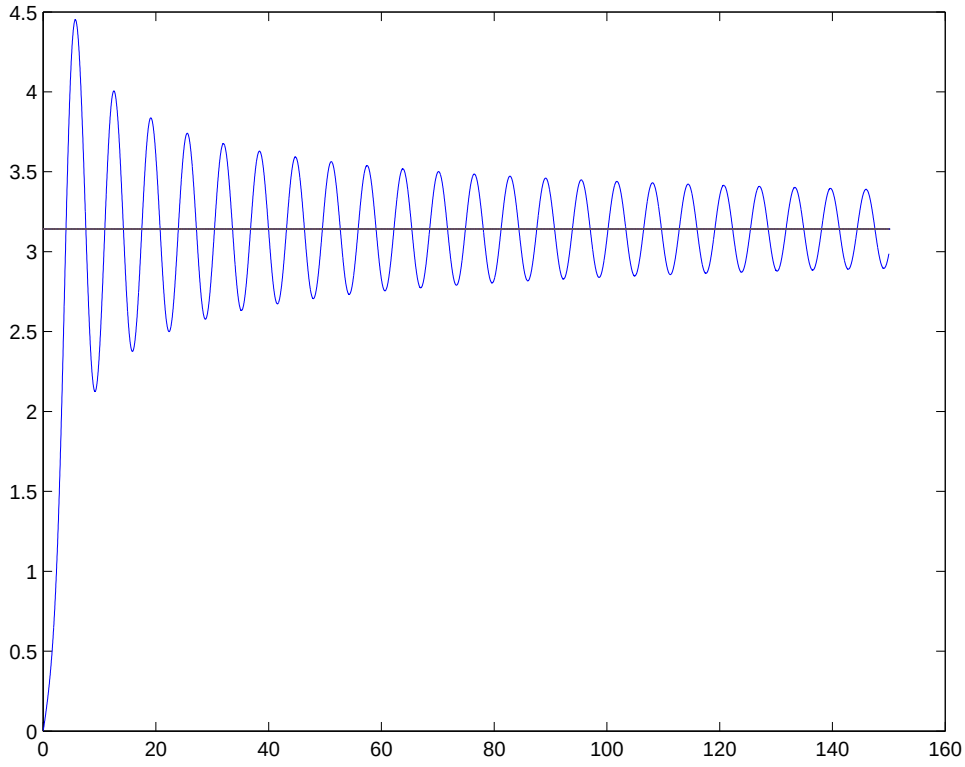

Figure 4.1: The radial profile of a generic non-stationary solution to the Landau-Lifshtiz equation

4.4 Vortex solutions to the Landau-Lifshitz equation

The connection between solutions to (4.1) of the structure (4.8) and vortices introduced in Chapter 2 is straightforward. One needs to transform the solution (4.8) written in the spherical coordinates by the stereographic projection which transforms (4.1) into nonlinear Schrödinger equation

$$iw_t = -\triangle w - 2\,\frac{\nabla w \cdot \nabla w}{1+|w|^2}\bar{w}\,. \tag{4.12}$$

The solution w to (4.12) is given by $w = u + iv$, where u and v are defined by

$$m_1 = \frac{2u}{1+u^2+v^2}\,, \quad m_2 = \frac{2v}{1+u^2+v^2}\,, \quad m_3 = \frac{u^2+v^2-1}{1+u^2+v^2}\,.$$

Here m is a solution to (4.1), $|m| = 1$. Then

$$u = \frac{\cos\psi \pm |\cos\psi||\cos\phi|}{\sin\phi}, \qquad v = u\tan\psi\,. \tag{4.13}$$

For simplicity ignore the absolute values in (4.13). The two choices of the sign $\pm$ in (4.13) yield two different formulas for a solution w to (4.12)

$$w = e^{i\psi}\cot\frac{\phi}{2}, \qquad \text{and} \qquad w = e^{i\psi}\tan\frac{\phi}{2}\,.$$

Clearly, this is the exactly same setting for a vortex solution as it was introduced in Chapter 2,

$$w(r,\theta,t) = e^{i(n\theta+\omega t+\theta_0)}U(r)\,. \tag{4.14}$$

The appropriate choice of the form of the function $U(r)$ in (4.14) is given by the sign of ω as will be later clarified in Lemma 4.4.2.

The following simple facts about the symmetries and scaling properties of the solutions to (4.9) will be stated without proof. Note that the proposition does not take into account the initial condition (4.10).

Proposition 4.4.1.

- *If $\phi(r)$ is a solution of (4.9) then $\phi^*(r) = -\phi(r)$ is a solution too.*
- *If $\phi(r)$ is a solution of (4.9) then $\phi^*(r) = 2\pi + \phi(r)$ is a solution too.*
- *If $\phi(r)$ is a solution of (4.9) for a parameter ω then $\phi^*(r) = \pi \pm \phi(r)$ is a solution of the same equation for a parameter $-\omega$.*

- *If $\phi(r)$ is a solution of (4.9) for a parameter ω then $\phi^*(r) = \phi(\lambda r)$ is a solution of the same equation for a parameter $\lambda^2\omega$. (Thus one can always assume that $\omega = 1$, $\omega = -1$ or $\omega = 0$.)*

First, consider the case $\omega = 0$. In two dimensions there exist stationary solutions to (4.1), the Belavin-Polyakov instantons. These solutions are harmonic maps from $\mathbb{R}^2$ into $\mathbb{S}^2$. The equation (4.9) becomes integrable and all the solutions satisfying (4.10) are

$$\phi(r) = 2\tan^{-1}\left(\frac{d}{2}r^n\right). \tag{4.15}$$

Note that such a solution has a finite energy (4.11).

The next lemma shows that a solution of the problem (4.9)–(4.10) is bounded.

Lemma 4.4.2. *Let $\phi(r)$ be a solution to (4.9)–(4.10) for $\omega = 1$ or $\omega = -1$ respectively. Then $\phi(r)$ is bounded, $0 < \phi(r) < 2\pi$ for all $r > 0$ or $-\pi < \phi(r) < \pi$ respectively.*

Proof. First, let $\omega > 0$. Multiply (4.9) by the term $r^2\phi_r(r)$ to obtain

$$\frac{\partial}{\partial r}\left(\frac{r^2\phi_r^2}{2}\right) + \frac{\partial}{\partial r}\left(\frac{n^2}{4}\cos 2\phi\right) = -\omega r^2\frac{\partial}{\partial r}\left(\cos\phi\right).$$

By integrating the last identity on interval (R, r) and using integration by parts it is possible to derive *the Pohozaev identity:*

$$\begin{aligned}&\frac{1}{2}\left(r^2\phi_r^2(r) - R^2\phi_r^2(R)\right) + \frac{n^2}{4}(\cos 2\phi(r) - \cos 2\phi(R))\\ &= 2\omega\int_R^r s(\cos\phi(s) - \cos\phi(r))ds + \omega R^2(\cos\phi(R) - \cos\phi(r)).\end{aligned} \tag{4.16}$$

Setting $R = 0$ in (4.16) and using $\lim_{r\to 0}\phi(r) = 0$ the initial condition (4.10) implies $\phi(s) > 0$ on $(0, r)$ for some $r > 0$. Then

$$\frac{1}{2}r^2\phi_r^2(r) - \frac{n^2}{2}\sin^2\phi(r) = 2\omega\int_0^r s(\cos\phi(s) - \cos\phi(r))ds. \tag{4.17}$$

If there exists $r > 0$ such that $\phi(r) = 0$ (assume that $\phi(s) > 0$ on $(0, r)$) then by (4.17)

$$0 \leq r^2\phi^2(r) = 4\omega \int_0^r s(\cos\phi(s) - 1)ds < 0\,,$$

which yields a contradiction. Hence $\phi(r) > 0$ for all $r > 0$. The very same argument can be used to prove that $\phi(r) < 2\pi$ for all $r > 0$. Similarly in the case $\omega < 0$ one can prove $-\pi < \phi(r) < \pi$ for all $r > 0$. □

Lemma 4.4.3. *Let $\phi(r)$ be a solution to (4.9)–(4.10) for $\omega > 0$ and let r be a point of local maximum (resp. a local minimum) of $\phi(r)$, $r > \frac{n}{\sqrt{\omega}}$. Then $\phi(r) > \pi$ (resp. $\phi(r) < \pi$). If $\omega < 0$ then $\phi(r) > 0$ (resp. $\phi(r) < 0$).*

Proof. Since $r^2\omega > n^2$, it follows $\omega + \cos\phi(r)\frac{n^2}{r^2} > 0$. Then by (4.9)

$$\phi_{rr} = -\frac{1}{r}\phi_r + \sin\phi\left(\omega + \cos\phi\frac{n^2}{r^2}\right) = \sin\phi\left(\omega + \cos\phi\frac{n^2}{r^2}\right)\,.$$

Thus the sign of ϕ_{rr} is the same as the sign of $\sin\phi$. The statement immediately follows by Lemma 4.4.2. Similar arguments prove the statement for $\omega < 0$. □

4.5 Non-existence of vortex solutions

In this section we demonstrate that the only possible type of a solution to (4.9)–(4.10) is an *infinitely oscillating solution* by eliminating all the other types.

The list all the possible behaviors of radial profiles of vortex-like solutions to (4.9)–(4.10) for $\omega > 0$ using Lemma 4.4.2–4.4.3 (omitting the trivial solutions $\phi(r) = k\pi$) is not so long (the similar classifications exists also for $\omega < 0$):

- *pure vortex solution* – growing for all $r > \frac{n}{\sqrt{\omega}}$, and satisfying

$$\lim_{r\to\infty}\phi(r) = \pi \quad \text{or} \quad 2\pi\,,$$

- *encapsulated vortex solution* – any solution satisfying

$$\lim_{r\to\infty}\phi(r)=0\,,$$

- *finitely oscillating solution* – any solution satisfying

$$\lim_{r\to\infty}\phi(r)=\pi\,,$$

  which is monotone on some interval (R,∞);

- *infinitely oscillating solution* (also called *oscillating solution*) – any solution satisfying

$$\lim_{r\to\infty}\phi(r)=\pi\,,$$

  which is not monotone on any interval (R,∞).

The main result of this section is stated in the next Theorem.

Theorem 4.5.1. *There are no solutions to (4.9)–(4.10) for $\omega > 0$ with the property $\lim_{r\to\infty}\phi(r)=0$, i.e. there are no encapsulated vortex solutions.*

Proof. Assume the contrary. Let $\phi(r)$ be a solution to (4.9)–(4.10) satisfying the boundary condition $\lim_{r\to\infty}\phi(r)=0$. Since $\phi(r)>0$ for some small positive r, it has at least one local maximum. Fix R to be any of them. Then (4.16) yields

$$\begin{aligned}&\frac{1}{2}r^2\phi_r^2(r)+\frac{n^2}{4}(\cos 2\phi(r)-\cos 2\phi(R))\\&=2\omega\int_R^r s(\cos\phi(s)-\cos\phi(r))ds+\omega R^2(\cos\phi(R)-\cos\phi(r))\,.\end{aligned}\quad(4.18)$$

Let us moreover assume that $\phi(R)\neq\pi$ ($\phi(R)\neq 0$ by Lemma 4.4.2). So $\cos 2\phi(R)<1$. By Lemma 4.4.3 such a solution must be decreasing for r large enough so we can choose r to satisfy both $\cos\phi(s)<\cos\phi(r)$ for all $s\in(R,r)$

and $\cos 2\phi(R) < \cos 2\phi(r)$. Then the left hand side of (4.18) is positive while the right hand side is negative yielding a contradiction.

In the case of $\phi(R) = \pi$ the equation (4.18) becomes

$$\begin{aligned} \frac{r^2\phi_r^2(r)}{2} &= 2\omega \int_R^r s(\cos\phi(s) - \cos\phi(r))ds \\ &\quad + \omega R^2(-1 - \cos\phi(r)) - \frac{n^2}{4}(\cos 2\phi(r) - 1)\,. \end{aligned} \tag{4.19}$$

Again choose r large enough to satisfy $\cos\phi(s) < \cos\phi(r)$ for all $s \in (R, r)$ so the integral in (4.19) becomes negative. Then

$$\begin{aligned} \frac{1}{2}r^2\phi_r^2(r) &\leq -\omega R^2(1 + \cos\phi(r)) + \frac{n^2}{4}(1 - \cos 2\phi(r)) \\ &= 2\cos^2\frac{\phi(r)}{2}\left(n^2\sin^2\frac{\phi(r)}{2} - \omega R^2\right)\,. \end{aligned} \tag{4.20}$$

On the other hand, for r large enough $\phi(r)$ is positive and close to zero. Hence $\cos^2\frac{\phi(r)}{2} > 0$ and $n^2\sin^2\frac{\phi(r)}{2} < 2\omega R^2$. This contradicts (4.20). □

A similar statement is true for $\omega < 0$ but first one needs to prove the following lemma which estimates the possible rate of decay of such solutions.

Lemma 4.5.2. *If there exists a positive solution $\phi(r)$ to (4.9)–(4.10) for $\omega < 0$, such that $\lim_{r\to\infty}\phi(r) = 0$ then $n\phi(r) + r\phi_r(r) \geq 0$, i.e. $\phi(r) \geq \frac{1}{r^n}\phi(r_0)r_0^n$ for any $r > r_0 > 0$.*

Proof. For the sake of brevity set $\omega = -1$. The equation (4.9) can be rewritten as

$$\phi_{rr} + \frac{1}{r}\phi_r - \frac{n^2}{r^2}\phi = -\sin\phi + \frac{n^2}{r^2}\left(\frac{\sin 2\phi}{2} - \phi\right)\,. \tag{4.21}$$

Since $\sin 2\phi < 2\phi$ for $\phi > 0$ and $\phi(r) < \pi$ by Lemma 4.4.2, the right hand side of (4.21) is always negative. Hence

$$\phi_{rr} + \frac{1}{r}\phi_r - \frac{n^2}{r^2}\phi < 0\,.$$

Following the same calculation as in [15] set $\phi(r) = r^n u(r)$. Then for any $r > r_0 > 0$

$$u(r) < u(r_0) + u_r(r_0)\frac{r_0}{2n}\left[1 - \left(\frac{r_0}{r}\right)^{2n}\right].$$

After substitution $\phi(r) = r^n u(r)$ finally obtain

$$\phi(r) < \left(\frac{r}{r_0}\right)^n \left[\phi(r_0) + \left(\frac{r_0\phi_r(r_0)}{2n} - \frac{\phi(r_0)}{2}\right)\left(1 - \left(\frac{r_0}{r}\right)^{2n}\right)\right]. \tag{4.22}$$

The inequality (4.22) holds for any $r > r_0 > 0$. If there exists a positive solution to (4.9) then the term in the bracket must be positive for every such a pair (r, r_0). Therefore

$$\phi(r_0) + \left(\frac{r_0\phi_r(r_0)}{2n} - \frac{\phi(r_0)}{2}\right)\left[1 - \left(\frac{r_0}{r}\right)^{2n}\right] > 0\,.$$

Because r can be arbitrarily large, the difference $1 - \left(\frac{r_0}{r}\right)^{2n}$ can be arbitrarily close to one. Thus it is necessary that

$$\phi(r_0) + \left(\frac{r_0\phi_r(r_0)}{2n} - \frac{\phi(r_0)}{2}\right) \geq 0\,.$$

Integration over (r_0, r) then implies

$$\phi(r) \geq \frac{1}{r^n}\phi(r_0)r_0^n\,.$$

□

Proposition 4.5.3. *There is no solution to the system (4.9)–(4.10) for $\omega < 0$ with the property $\lim_{r\to\infty}\phi(r) = 0$ which is monotone on some interval (R, ∞), i.e. there are no encapsulated vortex solutions.*

Proof. First, a proof that there are no positive solutions to (4.9)–(4.10) for $\omega = -1$ such that $\lim_{r\to\infty}\phi(r) = 0$ will be presented.

Using the Pohozaev identity (4.16) on interval $(0, r)$ one arrives at

$$r^2\phi_r^2(r) - n^2\sin^2\phi(r) = -4\int_0^r s\,(\cos\phi(s) - \cos\phi(r))\,ds\,. \tag{4.23}$$

By Lemma 4.4.3 a solution $\phi(r)$ may not attain a local minimum for r large enough. Hence, if there exists a positive solution to (4.9)–(4.10) such that $\lim_{r\to\infty}\phi(r) = 0$ it must decrease monotonically to zero on (r,∞) for some r large enough. Then Lemma 4.5.2 implies $0 > r\phi_r \geq -n\phi$ and $r^2\phi_r^2 \leq n^2\phi^2$. Combining it with (4.23) yields

$$-4\int_0^r s\left(\cos\phi(s) - \cos\phi(r)\right) ds \leq n^2(\phi^2 - \sin^2\phi)\,. \tag{4.24}$$

Pass to the limit $r \to \infty$ on both sides of (4.24), then

$$\lim_{r\to\infty} n^2(\phi^2 - \sin^2\phi) = 0$$

on the right hand side. On the other side

$$\lim_{r\to\infty} 4\int_0^r s\left(\cos\phi(r) - \cos\phi(s)\right) ds = 4\int_0^\infty s\left(1 - \cos\phi(s)\right) ds > 0$$

(the integrand is a positive quantity which justifies the limit) yields a contradiction for any nontrivial solution.

If $\phi(r)$ is not positive, it is by the assumption monotone on some interval (R,∞). Assume $\phi(r)$ decreases to zero at infinity (if it increases, one needs to perform the transformation $\tilde{\phi}(r) = -\phi(r)$ first). If $\phi(r)$ is not positive for all $r \in (0,\infty)$, then there exist $R > 0$, such that $\phi(R) = 0$ and $\phi(r) > 0$ for $r > R$. Hence one can exploit Lemma 4.5.2 on the interval (R,∞) and repeat the above arguments for positive solutions to prove the statement of the proposition just by replacing zero by R in the proof. □

Proposition 4.5.4. *There is no solution to the system (4.9)–(4.10) for $\omega > 0$ with the property $\lim_{r\to\infty}\phi(r) = \pi$ or $\lim_{r\to\infty}\phi(r) = 2\pi$ growing for all $r > \frac{n}{\sqrt{\omega}}$, i.e. there are no pure vortex solutions.*

Proof. First, assume that $\lim_{r\to\infty}\phi(r) = \pi$. Then $\tilde{\phi} = \pi - \phi$ solves (4.9) for $\omega < 0$ with the initial condition $\tilde{\phi}(0) = \pi$. Clearly $\lim_{r\to\infty}\tilde{\phi}(r) = 0$. The monotonicity ensures that the solution is decreasing on the interval $\left(\frac{n}{\sqrt{\omega}}, \infty\right)$. The non-existence of such a solution was already proved in Theorem 4.5.3.

Therefore also assume that $\lim_{r\to\infty}\phi(r) = 2\pi$. This is a slight modification of an argument used in the proof of Theorem 4.5.3.

Apply the Pohozaev identity (4.16) on a interval $(0, r)$ to obtain

$$r^2\phi_r^2(r) = n^2\sin^2\phi(r) + 4\omega\int_0^r s\left(\cos\phi(s) - \cos\phi(r)\right)ds\,. \tag{4.25}$$

The left hand side of (4.25) is a positive quantity $r^2\phi_r^2(r) \geq 0$. The integral can be rewritten as a sum of two integrals

$$4\omega\int_0^R s\left(\cos\phi(s) - \cos\phi(r)\right)ds + 4\omega\int_R^r s\left(\cos\phi(s) - \cos\phi(r)\right)ds\,.$$

Let R be chosen such that $\phi(r) > \frac{3}{2}\pi$ for all $r > R$. Then for $r > R$ the argument of the second integral is a negative quantity and one can pass to the limit $r \to \infty$:

$$4\omega\int_0^R s\left(\cos\phi(s) - \cos\phi(r)\right)ds \to 4\omega\int_0^R s\left(\cos\phi(s) - 1\right)ds < 0$$

and $n^2\sin^2\phi(r) \to 0$, $4\omega\int_R^r s\left(\cos\phi(s) - \cos\phi(r)\right) \to L < 0$. Hence the limit of the right hand side of (4.25) is negative — a contradiction. □

Proposition 4.5.5. *There is no solution to the system (4.9)–(4.10) for $\omega < 0$ with the property $\lim_{r\to\infty}\phi(r) = \pi$ or $\lim_{r\to\infty}\phi(r) = -\pi$ monotone for all $r > \frac{n}{\sqrt{\omega}}$, i.e. there are no pure vortex solutions.*

Proof. First, assume that $\lim_{r\to\infty}\phi(r) = \pi$ (for $\lim_{r\to\infty}\phi(r) = -\pi$ the proof is analogical using the transformation $\tilde{\phi} = -\phi$).

It is plausible to transform the solution to $\tilde{\phi} = \pi - \phi$ to obtain the solution $\tilde{\phi}$ to (4.9) for $\omega > 0$ satisfying the initial condition $\tilde{\phi}(0) = \pi$. For simplicity

all tildes tildes in the rest of this proof will be omitted. One can use the same arguments as in the proof of Theorem 4.5.4 to show the non-existence of such solutions: apply the Pohozaev identity on $(0, r)$ to get

$$r^2\phi_r^2 = n^2 \sin^2\phi + 4\omega \int_0^r s\,(\cos\phi(s) - \cos\phi(r))\,ds$$

and then send $r \to \infty$. The left-hand side has a positive limit while the right-hand side has a negative limit (justification of the existence of the limit can be done exactly as in the proof of Proposition 4.5.4). □

Proposition 4.5.6. *There is no solution to the system (4.9)–(4.10) for $\omega > 0$ with the property $\lim_{r\to\infty}\phi(r) = \pi$ monotone on some interval (R, ∞), $R > 0$, i.e. there are no finitely oscillating solutions.*

Proof. One can again combine the same arguments as in the proofs of previous theorems. First, by the transformation $\tilde{\phi} = \pi + \phi$ obtain a solution $\tilde{\phi}$ to (4.9) for $\omega < 0$ satisfying the initial condition $\tilde{\phi}(0) = -\pi$ with the property

$$\lim_{r\to\infty} \tilde{\phi}(r) = 0\,.$$

The non-existence of such a solution is then guaranteed by Proposition 4.5.3. The only difference is in the initial condition but the second part of the proof of Proposition 4.5.3 is independent on initial data. □

Notice that by Lemma 4.4.3 there are no *finitely oscillating solutions* for $\omega < 0$ which were not covered by Proposition 4.5.3 or 4.5.5.

4.6 Energy of oscillating solutions

The aim of this final section is to prove Theorem 4.3.1. The first statement of Theorem 4.3.1, the oscillating character of the solution, follows from Propo-

sitions 4.5.1–4.5.6 of the previous section where all the other possible profile behaviors of $\phi(r)$ for both $\omega > 0$ and $\omega < 0$ were ruled out. Thus one only need to show that such a solution has an infinite energy (4.11). This fact is not a priori clear (the stationary solutions (4.15) for $\omega = 0$ all have finite energy) because both terms in the energy formula (4.11) have the same scaling properties. This suggests a strong energetic instability of any vortex structures for $\omega \neq 0$.

The outline of the proof is following: First is a proof of the statement for $\omega > 0$ (the proof for $\omega < 0$ is analogical). By the scaling properties of the energy and the scaling invariance of the equation (4.9) (see Proposition 4.4.1) one can also assume without loss of generality that $\omega = 1$. Assume that the contrary is true – the solution has finite energy. Using that fact it is not difficult to show that the solution must "monotonically" decay to π (Lemma 4.6.1). Then the solution will be shifted to oscillate around 0 instead of π by the transformation $\phi \to \phi - \pi$. The transformed solution solves (4.9) with $\omega = -1$. Finally, the key ingredient is that for such a solution the energy (4.11) has the same character as the energy $E^* = \int r\phi^2 + r\phi_r^2 dr$. Finally, using the polar coordinates in the phase plane (similarly as in Sturm-Liuville theory), it will be demonstrated that the energy E^* (and so E) is infinite.

Let $\phi(r)$ be a solution to (4.9)–(4.10) for fixed parameter d in (4.10). It is convenient to introduce $(a_i)_1^\infty$, $(b_i)_1^\infty$ and $(c_i)_1^\infty$, the increasing infinite sequences of the intercepts of $\phi(r)$ with $y = \pi$ and the sequences of local maxima and local minima of $\phi(r)$ respectively. By neglecting first few terms and by Lemma 4.4.3 one may assume $a_1 < b_1 < a_2 < c_1 < a_3 < b_2 < \dots$, i.e. $a_{2i-1} < b_i < a_{2i} < c_i < a_{2i+1}$ for $i \geq 1$. For simplification define $(r_i)_1^\infty$, $r_1 = a_1$, $r_2 = b_1$, $r_3 = a_2$, $r_4 = c_1$, etc.,

i.e. the increasing sequence (r_i) is the "ordered" union of the sequences (a_i), (b_i) and (c_i).

Lemma 4.6.1. *Assume that the solution $\phi(r)$ to (4.9)–(4.10) has finite energy. Then*

$$\lim_{r\to\infty} \phi(r) = \pi \tag{4.26}$$

and the convergence is "monotone"

$$|\phi(b_i) - \pi| > |\pi - \phi(c_i)| > |\phi(b_{i+1}) - \pi| \qquad \text{for } i \geq i_0,$$

for some $i_0 \geq 1$, where (b_i), (c_i) are defined above.

Written in terms of the sequence (r_i):

$$|\phi(r_{2i}) - \pi| > |\pi - \phi(r_{2i+2})| \qquad \text{for } i \geq i_0.$$

Proof. The inequality $|ab| \leq \frac{a^2+b^2}{2}$ implies

$$\left| \int_a^b \phi_r(r) \sin\phi(r) dr \right| \leq \int_a^b |\phi_r(r) \sin\phi(r)|\, dr \leq \frac{1}{2} \int_a^b r\phi_r^2(r) + \frac{\sin^2\phi(r)}{r} dr\,.$$

Thus

$$|\cos\phi(b) - \cos\phi(a)| \leq \frac{1}{2} \int_a^b r\phi_r^2(r) + \frac{\sin^2\phi(r)}{r} dr\,. \tag{4.27}$$

Since the problem (4.9)–(4.10) is well-posed the integrals on the right-hand side of (4.27) are finite for $0 \leq a < b < \infty$. Then by (4.27)

$$|\cos\phi(r_{i+1}) - \cos\phi(r_i)| \leq \frac{1}{2} \int_{r_i}^{r_{i+1}} r\phi_r^2(r) + \frac{\sin^2\phi(r)}{r} dr$$

and

$$\sum_{i=1}^{\infty} |\cos(r_i) - \cos(r_{i+1})| \leq \frac{1}{2} \int_{r_1}^{\infty} r\phi_r^2(r) + \frac{\sin^2\phi(r)}{r} dr < \infty\,,$$

where the integral on the right-hand side converges by the assumption of the lemma

$$\int_0^\infty r\phi_r^2(r)dr < \infty \qquad \text{and} \qquad \int_0^\infty \frac{\sin^2\phi(r)}{r}dr < \infty\,.$$

Since $\cos\phi(r_{2i-1}) = -1$, for all $i \geq 1$, we have

$$|\cos\phi(r_{2i-1}) - \cos\phi(r_{2i})| + |\cos\phi(r_{2i}) - \cos\phi(r_{2i+1})| = 2|1 + \cos\phi(r_{2i})|\,.$$

Thus

$$\sum_{i=1}^{\infty} |1 + \cos(r_{2i})| < \infty\,, \qquad \lim_{i\to\infty} \cos\phi(r_{2i}) = -1$$

and (4.26) follows. The oscillating solution $\phi(r)$ converges to π, so it is possible to assume that $\pi/2 < \phi(r) < 3/2\pi$ for $r > R_0$ for some $R_0 > 0$.

Next, consider two consecutive local extremes at R and r (i.e. $(R, r) = (b_i, c_i)$ or $(R, r) = (c_i, b_{i+1})$), $r > R > R_0$, of $\phi(r)$. First, assume that

$$|\phi(R) - \pi| < |\phi(r) - \pi|\,. \tag{4.28}$$

The requirement $r > R > R_0$ assures that

$$0 > \cos\phi(r) > \cos\phi(R)\,. \tag{4.29}$$

By Pohozaev identity (4.16) applied on interval (R, r)

$$(\cos\phi(r) - \cos\phi(R))\left[\frac{n^2}{2}(\cos\phi(r) + \cos\phi(R)) + R^2\right] = 2\int_R^r s\,(\cos\phi(s) - \cos\phi(r))\,ds\,. \tag{4.30}$$

For R large enough ($R > |n|$) it holds

$$R^2 + \frac{n^2}{2}(\cos\phi(r) + \cos\phi(R)) \geq R^2 - n^2 > 0\,.$$

The inequality (4.29) implies $\cos\phi(r) - \cos\phi(R) > 0$, so the left-hand side of the equation (4.30) is positive. On the other hand, $\cos\phi(r)$ is the maximum value of

$\cos\phi(s)$ on the interval (R, r) so the integral on the right-hand side of (4.30) is negative. This yields a contradiction with the assumption (4.28). One can easily derive by the same argument that $|\pi - \phi(r)| = |\pi - \phi(R)|$ is not possible as well.

Simple considerations prove that for two consecutive local extremes located at R and r, $r > R > R_1$, $R_1 = \max\{R_0, |n|\}$, of $\phi(r)$ the following inequality holds.

$$|\pi - \phi(r)| < |\pi - \phi(R)| \,.$$

Let us mention two other consequences of a "monotone" convergence

$$0 > \cos\phi(R) > \cos\phi(r) \qquad \text{and} \qquad \cos\phi(r_{2i}) \searrow -1 \,.$$

□

It is very convenient to consider a solution $\phi(r)$ oscillating around $y = 0$ instead of around $y = \pi$. Therefore, introduce

$$\tilde{\phi} = \phi - \pi \,.$$

Then $\tilde{\phi}$ solves (see also Proposition 4.4.1)

$$\tilde{\phi}_{rr} + \frac{1}{r}\tilde{\phi}_r - \sin\tilde{\phi}\cos\tilde{\phi}\frac{n^2}{r^2} = -\sin\tilde{\phi} \,,$$

i.e. $\tilde{\phi}$ solves (4.9) for $\omega = -1$ with the initial condition $\tilde{\phi}(0) = -\pi$. Since the initial condition does not enter the arguments in this section (it was only used to prove the oscillating character of $\phi(r)$), we drop tildes and from now on assume only

$$\phi_{rr} + \frac{1}{r}\phi_r - \sin\phi\cos\phi\frac{n^2}{r^2} = -\sin\phi \tag{4.31}$$

and that $\phi(r)$ oscillates around 0. Clearly, the location of the points (r_i), (a_i), (b_i) and (c_i) does not change in this transformation and Lemma 4.6.1 implies

$$\phi(r) \to 0 \qquad \text{and} \qquad |\phi(r_{2i})| > |\phi(r_{2i+2})| \quad \text{for } i \geq i_0.$$

Lemma 4.6.2. *Let $\phi(r)$ be a non-trivial solution to (4.31) and (a_i) and i_0 be defined as above. Then for every $\varepsilon > 0$ there exists $i_1 \geq i_0$ such that for every $i \geq i_1$,*

$$\frac{5}{6}(1-\varepsilon)\int_{a_i}^{a_{i+1}} r\phi^2(r)dr \leq \int_{a_i}^{a_{i+1}} r\phi_r^2(r)dr \leq (1+\varepsilon)\int_{a_i}^{a_{i+1}} r\phi^2(r)dr\,. \qquad (4.32)$$

Proof. First, by the integration by parts

$$\int_{a_i}^{a_{i+1}} r\phi_r^2 dr = \phi r\phi_r|_{a_i}^{a_{i+1}} - \int_{a_i}^{a_{i+1}} \phi(\phi_r + r\phi_{rr})dr\,.$$

Since $\phi(a_i) = 0$, (4.31) gives

$$\phi_r + r\phi_{rr} = r\left(\frac{n^2}{r^2}\sin\phi\cos\phi - \sin\phi\right)\,.$$

Hence

$$\int_{a_i}^{a_{i+1}} r\phi_r^2(r)dr = \int_{a_i}^{a_{i+1}} r\phi\sin\phi\left(1 - \frac{n^2}{r^2}\cos\phi\right)dr\,. \qquad (4.33)$$

For any fixed n there exists $R_1 > 0$ such that for every r, $r > R_1$ the inequality $\left|\frac{n^2}{r^2}\cos\phi\right| < \varepsilon$ is true independently of a behavior of $\phi(r)$. Thus by (4.33)

$$(1-\varepsilon)\int_{a_i}^{a_{i+1}} r\phi\sin\phi dr \leq \int_{a_i}^{a_{i+1}} r\phi_r^2(r)dr \leq (1+\varepsilon)\int_{a_i}^{a_{i+1}} r\phi\sin\phi dr\,. \qquad (4.34)$$

The Taylor expansion of $\sin x$ implies the following simple calculus inequality

$$\frac{5}{6}x^2 < x\sin x < x^2 \quad \text{for every } |x| \leq 1,\ x \neq 0\,.$$

Setting $x = \phi(r)$ and shifting R_1 if necessary (condition $|\phi(r)| \leq 1$ is required) yields by (4.34)

$$\frac{5}{6}(1-\varepsilon)\int_{a_i}^{a_{i+1}} r\phi^2 dr \leq \int_{a_i}^{a_{i+1}} r\phi_r^2(r)dr \leq (1+\varepsilon)\int_{a_i}^{a_{i+1}} r\phi^2 dr\,.$$

□

Note that the fraction $\frac{5}{6}$ can be removed from (4.32) by a small modification of the proof.

Corollary 4.6.3. *Let $\phi(r)$ be a solution to (4.31) with finite energy. Then the integral $\int_0^\infty r\phi^2(r)dr$ must be finite too.*

Proof. Using Lemma 4.6.2 we only need to show that $\int_0^\varepsilon r\phi^2 dr$ and $\int_0^\varepsilon r\phi_r^2(r)dr$ are finite for some $\varepsilon > 0$. That fact follows immediately from well-posedness of the problem. □

Based on Corollary 4.6.3 one may introduce a new "energy" quantity

$$E^* = \int_0^\infty r\phi^2(r) + r\phi_r^2(r)dr\,. \tag{4.35}$$

For $\psi(r)$ a solution to (4.9)–(4.10) the energy E^* has then the same character as the energy E, i.e. both quantities are both finite or both infinite (the term $\int_1^\infty r\phi^2(r)dr$ clearly dominates the term $\int_1^\infty \frac{\phi^2(r)}{r}dr$). Therefore it is enough to show that E^* is infinite for an (oscillating) solution $\phi(r)$ and in the rest of the work when referring to energy we will always refer to E^*.

Introduce new "polar" coordinates in the phase plane of $\phi(r)$:

$$\rho^2(r) = \phi^2(r) + \phi_r^2(r) \qquad \text{and} \qquad \theta(r) = \tan^{-1}\frac{\phi_r(r)}{\phi(r)} \quad \text{for } \phi(r) \neq 0. \tag{4.36}$$

For $\phi(r) = 0$ define

$$\theta(r) = \frac{\pi}{2}\operatorname{sgn}|\phi_r(r)|\,.$$

Furthermore, denote $e(r) = r\rho^2$ the energy density

$$E^* = \int_0^\infty r\rho^2 dr = \int_0^\infty e(r)dr\,.$$

Lemma 4.6.4. *Let $\phi(r)$ be a non-trivial solution to (4.31) and let (a_i), (b_i) and (c_i) and i_0 be defined as above. Let (a,b) be either an interval (a_{2i-1}, b_i) or (a_{2i}, c_i) for $i \geq i_2$ for some $i_2 \geq i_0$. Then*

$$\int_a^b e(r)dr \geq a^2\phi_r^2(a)\ln\left(\frac{b}{a}\right). \tag{4.37}$$

Proof. First note that by the choice of the interval (a,b): $\phi\phi_r > 0$ on (a,b). Then by (4.36)

$$\frac{\partial}{\partial r}e(r) = \frac{\partial}{\partial r}r\rho^2 = \phi^2 + \phi_r^2 + 2r\phi_r(\phi + \phi_{rr}).$$

Using the equation (4.31) it is possible to obtain

$$\frac{\partial}{\partial r}e(r) \;=\; \phi^2 - \phi_r^2 + 2r\phi_r\left(\phi - \sin\phi + \frac{n^2}{r^2}\sin\phi\cos\phi\right). \tag{4.38}$$

Since $\phi\phi_r > 0$ on (a,b), one also have

$$\phi_r(\phi - \sin\phi) > 0.$$

The choice of i_0 in Lemma 4.6.1 ensures that $|\phi(r)| < \pi/2$ for all $r > a_i$. Then on (a,b)

$$\phi_r \sin\phi\cos\phi > 0.$$

The last inequality combined with (4.38) yields

$$\frac{\partial}{\partial r}e(r) > -\phi^2 - \phi_r^2 = -\rho^2 = -\frac{e(r)}{r}.$$

Integrating the last inequality on (a,R), $R \leq b$ get

$$e(R) \geq e(a)\frac{a}{R}.$$

Finally, an integration over $R \in (a,b)$ proves the statement of the lemma:

$$\int_a^b e(r)dr \geq ae(a)\ln\left(\frac{b}{a}\right).$$

□

In Lemma 4.6.4 the energy E^* on subintervals (a_{2i-1}, b_i) and (c_i, a_{2i+1}) where the product $\phi\phi_r$ is positive is estimated. To get an estimate in terms of a_i only one needs to prove a uniformity of the "'angular velocity" θ in the phase plane (Lemma 4.6.5).

Lemma 4.6.5. *Let $\phi(r)$ be a non-trivial solution to (4.31) and let θ and ρ be defined by (4.36). Then for every $\varepsilon > 0$ there exists $R(\varepsilon) > 0$ such that for all $r > R(\varepsilon)$, ($\phi(r) \neq 0$) it holds*

$$-1 - \varepsilon < \theta_r(r) < -1 + \varepsilon \,.$$

Proof. Since a short calculation gives

$$\theta_r = \frac{1}{1 + \frac{\phi_r^2}{\phi^2}} \cdot \frac{\phi_{rr}\phi - \phi_r^2}{\phi^2} = \frac{\phi_{rr}\phi - \phi_r^2}{\rho^2} = -1 + \frac{\phi_{rr}\phi + \phi^2}{\rho^2} \,,$$

it is enough to prove

$$|S(\phi)| = \left| \frac{\phi(\phi + \phi_{rr})}{\rho^2} \right| < \varepsilon \,, \tag{4.39}$$

for $r > R$ for some $R > 0$ which will immediately prove the lemma. By (4.31) the quantity $S(\phi)$ introduced in (4.39) is equivalent to

$$\begin{aligned} S(\phi) &= \frac{\phi\left(-\frac{1}{r}\phi_r + \phi - \sin\phi + \frac{n^2}{r^2}\sin\phi\cos\phi\right)}{\rho^2} \\ &= -\frac{1}{r}\frac{\phi\phi_r}{\phi^2 + \phi_r^2} + \frac{n^2}{r^2}\frac{\phi\sin\phi}{\phi^2 + \phi_r^2} + \frac{\phi^2 - \phi\sin\phi}{\phi^2 + \phi_r^2} \,, \end{aligned}$$

which may be estimated by

$$\begin{aligned} |S(\phi)| &\leq \frac{1}{2r} + \frac{n^2}{r^2}\frac{|\phi||\sin\phi|}{\phi^2 + \phi_r^2} + \frac{|\phi||\phi - \sin\phi|}{\phi^2 + \phi_r^2} \\ &\leq \frac{1}{2r} + \frac{n^2}{r^2}\frac{\phi^2}{\phi^2 + \phi_r^2} + \frac{\phi^2}{\phi^2 + \phi_r^2}\frac{\phi^2}{6} \\ &\leq \frac{1}{2r} + \frac{n^2}{r^2} + \frac{\phi^2}{6} \,. \end{aligned}$$

By Lemma 4.6.1 there exists $R = R(\varepsilon) > 0$ such that

$$\frac{1}{2r} + \frac{n^2}{r^2} + \frac{\phi^2(r)}{6} < \varepsilon\,,$$

for all $r > R$. This proves (4.39) and hence the whole statement of Lemma 4.6.5.

□

Corollary 4.6.6. *Let $\phi(r)$ be a non-trivial solution to (4.31) and let (a_i), (b_i) and (c_i) be defined as above. Then each b_i is approximately in the middle of the interval (a_{2i-1}, a_{2i}), i.e. there exists $1 > K > \frac{1}{2} > k > 0$ such that for every i large enough*

$$K > \frac{b_i - a_{2i-1}}{a_{2i} - a_{2i-1}} > k > 0\,.$$

(Similar statement holds for c_i inside the interval (a_{2i}, a_{2i+1})).

Proof. By the definition of $\theta(r)$, (a_i) and (b_i)

$$\int_{a_{2i-1}}^{b_i} \theta_r dr = \theta(b_i) - \theta(a_{2i-1}) = -\frac{\pi}{2}\,.$$

Then by Lemma 4.6.5 for any $\varepsilon > 0$ for all i large enough

$$(1-\varepsilon)(b_i - a_{2i-1}) < \frac{\pi}{2} < (1+\varepsilon)(b_i - a_{2i-1})\,. \tag{4.40}$$

Similarly

$$(1-\varepsilon)(a_{2i} - b_i) < \frac{\pi}{2} < (1+\varepsilon)(a_{2i} - b_i)\,. \tag{4.41}$$

Combining (4.40) with (4.41) one obtains

$$\frac{1}{2}\frac{1-\varepsilon}{1+\varepsilon} \leq \frac{b_i - a_{2i-1}}{a_{2i} - a_{2i-1}} \leq \frac{1}{2}\frac{1+\varepsilon}{1-\varepsilon}\,.$$

The statement of the corollary immediately follows. □

Now combine Corollary 4.6.6 with the estimate (4.37) of Lemma 4.6.4 to get the following corollary.

Corollary 4.6.7. *Let $\phi(r)$ be a non-trivial solution to (4.31), let (a_i), (b_i), (c_i) be defined as above, let k be defined as in Corollary 4.6.6 and let i_0 be defined as in Lemma 4.6.1. Then*

$$\int_{a_i}^{a_{i+1}} e(r)dr \geq k \ln\left(\frac{a_{i+1}}{a_i}\right) a_i^2 \phi_r^2(a_i)\,,$$

for all $i \geq i_2$ for some $i_2 \geq i_0$.

Proof. For simplicity, let the interval (a_i, a_{i+1}) contains b_j, i.e. $a_i < b_j < a_{i+1}$ (clearly $i = 2j-1$), in the other case ($a_i < c_j < a_{i+1}$) the proof is analogical. Then by (4.37)

$$\int_{a_i}^{b_j} e(r)dr \geq a_i^2 \phi_r^2(a_i) \ln\left(\frac{b_j}{a_i}\right)\,.$$

Since $\frac{b_j - a_i}{a_{i+1}-a_i} \geq k$ by Corollary 4.6.6 for i large enough ($i \geq i_2$) one has

$$\ln \frac{b_j}{a_i} \geq k \ln \frac{a_{i+1}}{a_i}$$

by a simple calculus inequality. Thus

$$\begin{aligned}\int_{a_i}^{a_{i+1}} e(r)dr &\geq \int_{a_i}^{b_j} e(r)dr \geq a_i^2 \phi_r^2(a_i) \ln\left(\frac{b_j}{a_i}\right) \\ &\geq k a_i^2 \phi_r^2(a_i) \ln\left(\frac{a_{i+1}}{a_i}\right)\,.\end{aligned}$$

□

Next we prove that the quantity $a_i^2 \phi_r^2(a_i)$ is increasing with an increasing index i.

Proposition 4.6.8. *Let $\phi(r)$ be a non-trivial solution to (4.31) and let (a_i) be defined as above. Then*

$$a_i^2 \phi_r^2(a_i) < a_{i+1}^2 \phi_r^2(a_{i+1})\,.$$

Proof. The Pohozaev identity applied to (4.31) on the interval (a_i, a_{i+1}) gives

$$\frac{1}{2}\left(a_{i+1}^2\phi_r^2(a_{i+1}) - a_i^2\phi_r^2(a_i)\right) = -2\int_{a_i}^{a_{i+1}} s(\cos\phi(s) - 1)ds > 0\,,$$

which proves the statement of Proposition 4.6.8. □

Finally everything is prepared to prove Theorem 4.3.1.

Proof. The proof of the theorem will be by a contradiction. Assume that the solution $\phi(r)$ has finite energy. Then also the modified solution $\tilde{\phi}(r) = \phi(r) - \pi$ has finite energy and solves (4.31). Drop the tildes and consider $\phi(r)$ to be a solution of (4.31). By Lemma 4.6.3 it has also finite modified energy E^* defined by (4.35). Let (a_i) be defined as above – the infinite sequence of the zero points of $\phi(r)$. Then by Corollary 4.6.7

$$\int_{a_i}^{a_{i+1}} e(r)dr \geq k\ln\left(\frac{a_{i+1}}{a_i}\right) a_i^2\phi_r^2(a_i)\,,$$

for $i \geq i_2$. Thus

$$E^* \geq \sum_{j=i_2}^{\infty}\int_{a_j}^{a_{j+1}} e(r)dr \geq \sum_{j=i_2}^{\infty} k\ln\left(\frac{a_{j+1}}{a_j}\right) a_j^2\phi_r^2(a_j)\,.$$

Also by Proposition 4.6.8

$$a_j^2\phi_r^2(a_j) \geq a_1^2\phi_r^2(a_1) = C > 0\,,$$

so

$$E^* \geq Ck\sum_{j=i_2}^{\infty}\ln\left(\frac{a_{j+1}}{a_j}\right) = Ck\lim_{j\to\infty}(\ln(a_j) - \ln(a_{i_2})) = \infty\,,$$

which yields the contradiction. □

Chapter 5

Discussion

In this section we discuss some of the important issues arising in this work. We also list some related problems which will be subject to our further investigations.

First, observe we used an assumption that the relative trap frequency Ω is smaller than 1, to prove the essential spectrum of the linearized operator is empty. The same assumption was also necessary to properly define the linearized operator. It is not clear how to define the operator for $\Omega \geq 1$ and whether its essential spectrum stays empty in this parameter regime. Since we show that the eigenvalues (the discrete spectrum) of the linearized problem suffer only a shift by a purely imaginary number depending on rotation, stability of this part of the spectrum is unaffected by rotation of the trap. Hence, in the transition through the bound $\Omega = 1$ the essential spectrum may play an important role in the stability of a single vortex. We emphasize that this may correspond to a physical intuition that for $\Omega > 1$ the effect of the centrifugal force dominates the effect of the trapping potential and that in this case a condensate may spin out of the trap.

Also note that the graph of the evolution of location of stable and unstable eigenvalues with a growing parameter p reveals an interesting phenomena. For

a Fourier mode $j = 2$ there appears to be a single eigenvalue crossing the others creating finite intervals of instability after each collision. We conjecture a possible connection of this behavior with the Krein signature of the eigenvalue. Particularly, when the fast-moving eigenvalue has the same Krein signature as the others, they do not collide and thus the stability pertains. On the other hand, the opposite Krein signature forces them to collide and split off the imaginary axis.

The signature of eigenvalues could also justify that there are no other unstable eigenvalues outside of the horizontal window we consider. It is so because the bound for number of unstable eigenvalues is equal to the precise number of unstable eigenvalues plus the number of stable eigenvalues with negative signature [50]. Another significant simplification would occur if one is able to determine the Krein signature directly from the Evans function since the Evans function should contain all the pertinent information (the same problem is mentioned in [50]).

After modifications, the method used in this thesis may be also helpful in solving a couple of related problems which may be subject to future investigations by the author of this thesis.

An interesting problem arising from computed behavior of the eigenvalues is to determine the behavior of the eigenvalues as $p \to \infty$ where the model approaches the fully nonlinear Thomas-Fermi regime. Similarly the precise description of the eigenvalues as $p \to p_0$ and behind, up to an attractive inter-particle potential (where the condensate is reported to be unstable), would be desirable to study, since by means of the Feshbach resonance [41] it is possible to perform such a transition in experiments.

The other interesting recent advances in BEC are experiments with *multi-component condensates*, either using a two-species ^{87}Rb [60] or even two-element ^{87}Rb–^{23}Na mixtures [61, 62, 63]. A numerical study of stability of vortices in this model was conducted in [64] but the limitation of the chosen method did not allow authors to reach the number of particles used in experiments. The implementation of the Evans function method should also in this case give a *reliable answer to stability questions*. Note, that this model has a much wider parameter regime than a single component BEC. Therefore there is a wider opportunity to realize a long term goal — *stable multiquantum vortices*.

Finally, in [65] Towers *et al.* discussed the stability of vortices in another model governed by the nonlinear Schrödinger equation. They posed the question whether truly stable ring solitons (vortices) can exists in a model with a realistic nonlinearity. As a such nonlinearity they suggest *a mixed quadratic* $\chi^{(2)}$ *(quadratic) –* $\chi^{(3)}$ *(cubic) nonlinearity*. Via direct simulations and a finite difference scheme for linear eigenvalue problem they found a parameter regime for which there exist stable vortex solutions. The Evans function method can also in this case provide *a more reliable calculation even for higher degree multiquantum vortices*.

Let me also mention one related problem. The already described model of BEC is only a simplification of Hartree-Fock approximation to nonlinear N-body Schrödinger equation. To obtain Gross-Pitaevskii equation one must consider instead of a non-local general interaction potential $W(x-y)$ only a local short-range interactions, i.e. $W(x-y) = \delta(x-y)$. Deconinck and Kutz [35] give numerical evidence that, despite the fact that the local model can be obtained by a correct asymptotic limit of a non-local one [26], stability of solutions is not

"asymptotically equivalent", i.e. stability is not preserved in this limit. Indeed in the case of periodic trapping potential in a simple one dimensional case they found a discrepancy in stability of explicitly calculated solutions. They perturbed inital data randomly and compared the long-time behavior to discover discrepancy in stability between local and non-local models. The source of this interesting phenomena is unclear. It is conjectured to appear only due to the transition from a non-local model to a local one. The question remains whether the same situation occurs for a more complicated two dimensional model in the case of more typical harmonic potential. To resolve this issue one must be able to detect instability of vortices in non-local equations. Although the code already developed for this thesis is able to construct vortex profiles even for non-local models, the design of the Evans function method is unfortunately not appropriate to handle this problem, since there is no analogue to the decoupling of modes as in the simple local case. The problem may be attainable by an implementation of a non-local Evans function introduced in [66].

Appendix A

Bifurcation

Appendix A contains the proof of Theorem 3.2.1, i.e. details regarding the proper use of the Crandall-Rabinowitz theorem [45] to justify initialization of the numerical algorithm for generating vortex solutions to the Gross-Pitaevskii equation. The notation $L^2(X, Y; \phi(x)dx)$ will denote a Hilbert space of functions $f : X \to Y$ with a bounded norm $\left(\int_X |f|^2 \phi(x)dx\right)^{1/2} < \infty$.

The Crandall-Rabinowitz theorem states the following:

Theorem A.1. *Let X and Y be Banach spaces. Let $(\overline{\lambda}, 0) \in \mathbb{R} \times X$ and let F be a C^2 mapping of an open neighborhood of $(\overline{\lambda}, 0)$ into Y. Let the null space $N(F_x(\overline{\lambda}, 0)) = span\{x_0\}$ be one-dimensional and $codim\, R(F_x(\overline{\lambda}, 0)) = 1$. Moreover, let $F_{x\lambda}(\overline{\lambda}, 0)x_0 \notin R(F_x(\overline{\lambda}, 0))$. If Z is a complement of $span\{x_0\}$ in X, then the solutions of $F(\lambda, x) = F(\overline{\lambda}, 0)$ near $(\overline{\lambda}, 0)$ form a curve $(\lambda(s), x(s)) = (\overline{\lambda} + \tau(s), sx_0 + sz(s))$, where $s \to (\tau(s), z(s)) \in \mathbb{R} \times Z$ is a continuously differentiable near $s = 0$ and $\tau(0) = 0$, $z(0) = 0$.*

Here $\lambda = p$, $x = w$, $\overline{\lambda} = p_0 = m + 1$ and

$$F(p, w) = w_{rr} + \frac{1}{r} w_r - \frac{m^2}{r^2} w + 2pw - r^2 w - 2|w|^2 w \,.$$

Recall, that in Chapter 3, section 3.2 it was shown that the only C^2 solution of the linearized equation

$$F_w(p_0, 0)w = w_{rr} + \frac{1}{r}w_r - \frac{m^2}{r^2}w + 2p_0 w - r^2 w = 0$$

satisfying the boundary conditions $w(0) = w(\infty) = 0$ is a constant multiple of

$$w_0 = r^m e^{-r^2/2} M(-n, m+1, r^2) = r^m e^{-r^2/2} c_n^{(m)} L_n^{(m)}(r^2)\,,$$

where $M(a, b, c)$ is a confluent hypergeometric function, which for these special parameters degenerates to a generalized Laguerre polynomial $L_n^{(m)}$, and $c_n^{(m)}$ is a positive normalization coefficient.

Also note that the operator $F(p, w)$ was obtained from the operator

$$\tilde{F}(p, u) = \triangle u - (x^2 + y^2)u + 2pu - 2|u|^2 u$$

by setting $u = e^{im\theta}w(r)$. This operator can be defined on $\mathbb{R} \times \mathcal{H}$, where $\mathcal{H}$ is the Hilbert space

$$\mathcal{H} = \{u : u \in H^2(\mathbb{R}^2, \mathbb{R}^2), (x^2 + y^2)u \in L^2(\mathbb{R}^2, \mathbb{R}^2)\}$$

with the usual norm

$$||u||_{\mathcal{H}}^2 = ||u||_{H^2}^2 + ||(x^2 + y^2)u||_{L^2}^2\,.$$

Note that by Sobolev embedding $\mathcal{H} \hookrightarrow L^6$. Clearly $\tilde{F}$ is densely defined within $\mathbb{R} \times L^2(\mathbb{R}^2, \mathbb{R}^2)$ since it contains the whole Schwartz space $\mathbb{R} \times \mathcal{S}(\mathbb{R}^2, \mathbb{R}^2)$ which is dense in $\mathbb{R} \times L^2(\mathbb{R}^2, \mathbb{R}^2)$. Now, define

$$X = \{w\ : w \in L^2(\mathbb{R}, \mathbb{R}; r), e^{im\theta}w(r) \in \mathcal{H}\}$$

with a norm

$$||w||_X = ||e^{im\theta}w(r)||_{\mathcal{H}}\ .$$

The space X is again by a Schwartz space argument dense in $L^2(\mathbb{R},\mathbb{R};rdr)$. On the other hand the choice of the domain $\mathbb{R}\times X$ of F implies

$$F:\mathbb{R}\times X\to Y:=L^2(\mathbb{R},\mathbb{R};rdr)\,.$$

Also note that each function $w\in X$, $m\neq 0$ satisfies $w(0)=\lim_{r\to\infty}w(r)=0$, if $m=0$ then $w(0)$ is finite and $\lim_{r\to\infty}w(r)=0$. The first condition holds since $e^{im\theta}w(r)\in H^2(\mathbb{R}^2,\mathbb{R}^2)$ and so $e^{im\theta}w(r)$ is a continuous function at $r=0$. Hence $w(0)=0$. The second condition follows from the property $w(r)\in L^2(\mathbb{R},\mathbb{R};rdr)$.

Operator F in a neighborhood of a point $(p_0,0)$ satisfies all the assumptions of the Crandall-Rabinowitz theorem. First, F is by the choice of its domain continuous operator, one can also check directly from the definition that F is a C^2 mapping, particularly in an open neighborhood of $(p_0,0)$. Furthermore, $F(p,0)$ is identically equal to zero.

The null space $N(F_w(p_0,0))$ is a kernel of the linearized operator which was proved to be a one-dimensional subspace of Y spanned by w_0. The eigenfunctions $w_n(r)$ of $F_w(p)$, $p=m+1+2n$, $n=0,1,2,\ldots$, are products of a fixed weight function $w_*(r)=r^me^{-r^2/2}$ and generalized Laguerre polynomials. These polynomials are orthonormal and complete in $L^2(\mathbb{R},\mathbb{R};rw_*^2(r)dr)$, since a completeness theorem of [67], page 31, applies. Therefore also $w_n(r)$ are orthonormal and complete in $L^2(\mathbb{R},\mathbb{R};rdr)$. Thus the operator $F_w(p_0,0)$ is a Fredholm operator and consequently $\operatorname{codim}R(F_w(p_0,0))=1$. Furthermore, $\frac{\partial}{\partial p}\frac{\partial}{\partial w}F(p_0,0)w_0=2w_0\notin R(F_w(p_0,0))$. The statement of Theorem 3.2.1 then follows.

Finally, note that the symmetry of the problem (both w and $-w$ are solutions) implies $\tau'(0)=0$.

Appendix B

Analysis of vortex profiles

In this Appendix a result concerning the spatial shape of the radial vortex profile satisfying

$$w_{rr} + \frac{1}{r}w_r - \frac{m^2}{r^2}w + 2p_0 w - r^2 w - 2|w|^2 w = 0 \tag{B-1}$$

is presented.

Lemma B.1. *Let $w(r)$ be a positive solution on $(0,\infty)$ to*

$$w_{rr} + \frac{1}{r}w_r - \frac{m^2}{r^2}w = 2(w(r)^2 - p(r)^2)w$$

where m, $m \neq 0$, is an integer and

$$2p(r)^2 = 2p_0 - r^2, \quad p_0 > 0,$$

satisfying $w(r) \to 0$ as $r \to 0^+$ and $r \to \infty$. Then $w(r)$ has a local maximum for some R, $R \in (m/\sqrt{2p_0}, \sqrt{2p_0})$ and is increasing on $(0,R)$ and decreasing on (R,∞). Moreover,

$$|w(r)|^2 < p_0 - m \tag{B-2}$$

for all $r \in \mathbb{R}^+$.

Proof. Assume that contrary is true, i.e. there exists a local minimum of $w(r)$. Since $w(0) = 0 = w(\infty)$, there must exists three consecutive local extrema: R_1 a

local maximum, r a local minimum and R_2 a local maximum, $R_1 < r < R_2$. Then $w_r(R_1) = w_r(r) = w_r(R_2) = 0$ and $w_{rr}(R_1) < 0$, $w_{rr}(r) > 0$ and $w_{rr}(R_2) < 0$. Then

$$\begin{aligned} 0 &> w_{rr}(R_1) = \left(\frac{m^2}{R_1^2} + R_1^2 + 2w^2(R_1) - 2p_0\right) w(R_1)\,, \\ 0 &< w_{rr}(r) = \left(\frac{m^2}{r^2} + r^2 + 2w^2(r) - 2p_0\right) w(r)\,, \\ 0 &> w_{rr}(R_2) = \left(\frac{m^2}{R_2^2} + R_2^2 + 2w^2(R_2) - 2p_0\right) w(R_2)\,. \end{aligned}$$

Hence

$$\begin{aligned} 2w^2(R_1) &< 2p_0 - \frac{m^2}{R_1^2} - R_1^2\,, \\ 2p_0 - \frac{m^2}{r^2} - r^2 &< 2w^2(r)\,, \\ 2w^2(R_2) &< 2p_0 - \frac{m^2}{R_2^2} - R_2^2\,. \end{aligned}$$

Since r is a local minimum of $w(r)$ and lies between local maxima R_1 and R_2, $w^2(r) < w^2(R_1)$, $w^2(r) < w^2(R_2)$. Then

$$\begin{aligned} 2p_0 - \frac{m^2}{R_1^2} - R_1^2 &> 2p_0 - \frac{m^2}{r^2} - r^2\,, \\ 2p_0 - \frac{m^2}{R_2^2} - R_2^2 &> 2p_0 - \frac{m^2}{r^2} - r^2\,, \end{aligned}$$

implying $G(r) > G(R_1)$ and $G(r) > G(R_2)$, where $G(x) = x^2 + \frac{m^2}{x^2}$. Since $G(x)$ is a convex function, this is impossible. Hence $w(r)$ can have only one local extreme – a maximum $w(R)$ at a point R. The location of R is restricted since by the previous inequalities

$$\frac{m^2}{R_1^2} + R_1^2 < 2p_0 - 2w^2(R) < 2p_0\,.$$

This implies $R \in (m/\sqrt{2p_0}, \sqrt{2p_0})$. Moreover, since $G(r) \geq 2m$, $w^2(R) < p_0 - m$. □

Appendix C

Essential spectrum of the linearized operator

Appendix C contains the proof of Theorem 3.3.1 which claims that the essential spectrum of the operator $A = J(L_c+L_w)$ is empty. The proof has three steps, first one shows that for $0 \leq \Omega < 1$ the essential spectrum of L_c is empty, $\sigma_{ess}(L_c) = \emptyset$. Then $\sigma_{ess}(JL_c) = \emptyset$. Finally, the generalization of Weyl's theorem (for non-self adjoint operators) yields the same property for JL.

Proof of Theorem 3.3.1.

First, denote

$$\begin{aligned} L_c &= -(-\frac{1}{2}\triangle + \frac{1}{2}r^2 + J\Omega\partial_\theta)\,, \\ L_w &= -\mu - 2|w|^2 - |w|^2 e^{2m\theta J} R\,. \end{aligned}$$

Then

$$A = J(L_c + L_w)\,. \tag{C-1}$$

We show that the essential spectrum of A is determined solely by the essential spectrum of L_c. Also, the angular momentum term ∂_θ is for $0 \leq \Omega < 1$ dominated

by the remaining terms of L_c in the following sense:

$$\begin{aligned}
\langle \partial_\theta \phi, \phi \rangle &= \int (x\phi_y - y\phi_x)\overline{\phi} dxdy \\
&\leq \int |x||\phi_y||\phi| + |y||\phi_x||\phi| dxdy \\
&\leq \frac{1}{2}\int |x|^2|\phi|^2 + |\phi_y|^2 + |y|^2|\phi|^2 + |\phi_x|^2 dxdy \\
&= \frac{1}{2}\int r^2|\phi|^2 dxdy + \frac{1}{2}\int |\nabla\phi|^2 dxdy \\
&= \frac{1}{2}\langle r^2\phi, \phi\rangle + \frac{1}{2}\langle -\triangle\phi, \phi\rangle ,
\end{aligned}$$

for $\phi = \Phi_i$, $i = 1, 2$. Similar argument implies for vectors Φ:

$$\langle -J\Omega\partial_\theta\Phi, \Phi\rangle \leq \Omega\langle \frac{1}{2}\left(-\triangle + r^2\right)\Phi, \Phi\rangle .$$

Therefore for $0 \leq \Omega < 1$:

$$\langle (-\frac{1}{2}\triangle + \frac{1}{2}r^2 + J\Omega\partial_\theta\Phi, \Phi\rangle \geq \frac{1-\Omega}{2}\langle (-\triangle + r^2)\Phi, \Phi\rangle .$$

Hence

$$\langle -L_c\Phi, \Phi\rangle \geq \frac{1-\Omega}{2}\langle (-\triangle + r^2)\Phi, \Phi\rangle . \tag{C-2}$$

Introducing a new Hamiltonian $H_c = \frac{1-\Omega}{2}\left(-\triangle + V\right)$ with a potential $V(r) = r^2$ the inequality (C-2) reduces to

$$\langle -L_c\Phi, \Phi\rangle \geq \langle H_c\Phi, \Phi\rangle . \tag{C-3}$$

Now one may apply *Theorem XIII.16* of Reed and Simon [68], pp. 120:

Theorem C.1 (Reed, Simon). *Let V be a locally bounded positive function with $V(x) \to \infty$ as $|x| \to \infty$. Define $-\triangle + V$ as a sum of quadratic forms. Then $-\triangle + V$ has purely discrete spectrum.*

The proof uses the minimax principle characterization of eigenvalues. The important ingredient is the estimate (C-3) along with the growth $V(r) \to \infty$ as $r \to \infty$. This proves that L_c and similarly $-L_c$ has only a discrete spectrum.

Next, we prove that the essential spectrum of JL_c is empty. Since L_c is a positive operator, 0 is not its eigenvalue and therefore L_c is invertible. Moreover, L_c does have only a discrete spectra and its eigenvalues are isolated with the only possible accumulation point ∞. Then by *Theorem XIII.64*, pp.245, of [68] the operator L_c^{-1} is compact. Here, only the shortened version of Theorem XIII.64 is presented.

Theorem C.2 (Reed, Simon). *Let A be a self-adjoint operator that is bounded from below. Then the following are equivalent ($\rho(B)$ denotes the resolvent set of an operator B):*

- $(A-\mu)^{-1}$ *is compact for some* $\mu \in \rho(A)$*;*
- $(A-\mu)^{-1}$ *is compact for all* $\mu \in \rho(A)$*;*
- $\mu_n(A) \to \infty$*, where* μ_n *is given by the min-max principle.*

Furthermore, consider the following identity:

$$\lambda I - JL_c = (\lambda L_c^{-1} J^{-1} - I) JL_c \,. \tag{C-4}$$

If $\lambda \notin \sigma_p(JL_c)$, then $\frac{1}{\lambda} \notin \sigma_p(L_c^{-1}J^{-1})$ and the right-hand side of (C-4) is invertible:

$$(\lambda I - JL_c)^{-1} = L_c^{-1} J^{-1} (\lambda L_c^{-1} J^{-1} - I)^{-1} \,.$$

Here L_c^{-1} is compact, $J^{-1} = -J$ is a bounded operator, $\lambda L_c^{-1} J^{-1} - I$ is a compact perturbation of identity, i.e. a Fredholm operator. Moreover, since

$\lambda \notin \sigma_p(L_c^{-1}J^{-1})$, the operator $\lambda L_c^{-1}J^{-1} - I$ has an empty kernel and is inverible and boundned. Therefore $(\lambda I - JL_c)^{-1}$ is compact. This implies that $\lambda I - JL_c$ is invertible with a compact inverse if λ is not an eigenvalue of JL_c. It remains to prove that the eigenvalues of JL_c are isolated and of finite multiplicity, which prohibits discrete spectra to be embedded in the essential spectrum.

To show that, consider the resolvent equation

$$(I\lambda - JL_c)u = f\,.$$

which is equivalent to

$$(I - T(\lambda))u = \left(\lambda L_c^{-1}J^{-1} - I\right)u = L_c^{-1}J^{-1}f\,.$$

The operator $\lambda L_c^{-1}J^{-1} - I$ is a (multiple of) compact perturbation of identity and therefore it is also Fredholm. Also, it is analytic everywhere except for the discrete spectra of $L_c^{-1}J^{-1}$. By a general result of Gohberg and Krein [69], p.21. or Kato [70], p.370, the set of values for which $I - T(\lambda)$ is not invertible is at most countable with their only possible accumulation point infinity. Therefore the eigenvalues of JL_c are isolated. Also, the spectral projection on the eigenspace associated with a particular eigenvalue of JL_c has finite dimensional range, since it is given by a integral

$$P_\lambda = \frac{1}{2\pi i}\int_\Gamma (\lambda I - JL_c)^{-1}\,d\lambda$$

of a compact operator. Hence the essential spectrum of JL_c is empty and consist of isolated eigenvalues of finite multiplicity with only accumulation point infinity, i.e.

$$\sigma_{ess}(JL_c) = \emptyset\,.$$

Finally, one can use the generalization of the Weyl's theorem to non self-adjoint operators to prove the equivalence of essential spectra

$$\sigma_{ess}(JL_c) = \sigma_{ess}(J(L_c + L_w)) .$$

It is enough to show that $J(L_c + L_w)$ is a relatively compact perturbation of JL_c, i.e. that $JL_w(\lambda I - JL_c)^{-1}$ is compact whenever $\lambda \notin \sigma_p(JL_c)$. Operator JL_w is bounded and therefore it remains to prove that $(\lambda I - JL_c)^{-1}$ is compact. But that fact was already proved in the previous paragraph. Hence if $\lambda \notin \sigma_p(JL_c)$, λ lies in the resolvent set $\rho(JL_c)$. What remains to prove is that the eigenvalues of $J(L_c + L_w)$ are isolated and of finite multiplicity. The proof of this statement is also the same as in the previous paragraph, using that

$$(\lambda - (JL_C + JL_w))u = f$$

is for $\lambda \notin \sigma_p(JL_c)$ equivalent to

$$(I - (\lambda I - JL_c)^{-1})JL_w)u = (\lambda I - JL_c)^{-1} f .$$

Hence the essential spectrum of JL is empty and consist of isolated eigenvalues of finite multiplicity with only accumulation point infinity. □

Appendix D

Bounds on eigenvalues

Appendix D contains two omitted proofs from Chapter 3: a bound on the index of possible unstable modes (Proposition 3.3.4) and a bound for the real part of an eigenvalue (Proposition 3.3.5).

Proof of Proposition 3.3.4.

For any $y \in D(L_j)$, $y \neq 0$:

$$\begin{aligned}
\langle L_j y, y\rangle &= \int_0^\infty \left[\frac{1}{2}\left(\frac{j+m}{r}\right)^2 |y_+|^2 + \frac{1}{2}\left(\frac{j-m}{r}\right)^2 |y_-|^2\right. \\
&\quad + \frac{1}{2} r^2 \left(|y_+|^2 + |y_-|^2\right) \\
&\quad + 2|w|^2 \left(|y_+|^2 + |y_-|^2\right) + |w|^2 \left(y_+ \overline{y}_- + \overline{y}_+ y_-\right) \\
&\quad \left. - \frac{1}{2}\left(\triangle_r y_+ \overline{y}_+ + \triangle_r y_- \overline{y}_-\right) - p\left(|y_+|^2 + |y_-|^2\right)\right] r dr \\
&> \int_0^\infty \left[\frac{1}{2}\frac{m^2}{r^2}\left(|y_+|^2 + |y_-|^2\right) + \frac{1}{2} r^2 \left(|y_+|^2 + |y_-|^2\right)\right. \\
&\quad + |w|^2 \left(|y_+|^2 + |y_-|^2\right) + \frac{1}{2}\left(|\partial_r y_+|^2 + |\partial_r y_-|^2\right) \\
&\quad \left. - p\left(|y_+|^2 + |y_-|^2\right)\right] r dr \,,
\end{aligned}$$

by integration by parts, by the assumption of the theorem

$$|j+m| > m\,, \qquad\qquad |j-m| > m\,,$$

and by the inequality

$$(y_+\overline{y}_- + \overline{y}_+ y_-) \leq \left(|y_+|^2 + |y_-|^2\right) .$$

The operator L_j is, similarly as the operator A in Section 3.3, defined on $D(L_j)$ by the appropriate quadratic form and thus the integrals used here are well defined.

Then

$$\begin{aligned}\langle L_j y, y\rangle &\geq \frac{1}{2}\int_0^\infty \left[|\partial_r y_+|^2 + \left(\frac{m^2}{r^2} + r^2 + 2|w|^2 - 2p\right)|y_+|^2\right] r dr \\ &\quad + \frac{1}{2}\int_0^\infty \left[|\partial_r y_-|^2 + \left(\frac{m^2}{r^2} + r^2 + 2|w|^2 - 2p\right)|y_-|^2\right] r dr \\ &= E_w(y_+) + E_w(y_-)\,,\end{aligned}$$

where

$$E_w(f) = \frac{1}{2}\int_0^\infty \left[|\partial_r f|^2 + \left(\frac{m^2}{r^2} + r^2 + 2|w|^2 - 2p\right)|f|^2\right] r dr\,. \tag{D-1}$$

The function $e^{im\theta}w(r)$ is a non-negative, $w \geq 0$, minimizer of the energy (3.5) (with $\Omega = 0$), with respect to the constraint (3.9), within the family $\phi(r,\theta) = e^{im\theta}f(r) \in D(q)$. For this class of functions the energy (3.5) is reduced to $E_w(f)$ of (D-1). Since $E_w(w) = 0$, it follows that $E_w(f) \geq 0$ for all $e^{im\theta}f \in D(q)$. Hence

$$\langle L_j y, y\rangle > 0\,,$$

and by (3.31) also

$$\langle i\lambda_0 R y, y\rangle = i\lambda_0\langle R y, y\rangle > 0\,. \tag{D-2}$$

Therefore $i\lambda_0$ (and by Lemma 3.3.3 also $i\lambda_\Omega$) must be real. □

Proof of Proposition 3.3.5.

First, recall the simple bootstrap argument justifying that $\Phi_\pm$ of (3.23)–(3.24) is $C^\infty(\mathbb{R}^2,\mathbb{R}^2)\cap L^2(\mathbb{R}^2,\mathbb{R}^2)$. Then, split the operator A to a vortex-profile-dependent part A_w and independent part A_c: $A = A_c + A_w$, where

$$\begin{aligned} A_c &= J\left[\frac{1}{2}\triangle - J\Omega\partial_\theta - \left(\frac{1}{2}r^2 - \mu\right)\right], \\ A_w &= -J\left[2|w(r)|^2 + |w(r)|^2 e^{2m\theta J} R\right]. \end{aligned}$$

Since J and R are constant matrices (bounded by 1 in the matrix norm) the estimate (B-2) implies that the norm of the profile dependent part A_w is bounded above:

$$||A_w||_{L^2} = \left|\left|-J\left(2|w|^2 + |w|^2 e^{2m\theta J} R\right)\right|\right|_{L^2} \leq 3M(w) < \infty\,, \tag{D-3}$$

where $|\cdot|_{L^2}$ denotes the operator norm in $L^2(\mathbb{R}^2,\mathbb{C}^2)$ and $M(w) = \max\limits_{r\in(0,\infty)} |w(r)|^2$.

Multiply (3.22) by the smooth complex conjugate $\overline{\Phi}$ and integrate over $(0,\infty)$ with respect to r and over $(0,2\pi)$ with respect to θ to obtain

$$\lambda||\Phi||^2 = \int_0^{2\pi}\int_0^\infty A_c\Phi\cdot\overline{\Phi}\, r dr d\theta + \int_0^{2\pi}\int_0^\infty A_w\Phi\cdot\overline{\Phi}\, r dr d\theta\,. \tag{D-4}$$

The second term on the right hand side of (D-4) can be estimated using (D-3)

$$\int_0^{2\pi}\int_0^\infty A_w\Phi\cdot\overline{\Phi}\, r dr d\theta\,. \leq 3M(w)||\Phi||^2\,. \tag{D-5}$$

Finally, the real part of $\int_0^{2\pi}\int_0^\infty A_c\Phi\cdot\overline{\Phi}\, r dr d\theta$ vanishes what can be justified by a simple but long integration by parts. The proof of this simple claim is omitted here. The statement of the proposition then immediately follows.

□

Appendix E

Asymptotic behavior

This appendix contains the asymptotic behavior results used in Chapter 3. The proof of the Gaussian decay of the vortex profile satisfying (3.15) is proved first and then the precise description of asymptotic behavior of solutions to the system of ordinary differential equations used in construction of the Evans function (Theorem 3.4.1) is presented.

Lemma E.1. *The real positive solution $w(r)$ to*

$$w_{rr} + \frac{1}{r}w_r - \frac{m^2}{r^2}w - r^2 w + 2pw - 2|w|^2 w \tag{E-1}$$

satisfying the homogeneous boundary conditions $w(0) = w(\infty) = 0$ decays exponentially as $r \to \infty$, i.e.

$$w(r) = O(r^p e^{-r^2/2})\,.$$

Proof. The proof is based on the same ODE technique as [15]. First, observe that $w(r)$ must decay to zero monotonically. Otherwise, there would exist a local maximum R of $w(r)$ for some $R >> 1$. Therefore if R is large enough then

$$w_{rr}(R) = \frac{m^2}{R^2}w(R) + R^2 w(R) - 2pw(R) + 2w^3(R) > 0\,. \tag{E-2}$$

Notice that in Appendix B it is proved that $w(r)$ is bounded and so the estimate (E-2) (with a different p) is true also for the attractive potential for which the term $2|w|^2w$ has the opposite sign. Hence $w_{rr}(R) > 0$ and R cannot be a local maximum. This immediately implies $w'(r) \to 0$ as $r \to \infty$.

The rest of the proof will be done in two steps. In the first step it is proved that $w(r) = O(e^{-cr})$ for any $c > 0$ and in the second step that $w(r) = O(e^{-r^2/2})$. The term w_{rr} can be estimated as

$$w_{rr} = -\frac{1}{r}w_r + \frac{m^2}{r^2}w + r^2w - 2pw + 2w^3 > c^2w \tag{E-3}$$

for any $c^2 > 0$ and $r > r_0$ by assuming r_0 is large enough. Multiply the inequality (E-3) by $w_r < 0$ to obtain

$$\frac{1}{2}\partial_r(w_r)^2 < c^2\frac{1}{2}\partial_r(w^2)$$

and integrate over (r, ∞)

$$-(w_r)^2 < -c^2w^2$$

using the boundary condition $w(\infty) = w'(\infty) = 0$. Then

$$-w_r > cw$$

and thus

$$w(r) = O(e^{-cr})\,.$$

On the other hand

$$w_{rr} = -\frac{1}{r}w_r + \frac{m^2}{r^2}w + r^2w - 2pw + 2w^3 > (r^2 - 2p)w\,, \tag{E-4}$$

for every $r > r_0$ for some fixed $r_0 = r_0(m, p)$. Multiplying the inequality (E-4) by the term $w_r < 0$ gives

$$\frac{1}{2}\partial_r(w_r)^2 < (r^2 - 2p)\frac{1}{2}\partial_r(w^2)\,.$$

on the interval (r_0, ∞). Integrating the inequality over (r, ∞) for any $r > r_0$ using the property $\lim_{r\to\infty} rw(r) = rO(e^{-cr}) = 0$ then yields

$$-(w_r)^2 < \int_r^\infty (r^2 - 2p)\partial_r(w^2)\, dr = (r^2 - 2p)w^2|_r^\infty - \int_r^\infty 2rw^2\, dr\,.$$

Using the fact $w'(\infty) = 0$ gives

$$(w_r)^2 > (r^2 - 2p)w^2 + \int_r^\infty 2rw^2\, dr > (r^2 - 2p)w^2\,.$$

For simplicity set $p = 0$. Then

$$(w_r)^2 > r^2w^2$$

implies for $w_r < 0$, $w > 0$:

$$w_r < -rw\,,$$

which in turn gives

$$w(r) < Ce^{-r^2/2}\,.$$

If $p \neq 0$ the argument is similar and yields

$$w(r) < Ce^{-r^2/2}r^p\,.$$

Note, that this proof does not justify the precise asymptotic behavior of $w(r)$ which should be $r^p e^{-r^2/2}$ by comparison with the linear part. □

Proof of Theorem 3.4.1.

The goal is to prove a precise description of the asymptotic behavior of nontrivial solutions of (3.31). The second order ODE system (3.31) can be rewritten as the first order system

$$y' = B(r, j, \lambda)y\,, \tag{E-5}$$

where

$$B = B_\infty + B_w\,, \qquad y = \left(y_+^{(j+m)}(r), \partial_r y_-^{(j+m)}(r), y_+^{(j-m)}(r), \partial_r y_-^{(j-m)}(r)\right)^T \quad \text{(E-6)}$$

and

$$B_\infty = \begin{pmatrix} 0 & 1 & 0 & 0 \\ k^+ & -1/r & 0 & 0 \\ 0 & 0 & 0 & 1 \\ 0 & 0 & k^- & -1/r \end{pmatrix}, \qquad B_w = |w|^2 \begin{pmatrix} 0 & 0 & 0 & 0 \\ 4 & 0 & 2 & 0 \\ 0 & 0 & 0 & 0 \\ 2 & 0 & 4 & 0 \end{pmatrix},$$

and

$$\begin{aligned} k^+(r) &= \frac{(j+m)^2}{r^2} + r^2 - 2p - 2i\lambda\,, \\ k^-(r) &= \frac{(j-m)^2}{r^2} + r^2 - 2p + 2i\lambda\,. \end{aligned}$$

The asymptotic analysis in Section 3.2 also applies to the linear system

$$y'_\infty = B_\infty(r, j, \lambda) y_\infty \quad \text{(E-7)}$$

and reveals that it has four independent solutions — the columns of the fundamental matrix of the system (E-7)

$$Y_\infty = \begin{pmatrix} M_+ & 0 & U_+ & 0 \\ M'_+ & 0 & U'_+ & 0 \\ 0 & M_- & 0 & U_- \\ 0 & M'_- & 0 & U'_- \end{pmatrix}, \quad \text{(E-8)}$$

where

$$\begin{aligned} M_+ &= r^{j+m}e^{-r^2/2}M\left(\frac{j+m+1+\alpha_+}{2}, j+m+1, r^2\right), \\ M_- &= r^{j-m}e^{-r^2/2}M\left(\frac{j-m+1+\alpha_-}{2}, j-m+1, r^2\right), \\ U_+ &= r^{j+m}e^{-r^2/2}U\left(\frac{j+m+1+\alpha_+}{2}, j+m+1, r^2\right), \\ U_- &= r^{j-m}e^{-r^2/2}U\left(\frac{j-m+1+\alpha_-}{2}, j-m+1, r^2\right) \end{aligned} \tag{E-9}$$

and

$$\alpha_+ = p + i\lambda\,, \qquad \alpha_- = p - i\lambda\,.$$

Note that the asymptotic behavior of the columns of the fundamental matrix Y_∞ as $r \to \infty$ is given by

$$y_{\infty 1} \sim e^{r^2/2}r^{\alpha_+}\left(1/r, 1, 0, 0\right)^T\,, \qquad y_{\infty 2} \sim e^{r^2/2}r^{\alpha_-}\left(0, 0, 1/r, 1\right)^T\,,$$

$$y_{\infty 3} \sim e^{-r^2/2}r^{-\alpha_+}\left(1/r, -1, 0, 0\right)^T\,, \qquad y_{\infty 4} \sim e^{-r^2/2}r^{-\alpha_-}\left(0, 0, 1/r, -1\right)^T\,.$$

Similarly as $r \to 0^+$, the solutions to (E-5) have the same asymptotics as the solutions of the uncoupled asymptotic linear system

$$y_0' = B_0(r, j, \lambda)y_0\,, \tag{E-10}$$

where

$$B_0 = \begin{pmatrix} 0 & 1 & 0 & 0 \\ l^+ & -1/r & 0 & 0 \\ 0 & 0 & 0 & 1 \\ 0 & 0 & l^- & -1/r \end{pmatrix}$$

and

$$l^+(r) = \frac{(j+m)^2}{r^2}\,, \qquad l^-(r) = \frac{(j-m)^2}{r^2}\,.$$

The asymptotic behavior of solutions which is relevant for our approach only in a close neighborhood of origin $r \to 0^+$ is

$$y_{01} \sim r^{|j+m|}\,(1, |j+m|/r, 0, 0)^T\,, \qquad y_{02} \sim r^{|j-m|}\,(0, 0, 1, |j-m|/r)^T\,,$$

$$y_{03} \sim r^{-|j+m|}\,(1, -|j+m|/r, 0, 0)^T\,, \qquad y_{04} \sim r^{-|j-m|}\,(0, 0, 1, -|j-m|/r)^T\,.$$

The Gaussian growth and decay of these vectors motivates the reparametrization of equation (E-5) by

$$x = \frac{r^2}{2}, \qquad\qquad r = \sqrt{2r}\,. \tag{E-11}$$

Then similarly as in [1] the system (E-5) transforms into

$$z(x)' = C(x)z(x)\,, \tag{E-12}$$

where

$$C(x) = r_x\left(MBM^{-1} + M'M^{-1}\right)$$

and M is the diagonal matrix 4×4 with the diagonal entries $(1, r_x, 1, r_x)$. A derivation of this formula and all the other details regarding the rescaling of the original system and its adjoint are discussed in Appendix F.

Then

$$C(x) = C_\infty(x) + C_w(x)\,, \tag{E-13}$$

where

$$C_\infty = \begin{pmatrix} 0 & 1 & 0 & 0 \\ m^+(x)/2x & -1/x & 0 & 0 \\ 0 & 0 & 0 & 1 \\ 0 & 0 & m^-(x)/2x & -1/x \end{pmatrix}$$

and

$$C_w = \frac{w^2(x)}{x} \begin{pmatrix} 0 & 0 & 0 & 0 \\ 2 & 0 & 1 & 0 \\ 0 & 0 & 0 & 0 \\ 1 & 0 & 2 & 0 \end{pmatrix} . \tag{E-14}$$

The functions m^+ and m^- are given by

$$m^+(x) = 2x + \frac{(j+m)^2}{2x} - \alpha_+ \qquad \text{and} \qquad m^-(x) = 2x + \frac{(j-m)^2}{2x} - \alpha_- .$$

It seems reasonable to expect that the asymptotic behavior of the system (E-12) as $x \to \infty$ is the same as of the system

$$\tilde{z}'(x) = C_\infty(x)\tilde{z}(x) ,$$

since w^2 has a Gaussian-like decay (Lemma E.1). To justify it we will apply the asymptotic theory of [71], particularly Theorem 11, Chapter IV.

Theorem E.2. *[71] Let $A(t)$ be continuously differentiable and let $B(t)$ be continuous for $t \geq t_0$ with*

$$\int_{t_0}^{\infty} |A'(t)|dt < \infty, \qquad \int_{t_0}^{\infty} |B(t)|dt < \infty .$$

Suppose that all characteristic roots $\lambda_1, \ldots, \lambda_n$ of

$$A_0 = \lim_{t\to\infty} A(t)$$

are simple, let ξ_i be a characteristic vector of A_0 belonging to the characteristic root λ_i, and let $\lambda_i(t)$ denote the characteristic root of $A(t)$ which converges to λ_i as $t \to \infty$, $(i = 1, \ldots, n)$.

If for some integer i none of the differences $\Re\{\lambda_i(t) - \lambda_j(t)\}$, $j \neq i$ change the sign, then the equation

$$x' = [A(t) + B(t)]\, x$$

has a solution $x_i(t)$ *such that for* $t \to \infty$

$$x_i(t) = \exp\{\int_{t_0}^{t} \lambda_i(s)ds\} \left[\xi_i + o(1)\right] .$$

First we note that the statement of the Theorem E.2 is true also if we assume that the eigenvalues $\lambda_1, \ldots, \lambda_n$ of A_0 are semi-simple. One only needs to check that the proof of Lemma 3 (continuous diagonalization of $A(t)$), page 112 of [71] is valid for semi-simple eigenvalues. We use Theorem E.2 only through the corollary.

Corollary E.3. *Let* $A(t)$ *be continuously differentiable and let* $B(t)$ *be continuous for* $t \geq t_0$ *with*

$$\int_{t_0}^{\infty} |A'(t)|dt < \infty, \qquad \int_{t_0}^{\infty} |B(t)|dt < \infty .$$

Suppose that all characteristic roots $\lambda_1, \ldots, \lambda_n$ *of*

$$A_0 = \lim_{t\to\infty} A(t)$$

are simple or semi-simple, let ξ_i *be a characteristic vector of* A_0 *belonging to the characteristic root* λ_i*, and let* $\lambda_i(t)$ *denote the characteristic root of* $A(t)$ *which converges to* λ_i *as* $t \to \infty$*,* $(i = 1, \ldots, n)$*. Furthermore, let* $x_i^0(t)$*,* $i = 1, \ldots, 4$ *be four independent solutions of the equation*

$$x' = A(t)x .$$

If none of the differences $\Re\{\lambda_i(t) - \lambda_j(t)\}$*,* $(0 < i < j \leq n)$ *change sign, then the equation*

$$x' = [A(t) + B(t)]\, x$$

has four independent solutions $x_i(t)$ *such that for* $t \to \infty$

$$x_i(t) \sim x_i^0(t)\,.$$

Proof. Let us apply Theorem E.2 for $i = 1, 2, 3, 4$. We obtain the existence of four (clearly independent) solutions $x_i(t)$ which satisfy

$$x_i(t) = \exp\left(\int_{t_0}^{t} \lambda_i(s)ds\right)\left[\xi_i + o(1)\right]\,.$$

On the other hand, solutions $x_i^0(t)$ of the system

$$x' = A(t)x$$

by the definition of eigenvalue satisfy

$$x_i^0(t) = \exp\left(\int_{t_0}^{t} \lambda_i(s)ds\right)\xi_i\,.$$

which proves the corollary. □

Now we are prepared to prove the asymptotic behavior as stated in Theorem 3.4.1 which is analogous to Lemma 4.1. of [1].

Proof. The asymptotic behavior as $r \to 0^+$ is the same as of the Bessel function. The proof based on a proper rescaling is omitted here. Unfortunately it is not possible to rescale (E-5) similarly as in [1] to establish the asymptotics, as $r \to \infty$. Instead, we use the scaling introduced in (E-11) and transform the system (3.35) into (E-12).

First, we show that the matrix $C_w(r)$ is integrable. Lemma E.1 reveals that $w(r)$ decays as $r \to \infty$ at least like $e^{-r^2/2}$. Since $x = r^2/2$, the function w^2/x is L^1 integrable on every interval $[x_0, \infty)$, $x_0 > 0$. Therefore

$$\int_{x_0}^{\infty} |C_w(x)|\,dx \le k \int_{x_0}^{\infty} \frac{w^2(x)}{x} dx < \infty\,. \tag{E-15}$$

Next, we prove that $C'_\infty(x)$ is integrable. We have

$$C'_\infty(x) = \frac{1}{x^2}\begin{pmatrix} 0 & 0 & 0 & 0 \\ \beta_+(x) & 1 & 0 & 0 \\ 0 & 0 & 0 & 0 \\ 0 & 0 & \beta_-(x) & 1 \end{pmatrix},$$

where

$$\beta_+(x) = \frac{1}{2}\left(\alpha_+ - \frac{(j+m)^2}{x}\right) \qquad \text{and} \qquad \beta_-(x) = \frac{1}{2}\left(\alpha_- - \frac{(j-m)^2}{x}\right).$$

Clearly,

$$\int_{x_0}^{\infty} |C'_\infty(x)|dx \le K \int_{x_0}^{\infty} \frac{1}{x^2}dx < \infty\,.$$

The matrix $C_\infty(x)$ tends to C_0 as $x \to \infty$ with

$$C_0 = \begin{pmatrix} 0 & 1 & 0 & 0 \\ 1 & 0 & 0 & 0 \\ 0 & 0 & 0 & 1 \\ 0 & 0 & 1 & 0 \end{pmatrix}.$$

The eigenvalues $\{-1, 1, -1, 1\}$ of A_0 are semi-simple. To make use of Corollary E.3 with independent variable x corresponding to t, $C_\infty(x)$ corresponding to $A(t)$, $C_w(x)$ corresponding to $B(t)$ and $z(x)$ corresponding to $x(t)$ we need to check just one remaining assumption:

none of the differences $\Re\{\lambda_i(t) - \lambda_j(t)\}$, $0 < i < j \le n$ change sign. (E-16)

We calculate the eigenvalues of $C_\infty(x)$

$$\begin{aligned}
\lambda_1^+ &= \frac{1}{2x}\left[-1 + \sqrt{4x^2 - 2\alpha_+ x + (j+m)^2 + 1}\right] \to 1\,, \\
\lambda_2^+ &= \frac{1}{2x}\left[-1 - \sqrt{4x^2 - 2\alpha_+ x + (j+m)^2 + 1}\right] \to -1\,, \\
\lambda_1^- &= \frac{1}{2x}\left[-1 + \sqrt{4x^2 - 2\alpha_- x + (j-m)^2 + 1}\right] \to 1\,, \\
\lambda_2^- &= \frac{1}{2x}\left[-1 - \sqrt{4x^2 - 2\alpha_- x + (j-m)^2 + 1}\right] \to -1\,.
\end{aligned}$$

To prove (E-16) we only need to show that $\Re\{\lambda_1^+(x) - \lambda_2^+(x)\}$ and $\Re\{\lambda_1^-(x) - \lambda_2^-(x)\}$ do not change sign as $x \to \infty$.

Let us first prove a simple auxiliary lemma.

Lemma E.4. *a) Let $a > 0$ and b are two real numbers. Then $\Re(\sqrt{a+bi}) = \Re(\sqrt{a-bi})$, where by square root we consider only its first sheet (i.e. positive real part).*

b) Let z is a complex number and c a positive real number $\Re z > c$. Then $\Re(\sqrt{z+c}) > \Re(\sqrt{z-c})$.

Proof. The statement a) is obvious. To prove b) first note that $|z+c| > |z-c|$ and $0 < \arg(z+c) < \arg(z-c) < \frac{\pi}{2}$. Therefore

$$\Re(\sqrt{z+c}) = |z+c| \cos\left(\frac{1}{2}\arg(z+c)\right) > |z-c| \cos\left(\frac{1}{2}\arg(z-c)\right) = \Re(\sqrt{z-c})\,.$$

□

Clearly it is enough to prove that $\Re\{\lambda_1^+ - \lambda_1^-\}$ and $\Re\{\lambda_2^+ - \lambda_2^-\}$ do not change sign as $x \to \infty$. We prove the first statement, the proof of the other is analogous. We have

$$\begin{aligned}
\Re\{\lambda_1^+ - \lambda_1^-\} &= \Re\left\{\frac{1}{2}\left[\sqrt{4x^2+1+(j+m)^2-2\alpha_+ x}\right.\right. \\
&\qquad \left.\left. -\sqrt{4x^2+1+(j-m)^2-2\alpha_- x}\right]\right\} \\
&= \Re\left\{\sqrt{A+b-ci} - \sqrt{A-b+ci}\right\}\,,
\end{aligned}$$

where

$$\begin{aligned}
A &= 4x^2+1+j^2+m^2-2px\,, \\
b &= 2jm+2\lambda_i x\,, \\
c &= 2\lambda_r x\,.
\end{aligned}$$

Then $A > 0$ and $A > b$ as $x \to \infty$.

We apply Lemma E.4, part a) to obtain

$$\Re\{\lambda_1^+ - \lambda_1^-\} = \Re\left\{\sqrt{A+b-ci} - \sqrt{A-b-ci}\right\} = \Re\left\{\sqrt{z+b} - \sqrt{z-b}\right\}$$

with $z = A - ci$.

For $\lambda_i > 0$, $b > 0$ for x large enough and then

$$\Re\{\lambda_1^+ - \lambda_1^-\} = \Re\left\{\sqrt{z+b} - \sqrt{z-b}\right\} > 0$$

by Lemma E.4, part b).

Similarly for $\lambda_i < 0$ we get $b < 0$ for x large enough and

$$\Re\{\lambda_1^+ - \lambda_1^-\} = \Re\left\{\sqrt{z+b} - \sqrt{z-b}\right\} < 0\,.$$

Finally, for $\lambda_i = 0$, the parameter $b = 2jm$ is constant for all x. Since $m \neq 0$ if $j \neq 0$ then $b = 2jm \neq 0$. This implies that $\Re\{\lambda_1^+ - \lambda_1^-\}$ does not change sign as $x \to \infty$. This is caused by the presence of two different (independent) solutions with the same decay rate as $r \to \infty$. Although the statement of the theorem is still true, the argument in the case $\lambda_i = 0$ and $j = 0$ must be different.

First, observe that the system (3.35) reduces in that case to

$$\left[\triangle_r - \frac{m^2}{r^2} - r^2 + 2(p + i\lambda)\right] y_+ + 4|w|^2 y_+ + 2|w|^2 y_- \;=\; 0\,, \qquad \text{(E-17)}$$

$$\left[\triangle_r - \frac{m^2}{r^2} - r^2 + 2(p - i\lambda)\right] y_- + 4|w|^2 y_- + 2|w|^2 y_+ \;=\; 0\,. \qquad \text{(E-18)}$$

Let (y_+, y_-) be any fixed solution to (E-17)–(E-18). Set $u = y_+ - \overline{y_-}$ and $v = y_+ + \overline{y_-}$. Then (E-17)–(E-18) transforms into a decoupled system (the special property $\overline{p + i\lambda} = p - i\lambda$ is used here)

$$\left[\triangle_r - \frac{m^2}{r^2} - r^2 + 2(p + i\lambda)\right] u + 4|w|^2 u - 2|w|^2 \overline{u} \;=\; 0\,, \qquad \text{(E-19)}$$

$$\left[\triangle_r - \frac{m^2}{r^2} - r^2 + 2(p + i\lambda)\right] v + 4|w|^2 v + 2|w|^2 \overline{v} \;=\; 0\,. \qquad \text{(E-20)}$$

The asymptotic behavior of solutions to both (E-19) and (E-20) can be treated similarly as in the case $j \neq 0$, although the proof is slightly complicated by the presence of the complex conjugate. Nevertheless, after the same rescaling as in the previous case $x = r^2/2$ the equation (E-19) can be rewritten as a 2×2 system of ordinary differential equations

$$\nu' = A(x)\nu + B(x)\nu + C(x)\overline{\nu}\,,$$

where $\nu = (u, u')^T$ and

$$A(x) = \begin{pmatrix} 0 & 1 \\ \frac{m(x)}{2x} & -\frac{1}{x} \end{pmatrix}\,, \quad B(x) = |w|^2 \begin{pmatrix} 0 & 0 \\ 4 & 0 \end{pmatrix}\,, \quad C(x) = -|w|^2 \begin{pmatrix} 0 & 0 \\ 2 & 0 \end{pmatrix}\,.$$

Let us denote the small terms as $g(x, \nu) = B(x)\nu + C(x)\overline{\nu}$.

The statement of Theorem 11, Chapter IV [71] does not directly apply in this case since the system is not linear, but the proof relies on a more general Theorem 11, Chapter III [71], which states that there exists a one-to-one bicontinuous correspondence (preserving the asymptotic behavior) between solutions of the linear equation $z' = A(t)z$ and solutions of the perturbed equation $z' = A(t)z + f(t, z)$. The assumptions on $A(t)$ are identical to the previously required conditions for the asymptotic 4×4 system and it is easy to check that they are satisfied. The assumptions on $f(t, x)$ are

$$\int_{t_0}^{\infty} |f(t, 0)|dt < \infty$$

and

$$|f(t, z_1) - (t, z_2)| \leq \gamma(t)|z_1 - z_2|\,.$$

Both conditions are met when $f(t, z) = C(t)z + D(t)\overline{z}$, if $C(t)$ and $D(t)$ are L^1 integrable matrices. Hence even after $g(x, \nu)$ is properly rescaled as in the case of $j \neq 0$ the statement applies to (E-19). The argument for (E-20) is the same.

This proves the asymptotic behavior of solutions to (E-19)–(E-20). To find find out the behavior of (E-17)–(E-18) observe that if (u, v) satisfy (E-19)–(E-20), then $(u + v, \overline{v - u})$ solves (E-17)–(E-18). Therefore there is an equivalence between this two systems and the asymptotics of solutions to (E-17)–(E-18) can be deduced. The results are same as in the case $j \neq 0$. □

Appendix F

Rescaling formulas

This Appendix contains all the necessary formulas for rescaling of the system of ordinary differential equations used in the numerical implementation of the Evans function. Rescaling of the eigensystem described in Appendix E is inevitable since the Gaussian growth of the solutions on the stable manifold produces a significant numerical error. On the the hand, the rescaled system has bounded matrix elements, and numerically does not pose any significant complication. In the actual implementation of the code the logarithmic rescaling close to the origin appeared to crucial.

For simplicity only 2×2 linear first order ordinary differential equation systems obtained by reduction of linear second order ordinary equations will be considered. The generalization to 4×4 system obtained by reduction of two coupled second order ODE's is straightforward.

Recall a rescaling lemma from [1]:

Proposition F.1. *Let* $\overrightarrow{y}(r) = (y(r), y'(r))^T$ *and let* B *be a* 2×2 r*-dependent matrix. Rescaling*

$$\xi(x) = h(r)y(r),$$

where $r = r(x)$ *transforms system*

$$\overrightarrow{y}'(r) = B(r)\overrightarrow{y}(r)$$

into

$$\overrightarrow{\xi}'(x) = r_x C(x) \overrightarrow{\xi}(x)\,,$$

where $\overrightarrow{\xi}(x) = (\xi(x), \xi'(x))^T$, $\overrightarrow{\xi} = M\overrightarrow{y}$,

$$M = \begin{pmatrix} h & 0 \\ h'r_x & hr_x \end{pmatrix} \tag{F-1}$$

and

$$C(x) = MBM^{-1} + M'M^{-1}\,.$$

The system considered in the proposition will be referred to as "the original system" with its counterpoint the adjoint system for which the analogous statement reads:

Proposition F.2. *Let* $\overrightarrow{z}(r) = (z(r), z'(r))$ *and let* B *be a* 2×2 r*-dependent matrix. Rescaling*

$$\zeta(x) = \tilde{h}(r)z(r),$$

where $r = \tilde{r}(x)$ *transforms system*

$$\overrightarrow{z}'(r) = -\overrightarrow{z}(r)B(r)$$

into

$$\overrightarrow{\zeta}'(x) = -\overrightarrow{\zeta}(x)\tilde{r}_x\tilde{D}(x)\,,$$

where $\overrightarrow{\zeta}(x) = (\zeta(x), \zeta'(x))$, $\overrightarrow{\zeta} = \overrightarrow{z}\tilde{N}$,

$$\tilde{N} = \begin{pmatrix} \tilde{h} & \tilde{h}'\tilde{r}_x \\ 0 & \tilde{h}\tilde{r}_x \end{pmatrix} \tag{F-2}$$

and

$$\tilde{D}(x) = \tilde{N}^{-1}B\tilde{N} - \tilde{N}^{-1}\tilde{N}'\,.$$

It is desired to conserve the property $\overrightarrow{z}(r) \cdot \overrightarrow{y}(r) = \text{const}$ for the pair of vectors $\overrightarrow{\xi}(x)$ and $\overrightarrow{\zeta}(x)$. Assume that the rescaling $\overrightarrow{\xi}(x) = M(r)\overrightarrow{y}(r)$ is given and search for such $N(r)$, $\overrightarrow{\zeta}(x) = \overrightarrow{z}(r)N(r)$, that will guarantee $\overrightarrow{\zeta}(x) \cdot \overrightarrow{\xi}(x) = \text{const}$. Clearly, it is necessary to set $N(r) = M^{-1}(r)$ (up to a constant multiple). Given (F-1) the inverse must be

$$N(r) = M^{-1} = \begin{pmatrix} 1/h & 0 \\ -h'/h^2 & 1/(hr_x) \end{pmatrix} .$$

The structure of (F-2) yields that this is possible only for $h' = \tilde{h}' = 0$. Therefore for simplicity set $h(r) = \tilde{(h)}(r) = 1$ and then $\tilde{N}(r) = N(r)$ implies

$$\tilde{N}(r) = \begin{pmatrix} 1 & 0 \\ 0 & 1/r_x \end{pmatrix} .$$

Hence $\tilde{r}(x) = 1/r_x$. The adjoint system then must according to Proposition F.2 have the form

$$\overrightarrow{\zeta}'(x) = -\overrightarrow{\zeta}(x) = \frac{1}{r_x}\tilde{D}(x)$$

for

$$\begin{aligned} \tilde{D}(x) &= \left(\tilde{N}^{-1}B\tilde{N} - \tilde{N}^{-1}\tilde{N}'\right) = \left(MBM^{-1} - M(M^{-1})'\right) \\ &\quad \left(MBM^{-1} + M'M^{-1}\right) , \end{aligned}$$

i.e. the rescaled adjoint system has almost the same form as the rescaled original system except of a different factors r_x and $1/r_x$.

In the systems considered in Chapter 3 two different rescaling were introduced:

$$x = \ln r \quad \text{as } r \to 0^+ \qquad \text{and} \qquad x = \frac{r^2}{2} \quad \text{as } r \to \infty.$$

Since $r_x = r$ and $r_x = 1/r$ respectively in these cases, the scaling of the adjoint system (preserving the constant inner product of solutions) must be the exact

opposite

$$x = \frac{r^2}{2} \quad \text{as } r \to 0^+ \qquad \text{and} \qquad x = \ln r \quad \text{as } r \to \infty$$

which may seem unexpected at the first glance. Note that as pointed above the generalization to 4×4 systems is straightforward.

The exterior systems associated with the original system and the adjoint system were also discussed in [1]. The original system $y'(r) = B(r)y(r)$ transforms into $\hat{y}'(r) = \hat{B}(r)\hat{y}(r)$ and the adjoint system $z'(r) = -z(r)B(r)$ into $\hat{z}'(r) = -\hat{z}(r)\hat{B}(r)$. The definition of $\hat{B}$ is $\hat{B} = B \wedge E$, where E is the 4×4 identity matrix and the wedge (exterior) product of two matrices is introduced in the next definition.

Definition F.3. *Let A and B be square matrices of the same dimension. We denote by $A \wedge B$ the exterior product:*

$$(A \wedge B)_{j\wedge k, i\wedge i'} = a_{ij}b_{i'k} - a_{ik}b_{i'j}\,.$$

Note that the $j \wedge k$ column of $A \wedge A$ is the wedge product of the j-th and k-th columns of A.

The next lemma describes the relation between and the vector wedge product and a linear mapping represented by A. This handy formula is used a couple of times in the numerical code.

Lemma F.4. *Let A be a $n \times n$ matrix and let v and w be vectors $n \times 1$. Then*

$$(Av) \wedge (Aw) = (A^T \wedge A^T)(v \wedge w)\,.$$

Moreover

$$(v^T A) \wedge (w^T A) = (v^T \wedge w^T)(A \wedge A)\,.$$

Proof. Let $A = (a_{ij})$, $v = (v_i)$, and $w = (w_i)$. Then for j, k, $1 \le j < k \le n$:

$$\begin{aligned}
[(Av) \wedge (Aw)]_{j\wedge k} &= (Av)_j(Aw)_k - (Av)_k(Aw)_j \\
&= (a_{ji}v_i)(a_{ki'}w_{i'}) - (a_{ki}v_i)(a_{ji'}w_{i'}) \\
&= \sum_{i,i'}(a_{ji}a_{ki'} - a_{ki}a_{ji'})v_iw_{i'} \\
&= \sum_{i<i'}(a_{ji}a_{ki'} - a_{ki}a_{ji'})(v_iw_{i'} - v_{i'}w_i) \\
&= \sum_{i<i'}(a_j^T \wedge a_k^T)(v \wedge w)_{i\wedge i'} \\
&= (A^T \wedge A^T)_{j\wedge k}(v \wedge w)\,.
\end{aligned}$$

Hence

$$(Av) \wedge (Aw) = (A^T \wedge A^T)(v \wedge w)\,.$$

The proof of the second statement is analogous. □

Finally, it is necessary to resolve the question how the rescaling of both original and adjoint system will influence the exterior products. Assume $y'(r) = B(r)y(r)$ is rescaled into $\xi'(x) = r_xC(x)\xi(x)$. Then the system for exterior products corresponding to the rescaled problem is

$$\hat{\xi}'(x) = r_x(C \wedge E)(x)\hat{\xi}(x)\,. \tag{F-3}$$

Similarly the system for exterior products associated with the rescaled adjoint system $\zeta'(x) = -\zeta(x)(1/r_x)C(x)$ is given by

$$\hat{\zeta}'(x) = -\hat{\zeta}(x)\frac{1}{r_x}(C \wedge E)(x)\,. \tag{F-4}$$

It is easy to prove that the product of the fundamental matrices of (F-3) and (F-4) is identity and thus it is in in agreement with the definition of the Evans function in Chapter 3.

Appendix G

Galerkin approximation

Appendix G contains the analytical background for finding the eigenfunction for an already calculated eigenvalue of the system (3.31). This procedure makes use of a Galerkin approximation and is similar to one used in [4].

Consider an eigenvalue problem

$$Ly = i\lambda Ry \tag{G-1}$$

where $y = (y_+, y_-)^T$,

$$R = \begin{pmatrix} 1 & 0 \\ 0 & -1 \end{pmatrix} \quad \text{and} \quad L = \begin{pmatrix} H_{j+m} - p & 0 \\ 0 & H_{j-m} - p \end{pmatrix} + |w|^2 \begin{pmatrix} 2 & 1 \\ 1 & 2 \end{pmatrix}$$

and $H_k = -\frac{1}{2}\triangle_r + \frac{k^2}{2r^2} + \frac{1}{2}r^2$, λ is an given eigenvalue (or its numerical approximation). The asymptotic analysis reveals the expected asymptotic behavior of y:

$$y \sim \begin{pmatrix} r^{j+m} \\ r^{j-m} \end{pmatrix} \quad \text{as } r \to 0^+ \quad \text{and} \quad y \sim e^{-\frac{r^2}{2}} \begin{pmatrix} r^{p+i\lambda-1} \\ r^{-p-i\lambda-1} \end{pmatrix} \quad \text{as } r \to \infty$$

Therefore we set

$$y = r^{j+m} e^{-\frac{r^2}{2}} \sum_{n=0}^{\infty} a_n \begin{pmatrix} L_n(r^2) \\ 0 \end{pmatrix} + r^{j-m} e^{-\frac{r^2}{2}} \sum_{n=0}^{\infty} b_n \begin{pmatrix} 0 \\ L_n(r^2) \end{pmatrix}. \tag{G-2}$$

Here $L_n(r^2)$ is a Laguerre polynomial satisfying

$$xL_n''(x) + (1-x)L_n'(x) + nL_n(x) = 0\,, \qquad n = 0, 1, 2, \ldots \tag{G-3}$$

Also, we will need an recurrence formula for derivatives of Laguerre polynomials

$$xL_n'(x) = n\left(L_n(x) - L_{n-1}(x)\right)\,, \qquad n = 1, 2, \ldots \tag{G-4}$$

Finally, Laguerre polynomials form an orthonormal basis with respect to a particular scalar product:

$$\int_0^\infty e^{-x} L_n(x) L_m(x) dx = \delta_{mn}\,. \tag{G-5}$$

These relations imply

$$rL_n''(r^2) + (1-2r^2)L_n'(r^2) + 4rnL_n(r^2) = 0\,, \qquad n = 0, 1, 2, \ldots \tag{G-6}$$

and

$$rL_n'(r^2) = 2n\left(L_n(r^2) - L_{n-1}(r^2)\right)\,, \qquad n = 1, 2, \ldots \tag{G-7}$$

and also

$$\int_0^\infty e^{-r^2} L_n(r^2) L_m(r^2) 2r dr = \delta_{mn}\,. \tag{G-8}$$

Let $F_n^{(k)} = L_n(r^2) r^k e^{-r^2/2}$. Then a short calculation gives

$$H_k F_n^{(k)} = \left[-2r^2 L_n'' - 2(k+1-r^2)L_n' + (k+1)L_n\right] r^k e^{-r^2/2}\,.$$

Inserting (G-6) into this expression yields

$$H_k F_n^{(k)} = \left[2(-2r^3 + r^2 + r - k - 1)L_n'(r^2) + (k+1+8r^2 n)L_n(r^2)\right] r^k e^{-r^2/2}\,.$$

To avoid use of derivatives we replace L_n' in the expression using (G-7):

$$\begin{aligned} H_k F_n^{(k)} \;=\; & \Big[4n\left(-2r^2 + r + 1 - \frac{k+1}{r}\right)\left(L_n(r^2) - L_{n-1}(r^2)\right) \\ & + (k+1+8r^2 n)L_n(r^2)\Big] r^k e^{-r^2/2} \end{aligned}$$

Consequently, the system (G-1) transforms into a system

$$
\begin{aligned}
i\lambda r^{j+m}e^{-r^2/2}\sum_n a_nL_n &= \sum_n (j+m+1-p-8r^2n)r^{j+m}e^{-r^2/2}L_na_n \\
&\quad + 4\sum_n \left(-2r^2+r+1\right)(L_n-L_{n-1})a_nr^{j+m}e^{-r^2/2} \\
&\quad - 4\sum_n \frac{j+m+1}{r}(L_n-L_{n-1})a_nr^{j+m}e^{-r^2/2} \\
&\quad + 2|w|^2r^{j+m}e^{-r^2/2}\sum_n a_nL_n \\
&\quad + |w|^2r^{j-m}e^{-r^2/2}\sum_n b_nL_n\,, \qquad \text{(G-9)} \\
i\lambda r^{j-m}e^{-r^2/2}\sum_n b_nL_n &= \sum_n (j-m+1-p-8r^2n)r^{j-m}e^{-r^2/2}L_nb_n \\
&\quad + 4\sum_n \left(-2r^2+r+1\right)(L_n-L_{n-1})b_nr^{j-m}e^{-r^2/2} \\
&\quad - 4\sum_n \frac{j-m+1}{r}(L_n-L_{n-1})b_nr^{j-m}e^{-r^2/2} \\
&\quad + 2|w|^2r^{j-m}e^{-r^2/2}\sum_n b_nL_n \\
&\quad + |w|^2r^{j+m}e^{-r^2/2}\sum_n a_nL_n\,, \qquad \text{(G-10)}
\end{aligned}
$$

Finally, by multiplying (G-9) by a factor $e^{r^2/2}r^{-(j+m)}$ and integrating over $(0,\infty)$ with respect to $e^{-r^2}L_k(r^2)2rdr$ (to assure orthonormality of L_n) one gets

$$
\begin{aligned}
i\lambda a_k &= (j+m+1-p)a_k + 8\sum_n a_n\int_0^\infty r^2L_nL_ke^{-r^2}2rdr \\
&\quad - 4(j+m+1)\sum_n 2na_n\int_0^\infty L_k(L_n-L_{n-1})e^{-r^2}dr \\
&\quad + 4\sum_n na_n\int_0^\infty(-2r^2+r+1)L_k(L_n-L_{n-1})e^{-r^2}2rdr \\
&\quad + 2\sum_n a_n\int_0^\infty |w|^2L_kL_ne^{-r^2}2rdr \\
&\quad + \sum_n b_n\int_0^\infty \frac{|w|^2}{r^{2m}}L_kL_ne^{-r^2}2rdr\,. \qquad \text{(G-11)}
\end{aligned}
$$

Similarly (G-10) transforms into

$$\begin{aligned}
-i\lambda b_k &= (j-m+1-p)b_k + 8\sum_n b_n \int_0^\infty r^2 L_n L_k e^{-r^2} 2r dr \\
&\quad - 4(j-m+1)\sum_n 2nb_n \int_0^\infty L_k (L_n - L_{n-1}) e^{-r^2} dr \\
&\quad + 4\sum_n nb_n \int_0^\infty (-2r^2 + r + 1) L_k (L_n - L_{n-1}) e^{-r^2} 2r dr \\
&\quad + 2\sum_n b_n \int_0^\infty |w|^2 L_k L_n e^{-r^2} 2r dr \\
&\quad + \sum_n a_n \int_0^\infty |w|^2 r^{2m} L_k L_n e^{-r^2} 2r dr \,. \qquad \text{(G-12)}
\end{aligned}$$

This motivates the introduction of matrices B, C, E and F consisting of the following integrals:

$$\begin{aligned}
B_{ij} &= \int_0^\infty \frac{|w|^2}{r^{2m}} L_i(r^2) L_j(r^2) e^{-r^2} 2r dr \,, \\
C_{ij} &= \int_0^\infty |w|^2 r^{2m} L_i(r^2) L_j(r^2) e^{-r^2} 2r dr \,, \\
F_{ij} &= \int_0^\infty |w|^2 L_i(r^2) L_j(r^2) e^{-r^2} 2r dr \,, \\
E^{(1)}_{ij} &= 2\int_0^\infty L_i(r^2) \left(L_j(r^2) - L_{j-1}(r^2) \right) e^{-r^2} dr \,, \\
E^{(2)}_{ij} &= 2\int_0^\infty (-2r^2 + r + 1) L_i(r^2) \left(L_j(r^2) - L_{j-1}(r^2) \right) e^{-r^2} dr \,, \\
G_{ij} &= \int_0^\infty r^2 L_i(r^2) L_j(r^2) e^{-r^2} 2r dr \,.
\end{aligned}$$

Then the system (G-11)–(G-12) reads

$$\begin{aligned}
i\lambda a_k &= (j+m+1-p)a_k + 8\sum_n n a_n G_{kn} - 4(j+m+1)\sum_n a_n n E^{(1)}_{kn} \\
&\quad + 4\sum_n a_n E^{(2)}_{kn} + 2\sum_n a_n F_{kn} + \sum_n b_n B_{kn} \,, \qquad \text{(G-13)} \\
-i\lambda b_k &= (j-m+1-p)b_k + 8\sum_n n b_n G_{kn} - 4(j-m+1)\sum_n b_n n E^{(1)}_{kn} \\
&\quad + 4\sum_n b_n E^{(2)}_{kn} + 2\sum_n b_n F_{kn} + \sum_n a_n C_{kn} \,, \qquad \text{(G-14)}
\end{aligned}$$

This infinitely-dimensional system will is in the numerical approximation truncated to a finite $2n \times 2n$ system for a solution vector $v = (a, b)^T$

$$Mv = 0$$

where M is a block matrix

$$M = \begin{pmatrix} A & B \\ C & D \end{pmatrix}$$

with

$$\begin{aligned} A &= (j + m + 1 - p - i\lambda)I + 8GT - 4(j + m + 1)E^{(1)}T + 4E^{(2)}T + 2F\,, \\ D &= (j - m + 1 - p + i\lambda)I + 8GT - 4(j - m + 1)E^{(1)}T + 4E^{(2)}T + 2F\,, \end{aligned}$$

where I is the $n \times n$ identity matrix and T is a matrix with diagonal entries $(0, 1, 2, \ldots, n-1)$ and all other elements zero.

In the actual implementation $n = 20$ was used and the complex system was decomposed to a real and imaginary part. This procedure then yields $4n \times 4n$ real system. The eigenfunction then corresponds to a non-zero solution vector. In practice the matrix M is not singular since λ is only a numerical approximation of the eigenvalue, elements of matrices B, C, E, F are only numerically evaluated (they also depend on numerically obtained function w on a finite interval) and finally, only a finite number of basis elements corresponding to a_n and b_n is used. It motivates a search for solution with fixed norm with a smallest possible remainder Mv, or equivalently a search for an eigenvector corresponding to the smallest singular value of $M^T M$.

BIBLIOGRAPHY

[1] R.L. Pego, H.A. Warchall, Spectrally stale encapsulated vortices for nonlinear Schrödinger equations. *J. Nonlinear Sci.***12** (2002), 347–394.

[2] F. Dalfovo, S. Giorgini, L.P. Pitaevskii, S. Stringari, Theory of Bose-Einstein condensation in trapped gases. *Rev. Mod. Phys.* **71** (1999), no. 3., 463–512.

[3] M. Edwards, R.J. Dodd, C.W. Clark, K. Burnett, Zero-temperature, mean-field theory of atomic Bose-Einstein condensates. *J. Res. Natl. Inst. Stand. Technol.* **101** (1996), 553.

[4] J.J. García-Ripoll, V.M. Pérez-García, Stability of vortices in inhomogeneous Bose condensates subject to rotation: A three-dimensional analysis. *Phys. Rev. A*, **60** (1999), no. 6, 4864–4874.

[5] H. Pu, C.K. Law, J.H. Eberly, N.P. Bigelow, Coherent disintegration and stability of vortices in trapped Bose condensates. *Phys. Rev. A* **59** (1999), 1533.

[6] W. Bao, D. Jaksch, P.A. Markowich, Numerical solution of the Gross-Pitaevskii equation for Bose-Einstein condensation. *J Comp. Phys.*, **187** (2003), 318–342.

[7] R. Kollár, On non-existence of vortex solutions to the Landau-Lifshitz magnetization equation. Preprint 2003, submitted to *Trans. AMS*.

[8] F.A. Berezin, M.A. Shubin, *The Schrödinger Equation*. Kluwer Acad. Publ., 1991.

[9] L.M. Pismen, J. Rubinstein, Dynamics of Defects, *Nematics (Orsay, 1990, J.M. Coron ed.*, 303–326, NATO Adv. Sci. Inst. Ser. C Math. Phys. Sci., 332. Kluwer Acad. Publ., 1991.

[10] A.L. Fetter, A.A. Svidzinsky, Vortices in a trapped dilute Bose-Einstein condensate. *J. Phys. Condens. Matter*, **13** (2001) no. 12, R135.

[11] P.-L. Lions, Solutions complexes d'équations ellitiques semilinéaires dans $\mathbb{R}^n$. *C. R. Acad. Sci. Paris Sér. I Math.* **302** (1986), 673–676.

[12] J.C. Neu, Vortices in complex scalar fields. *Physica D* **43** (1990), 385–406.

[13] M.I. Weinstein, On the vortex solutions of some nonlinear scalar field equations. *Rocky Mtn. J. Math.* **21** (1991), 821–827.

[14] J. Iaia, H. Warchall, Encapsulated-vortex solutions to equivariant wave equations: Existence. *SIAM J. Math. Anal.* **30** (1998), no. 1, 118–139.

[15] J. Iaia, H. Warchall, Nonradial solutions of a semilinear elliptic equation in two dimensions. *J.Diff. Eq.* **119** (1995), no. 2, 533–558.

[16] M.I. Weinstein, J. Xin, Dynamic stability of vortex solutions of Ginzburg-Landau and nonlinear Schrödinger equations. *Comm. Math. Phys.* **180** (1996), no.2, 389–428.

[17] R.L. Pego, M.I. Weinstein, Eigenvalues, and instabilities of solitary waves. *Phil. Trans. Roy. Soc. London A* **340** (1992), 47–94.

[18] I. Towers, A.V. Buryak, R.A. Sammut, B.A. Malomed, L.-C. Crasovan, D. Mihalache, Stability of spinning ring solitons of the cubic-quintic nonlinear Schrödinger equation. *Phys. Lett. A* **288** (2001), 292–298.

[19] M. Grillakis, J. Shatah, W. Strauss, Stability theory of solitary waves in the presence of symmetry, I. *J. Func. Anal.* **74** (1987), 160–197.

[20] A. De Bouard, Instability of stationary bubbles. *SIAM J. Math. Anal.* **26** (1995), no. 3, 566–582.

[21] M.H. Anderson, J.R. Ensher, M.R. Matthews, C.E. Wieman, E.A. Cornell, Observation of Bose-Einstein condensation in a dilute atomic vapor. *Science*, **269** (1995), 198–201.

[22] K.B. Davis, M.O.Mewes, M.R. Andrews, N.J. van Druten, D.S. Durfee, D.M. Kurn, W. Ketterle, Bose-Einstein condensation in a gas of sodium atoms. *Phys. Rev. Lett.*, **75** (1995), 3969–3973.

[23] C.J. Pethick, H. Smith, *Bose-Einstein Condensates in Dilute Gases*. Cambridge Press, 2002.

[24] E.H. Lieb, R. Seiringer, J. Yngvanson, A rigorous derivation of the Gross-Pitaevskii energy functional for a two-dimensional Bose gas. *Comm. Math. Phys.*, **224** (2001), no.1, 17–31.

[25] E.H. Lieb, R. Seiringer, J.P.Solovej, J. Yngvanson, The ground state of the Bose gas. *Current developments in mathematics*, 2001, 131–178, *Int. Press, Sommerville, MA, 2002.*

[26] E.H. Lieb, R. Seiringer, Proof of Bose-Einstein condensation for dilute trapped gases. *Phys. Rev. Lett.* **88** (2002), 170409.

[27] R.K. Jackson, M.I. Weinstein, Geometric analysis of bifurcation and symmetry breaking in a Gross-Pitaevskii equation. 2003, to appear in *J. Stat. Phys.*

[28] Y. Castin, R. Dum, Bose-Einstein condensates with vortices in rotating traps. *Eur. Phys. J. D*, **7** (1999), 399–412.

[29] A. Aftalion, Q.Du, Vortices in a rotating Bose-Einstein condensate: critical angular velocities and energy diagrams in the Thomas-Fermi regime. *Phys.Rev. A*, **64** (2001), 063603.

[30] T.P. Simula, S.M.M. Virtanen, M.M. Salomaa, Stability of multiquantum vortices in dilute Bose-Einstein condensates. *Phys.Rev. A*, **65** (2002), 033614.

[31] R. Seiringer, Gross-Pitaevskii theory of the rotating Bose gas. *Comm. Math. Phys.*, **229** (2002), 491–509.

[32] T. Isoshima, K. Machida, Vortex stabilization in dilute Bose-Einstein condensate under rotation. *J. Phys. Soc. Jpn.* **68** (1999), 487–492.

[33] S.M.M. Virtanen, T.P. Simula, M.M. Salomaa, Structure and stability of vortices in dilute Bose-Einstein condensates at ultralow temperatures. *Phys. Rev. Lett.* **86** (2001), 2704–2707.

[34] J.J. García-Ripoll, G. Molina-Terriza, V.M. Pérez-García, L. Torner, Structural instability of vortices in Bose-Einstein condensates. Preprint, 2001, arXiv/cond-mat/0106210.

[35] B. Deconinck, J.N. Kutz, Singular instability of exact stationary solutions of the nonlocal Gross-Pitaevskii equation. *Phys. Rev. Lett.*, **87** (2001), no. 14, 140403.

[36] P.G. Keverkidis, D.J. Frantzeskakis, B.A. Malomed, A.R. Bishop, I.G. Keverkidis Dark-in-bright solitons in Bose-Einstein condensates with attractive interactions. Preprint, 2003, arXiv/cond-mat/0304676.

[37] L.D. Carr, J.N. Kutz, W.P. Reinhardt, Stability of stationary states in cubic nonlinear Schrödinger equation: Applications to the Bose-Einstein condensate. *Phys. Rev. E* **63** (2001), 066604.

[38] S. Komineas, N. Papanicolaou, Solitons, solitonic vortices and vortex rings in a cylindrical Bose-Einstein condensate, Preprint, 2003, arXiv/cond-mat/0304123.

[39] J. Alexander, R.Gardner, C.K.R.T. Jones, A topological invariant arising in the stability analysis of traveling waves. *J. Reine Angew. Math.*, **410** (1990), 167–212.

[40] T. Isoshima, K. Machida, Vortex stabilization in Bose-Einstein condensate of alkali-metal atom gas. *Phys. Rev. A*, **59** (1999), 2203–2212.

[41] H.Feshbach, *Theoretical Nuclear Physics*. Wiley, New York, 1992.

[42] Z. Muslimani, private communication, (2004).

[43] J.J. García-Ripoll, V.M. Pérez-García , V. Vekslerchik, Construction of exact solutions by spatial translation in nonhomogeneous nonlinear Schrödinger equations. Preprint, 2001, arXiv/cond-mat/0106535.

[44] M. Abramowitz, I.A. Stegun, *Handbook of mathematical functions with formulas, graphs, and mathematical tables.* National Bureau of Standarts Applied Mathematics Series 55, 1964.

[45] M.G. Crandall, P.H. Rabinowitz, Bifurcation, perturbation of simple eigenvalues and linearized stability. *Arch. Rational Mech. Anal.*, **52** (1973), 161–180.

[46] E.L. Allgower, K. Georg, *Numerical Continuation Methods: An Introduction.* Series in Computational Mathematics 13, Springer Verlag, Heidelberg, 1990.

[47] J. Stoer, R. Bulirsch, *Introduction to Numerical Analysis.* 2nd ed., Springer, 1993.

[48] R. D'Agosta, B.A. Malomed, C. Presilla, Stationary solutions of the Gross-Pitaevskii equation with linear counterpart. *Phys. Lett. A* **275** (2000), 424–434.

[49] M. Reed, B. Simon, Methods of Modern Mathematical Physics I: Functional Analysis. Academic Press Inc., 1972.

[50] T. Kapitula, P.G. Kevrekidis, B. Sandstede, Counting eigenvalues via the Krein signature in infinite-dimensional Hamiltonian systems. Preprint 2003, to appear in *Physica D.*

[51] T.R. Taha, M.J. Ablowitz, Analytical and numerical aspects of certain nonlinear evolution equations. II. Numerical, nonlinear Schrödinger equation. *J. Comput. Phys* **55** (1984), 203–230.

[52] J.-G. Liu, private communication (2002).

[53] L. Landau, E. Lifshitz, On the theory of dispersion of magnetic permeability in ferromagnetic bodies. *Physik. Z. Sowietunion* **8** (1935), 153–169.

[54] S. Komineas, N. Papanicolaou, Topology and dynamics in ferromagnetic media. *Physica D* **99** (1996), 81–107.

[55] A. Visintin, On some models of ferromagnetism, in *Free boundary problems*. Gakkotosho, Tokyo (2000), 411–428.

[56] A.M. Kosevich, B.A. Ivanov, A.S. Kovalev, Magnetic solitons. *Phys. Rep.* **194** (1990), 119–237.

[57] W.F. Brown, *Micromagnetics*, Robert E. Krieger Publishing Co., Inc., Huntington, New York, 1978, 25–45.

[58] W. E, X.-P. Wang, Numerical methods for the Landau-Lifshitz equation, *SIAM J. Numer. Anal.* **38** (2000), no. 5, 1647–1665

[59] S. Gustafson, J. Shatah, The stability of localized solutions of Landau-Lifshitz equations. *Comm. Pure Appl. Math.* **55** (2002), no. 9, 1136–1159.

[60] M.R. Matthews, B.P Anderson, P.C. Haljan, D.S. Hall, C.E. Wieman, E.A. Cornell, Vortices in Bose-Einstein condensates. *Phys. Rev. Lett.* **83** (2000), 2498.

[61] T.-L. Ho, V.B. Shenoy, Binary mixtures of Bose condensates of alkali atoms. *Phys. Rev. Lett.* **78** (1996), 586.

[62] R. Ejnisman, H. Pu, Y.E. Young, N.P. Bigelow, Studies of two-species Bose-Einstein condensation. *Opt. Express* **2** (1998), no. 8, 330–337.

[63] Experiments undergoing, e.g. at Nicholas Bigelow's Quantum Optic Group at University of Rochester.
URL: http://pas.rochester.edu/∼catgroup/bose.htm

[64] J.J. García-Ripoll, V.M. Pérez-García, Stable and unstable vortices in multicomponent Bose-Einstein condensates. *Phys. Rev. Lett.* **84** (2000), no. 19, 4264.

[65] I. Towers, A.V. Buryak, R.A. Sammut, B.A. Malomed, Stable localized vortex solutions. *Phys. Rev. E* **63** (2001), 055601.

[66] B. Sandstede, A. Scheel, Evans function and blow-up methods in critical eigenvalue problems. *Discrete and Contin. Dyn. Syst. Ser. B* **10** (2004), 941-964.

[67] J.R. Higgins, *Completeness and basis properties of sets of special functions.* Cambridge Univ. Press, 1977.

[68] M. Reed, B. Simon, *Methods of Modern Mathematical Physics IV: Analysis of Operators.* Academic Press Inc., 1978.

[69] I.C. Gohberg, M.G. Krein, *Introduction to the Theory of the Linear Nonselfadjoint Operators.* Transactions Mathematical Monographs, no. 18. Providence, RI: American Mathematical Society, 1969.

[70] T. Kato, *Perturbation Theory for Linear Operators.* Springer, 1976.

[71] W.A. Coppel, *Stability and Asymptotic Behavior of Differential Equations.* D.C. Heath and Co., Boston, 1965.